THE ROLE OF INOSITOL POLYPHOSPHATE MULTIKINASE IN HUNTINGTON'S DISEASE

by

Ishrat Ahmed

A dissertation submitted to Johns Hopkins University in conformity with the requirements for the degree of Doctor of Philosophy

Baltimore, Maryland

May 2015

ABSTRACT

Huntington's disease (HD) is a progressive neurodegenerative disorder characterized by several motor signs including chorea, rigidity, and bradykinesia, as well as cognitive and psychiatric symptoms. This disease is caused by a poly-glutamine repeat expansion in the N-terminal region of huntingtin (Htt) and mainly affects the striatum despite the ubiquitous expression of Htt. Several mechanisms have been suggested for the striatal specificity of HD ranging from changes in striatal-enriched proteins like Rhes to excitotoxicity from corticostriatal projections. The transcription factor Ctip2, which is preferentially expressed in the striatum, hippocampus, and cortical subplate, is also impaired in HD. Given the putative role of Ctip2 in the regulation of inositol polyphosphate multikinase (IPMK), we hypothesized that IPMK is involved in the pathophysiology of HD.

IPMK is known for its various functions in regulating cell survival and death through soluble kinase and PI3-kinase activities, which produce the inositol phosphates IP_4 and IP_5, and the phosphatidylinositol PIP_3, respectively. IPMK also displays various non-catalytic interactions, including the regulation of mTOR signaling and CBP/p300-mediated transcription. We have detected a significant loss of IPMK in post-mortem HD striatal tissues and various cellular and animal models of the disease. The depletion of IPMK protein and mRNA result from mutant Htt-induced impairment of Ctip2, as well as alterations in IPMK protein stability. Overexpression of IPMK rescues the mitochondrial metabolic activity deficit in a cellular model of HD. This rescue requires the lipid kinase

activity of IPMK and implicates the Akt signaling pathway downstream of IPMK signaling in HD. More importantly, viral delivery of IPMK in the striatum improves striatal pathology and motor performance of a transgenic mouse model of HD.

Our findings indicate that IPMK is an important player in the pathophysiology of HD. Furthermore, this Ctip2/IPMK/Akt signaling pathway provides a novel therapeutic target and approach to enhancing Akt signaling in HD and potentially other neurodegenerative diseases.

Thesis Advisor

Dr. Solomon H. Snyder, M.D.

Thesis Committee

Dr. Rejji Kuruvilla, Ph.D.

Dr. Mark P. Mattson, Ph.D.

Dr. Hongjun Song, Ph.D.

Designated Readers

Dr. Solomon H. Snyder, M.D.

Dr. Mark P. Mattson, Ph.D.

ACKNOWLEDGEMENTS

I would like to express the deepest gratitude to my research advisor Dr. Solomon H. Snyder for the opportunity to work under his guidance. His invaluable advice, patience, and constructive guidance, have led me to acquire the ability to think critically about experiments while putting together the pieces that ultimately became my thesis project. I also truly appreciate Dr. Snyder's encouragement and support in additional scientific endeavors, including mentoring. The knowledge and experience I have acquired through these activities are also life-long assets. I will always be indebted to Dr. Snyder for including me in his scientific family.

I also sincerely thank my thesis committee, Dr. Hongjun Song, Dr. Mark P. Mattson, and Dr. Rejji Kuruvilla, for their guidance and scientific input on my project. Their advice, support, and enthusiasm throughout this training has been invaluable. I also appreciate the guidance and support of my pre-thesis advisors Dr. Michael Caterina and Dr. Valina L. Dawson.

My special and sincere thanks to Dr. Bindu Paul, Dr. Seyun Kim, Dr. Juan Sbodio, Dr. Maged Harraz, Dr. Richa Tyagi and Dr. Maimon Hubbi who have provided valuable advice and encouragement. Their scientific input and sincere efforts have enabled me to complete this thesis efficiently. Many thanks also to my colleagues Jonathan Grima and Lauren Albacarys who have worked with me on several experiments. I truly appreciate their enthusiasm and friendship. I would like to thank Dr. Scott Vandiver, Dr. Gary Ho

and Dr. Michael Koldobskiy whose scientific and academic advice and friendship have made this experience even more enjoyable. I also appreciate the efforts of Lynda Hester and Roxanne Barrow, senior research associates in the laboratory, whose expertise have greatly increased the efficiency of my research projects.

I have also had the joy to collaborate on additional projects with several other members of the laboratory, including Dr. Prasun Guha and Risheng Xu. Our scientific conversations have been enlightening. Dr. Eunchai Kang, a post-doctoral fellow in the laboratory of Dr. Hongjun Song, has also been an excellent collaborator on a separate project on IPMK and neurogenesis. Her enthusiasm has led to a very enjoyable and exciting collaboration. I also appreciate the collaborative efforts of Dr. Shaida Andrabi, Joe Bedont and Joshua Crawford, who have enabled me to follow my curiosity and explore branches of this thesis project through their scientific expertise and support.

I have had several academic families over my many years at Johns Hopkins. My journey into cellular and molecular neuroscience began as an undergraduate student and continued as a Master's student. Many thanks to my research advisors, Dr. Ted Dawson and Dr. Joseph Savitt, who encouraged me to pursue the MD/PhD training and merge my love for patient care and the pursuit of scientific knowledge. Their kindness, support, and guidance have motivated me and prepared me for the MD/PhD training.

The MD/PhD program at Hopkins has truly been a second family away from home. I appreciate Dr. Bob Siliciano and Dr. Andrea Cox's support in my endeavors. Sharon

Welling, Bern Harper, and Martha Buntin are always available with kindness and enthusiasm. Without them, the program would not be the family it is today. I gratefully acknowledge the neuroscience department, especially Beth Wood-Roig and Rita Ragan, who have welcomed me into the program and ensured that my graduate training moved forward smoothly. Many thanks to my friends in the neuroscience graduate program, as well as in medical school, who have made this experience even more enjoyable.

Lastly, I owe my deepest gratitude to my parents, Dr. Aziz Ahmed and Shamsun Nahar, and my brother, Irfan Ahmed, who have always encouraged me to pursue my curiosity and follow my dreams. I truly appreciate their encouragement, support and advice throughout my time at Johns Hopkins.

Portions of this thesis have been submitted for publication elsewhere and thus some of this thesis includes contributions from my mentor Dr. Solomon H. Snyder. This work was funded by the US Public Health Service Grant MH-18501 and the Cure Huntington's Disease Initiative (CHDI). I also appreciate funding from the Medical Scientist Training grant (T32 GM007309).

TABLE OF CONTENTS

LIST OF TABLES

1. INOSITOL POLYPHOSPHATE MULTIKINASE

2. HUNTINGTON'S DISEASE

3. ROLE OF IPMK IN HUNTINGTON'S DISEASE

LIST OF FIGURES

1. INOSITOL POLYPHOSPHATE MULTIKINASE

2. HUNTINGTON'S DISEASE

3. ROLE OF IPMK IN HUNTINGTON'S DISEASE

ABBREVIATIONS

3-NP	3-nitroproprionic acid
5-IP_7	5-PP-Ins(1,2,3,4,6)P_5
AAV2	Adeno-associated virus serotype 2
ACBD3	Acyl-CoA binding domain containing 3
ACUC	Animal Care and Use Committee
AD	Alzheimer's disease
AMP	Adenosine monophosphate
AMPK	5' AMP-activated protein kinase
APC	Adenomatous polyposis coli protein
ASO	Anti-sense oligonucleotide
ATP	Adenosine triphosphate
Baf	Bafilomycin
BAD	Bcl-2-associated death promoter
Bcl11b	B cell lymphoma/leukemia 11B
BDNF	Brain-derived neurotrophic factor
Bmal1	Brain and muscle Arnt-like protein 1
BTK	Bruton's tyrosine kinase
Ca^{2+}	Calcium ion
CDK5	Cyclin-dependent kinase 5
CBP	CREB-binding protein
ChIP-seq	Chromatin immunoprecipitation followed by sequencing
CHDI	Cure Huntington's Disease Initiative
CHX	Cycloheximide

CK1	Casein kinase 1
CK2	Casein kinase 2
Clock	Circadian locomotor output cycles kaput
CMA	Chaperone-mediated autophagy
COUP-TF	Chicken ovalbumin upstream promoter transcription factor
CRE	cAMP response element
CREB	cAMP response element-binding protein
CRM1	Chromosomal maintenance 1
Cry	Cryptochrome
Ctip2	COUP-TF-interacting protein 2
DAD	Deacetylase-activation-domain
DAG	Diacylglycerol
DMEM	Dulbecco's modified Eagle's medium
Drp1	Dynamin-related protein 1
Dvl	Disheveled
ERK	Extracellular signal-regulated kinase
FGF-2	Basic fibroblast growth factor
FOXO1	Forkhead box protein O1
Fz	Frizzled
GABA	γ-Aminobutyric acid
GAP or Gap	GTPase-activating protein
GFAP	Glial fibrillary acidic protein
GluR6	Glutamate receptor ionotropic, kainate 2
GPe	Globus pallidus *externa*
GPi	Globus pallidus *interna*

GSK3β	Glycogen synthase kinase 3β
GTP	Guanosine triphosphate
Het	Heterozygous
Htt	Huntingtin
Hb	Hemoglobin
HD	Huntington's disease
HDCR	Huntington's disease collaborative research group
HDAC	Histone deacetylase enzyme
HEAT	Huntingtin, elongation factor 3, protein phosphatase 2A, and yeast kinase TOR1
HK2	Hexokinase 2
HSC70	Heat-shock cognate 70
IEG	Immediate early gene
IP	Inositol phosphate
IP_3	Inositol trisphosphate [$Ins(1,4,5)P_3$]
IP_4	Inositol tetrakisphosphate [$Ins(1,3,4,5)P_4$ and $Ins(1,4,5,6)P_4$]
IP_5	Inositol pentakisphosphate [$Ins(1,3,4,5,6)P_5$]
IP_6	Inositol hexakisphosphate [$Ins(1,2,3,4,5,6)P_5$]
IP_3K	$Ins(1,4,5)P_3$-kinase
IP6K	$InsP_6$ kinase or inositol hexakisphosphate kinase
IPK1 or IPPK	Inositol 1,3,4,5,6-pentakisphosphate 2-kinase
IPK	Inositol phosphate kinase
IPMK	Inositol polyphosphate multikinase
ITK	Interleukin-2-inducible T cell kinase
LAMP2A	Lysosome-associated membrane protein 2A

LBD	Ligand binding domain
LEF/TCF	Lymphoid enhancing factor/T-cell factor
LKB1	Liver kinase B1
LRP6	Low-density lipoprotein receptor related protein 6
MADS	Mcm1, agamous, deficiens and SRF
Mcm1	Minichromosome maintenance protein 1
MEF	Mouse embryonic fibroblast
MFN	Mitofusin
mHtt	Mutant huntingtin
MSN	Medium spiny neurons
mTOR	Mammalian target of rapamycin
mTORC1	mTOR complex 1 (mTOR and raptor)
mTORC2	mTOR complex 2 (mTOR and rictor)
MTT	3-(4,5-dimethylthiazol-2-yl)-2,5-diphenyltetrazolium bromide
NES	Nuclear export signal
NLS	Nuclear localization signal
nPAS2	Neuronal PAS domain protein 2
OTCase	Ornithine carbamoyltransferase
PD	Parkinson's disease
PDK1	Pyruvate dehydrogenase kinase, isozyme 1
Per1	Period circadian clock 1
PGC-1α	Peroxisome proliferator-activated receptor γ coactivator-1α
PH	Pleckstrin homology
PHLPP1	PH domain leucine-rich repeat protein phosphatase 1
PI3K	Phosphoinositide 3-kinase

PIP or PI(3)P	Phosphatidylinositol (3)-bisphosphate [PtdIns(3)P]
PIP_2 or $PI(3,4)P_2$	Phosphatidylinositol (4,5)-bisphosphate [$PtdIns(4,5)P_2$]
PIP_3 or $PI(3,4,5)P_3$	Phosphatidylinositol (3,4,5)-triphosphate [$PtdIns(3,4,5)P_3$]
PFA	Paraformaldehyde
PKB	Protein kinase B
PLC	Phospholipase C
PLC-γ1	Phospholipase C, gamma 1 isoform (PLCG1)
PMD	Post-mortem delay
Q7 or Q7/Q7	$STHdh^{Q7/Q7}$ immortalized striatal cell line
Q111 or Q111/Q111	$STHdh^{Q111/Q111}$ immortalized striatal cell line
Q7/Q111	$STHdh^{Q7/Q111}$ immortalized striatal cell line
Raptor	Regulatory associated protein of mTOR
Rictor	Rapamycin-insensitive companion of mTOR
NMDAR	N-methyl-D-aspartate receptor
ROS	Reactive oxygen species
SF-1	Steroidogenic factor-1
SGK	Serum- and glucocorticoid- induced kinase
SIRT1	Sirtuin1
SMRT	Silencing mediator for retinoid and thyroid receptors
SYN	Synapsin
TrkB	Tropomyosin receptor kinase B
NCoR	Nuclear receptor co-repressor
Rhes or Rasd2	Ras homolog enriched in striatum
SNpc	Substantia nigra *pars compacta*
SNr	Substantia nigra *pars reticulata*

Sp1	Specificity 1
SRE	Serum response elements
SRF	Serum response factor
STN	Subthalamic nucleus
SUMO	Small ubiquitin-like modifier
SWI/SNF	SWItch/Sucrose Non-Fermentable complex
T-ALL	T-acute lymphoblastic leukemia
TSC2	Tuberous sclerosis 2
UPS	Ubiquitin-proteasome system
UTR	Untranslated region
VA	Ventral anterior nucleus of the thalamus
VL	Ventral lateral nucleus of the thalamus
VPS34	Vacuolar protein sorting-associated protein 34
WT	Wild type
XLA	X-linked agammaglobulinemia
Xid	X-linked immunodeficiency

INTRODUCTION

Huntington's disease (HD) is a progressive and fatal neurodegenerative disorder. It shares several common features with other neurodegenerative diseases such as Alzheimer's disease (AD) and Parkinson's disease (PD). These similar clinical and pathological features include delayed onset of symptoms, selective neuronal vulnerability, protein aggregation, and impaired cellular processes such as abnormal proteasomal degradation and mitochondrial deficits. The resulting neuronal dysfunction and neuronal death contribute to the motor and cognitive deficits as well as psychiatric symptoms evident in patients afflicted with these diseases. Although much progress has been made in understanding the molecular mechanisms involved in these diseases, the mechanisms resulting in selective neuronal death are unclear and a cure is still lacking for these neurodegenerative diseases.

Huntington's disease is unique among these diseases in that the genetic cause of HD, mutant huntingtin (mHtt), is well established. Given the similarities of HD with PD and AD, understanding the mechanisms for impaired cellular functions in HD may shed light on the pathophysiology of these other neurodegenerative diseases. Although much progress has been made in understanding HD and the role of mHtt in impairing cellular functions, the mechanisms for the selective neuronal dysfunction and death remain to be elucidated. Various cell autonomous mechanisms, as well as mechanisms relying on cell-cell interactions such as excitotoxicity from corticostriatal projections have been suggested. It is likely that these mechanisms act synergistically and target several key

proteins resulting in the impairment of a vast signaling network. Although key signaling pathways such as the BDNF/TrkB/Akt pathway have been identified, it is unclear how these pathways link together.

The inositol polyphosphate pathway is a complex, evolutionarily-conserved pathway that is required for numerous cellular functions ranging from endocytosis to ion channel regulation. Although most enzymes in this pathway phosphorylate inositol phosphates, inositol polyphosphate multikinase (IPMK) is a multi-functional enzyme that displays an inositol phosphate kinase activity, a lipid kinase activity, and several non-catalytic functions. Through these various catalytic and non-catalytic functions, IPMK regulates both cell survival and death.

Given the pleiotropic functions of IPMK, we sought to determine whether this enzyme plays a central role in the pathophysiology of HD and identify which of its multiple functions are relevant in this disease. Furthermore, the regulation of IPMK expression and activity remains to be elucidated. Ultimately, understanding the role of IPMK in this disease may clarify the vast signaling network contributing to HD and also provide novel therapeutic targets.

CHAPTER 1

INOSITOL POLYPHOSPHATE MULTIKINASE

1.1 Cellular functions of IPMK

Inositol polyphosphate multikinase (IPMK) is a multi-functional enzyme belonging to the family of inositol phosphate kinases, which share motifs allowing for inositol phosphate binding and adenosine triphosphate (ATP) binding (1). This family also includes the $InsP_6$ kinases (IP6K) and $Ins(1,4,5)P_3$-kinases (IP_3K). IPMK and other members of the inositol phosphate kinase family display a soluble inositol phosphate kinase activity. IPMK also demonstrates a lipid kinase activity, as well as several non-catalytic functions.

IPMK was first identified as a crucial enzyme in the inositol polyphosphate pathway where it specifically acts as a dual-function inositol trisphosphate (IP_3) and inositol tetrakisphosphate (IP_4) kinase (2-5). Overall, the inositol polyphosphate pathway consists of almost 60 inositol phosphate isomers (1). Collectively, these isomers are involved in a variety of cellular functions ranging from channel regulation to chromatin remodeling (6). The lipid kinase activity of IPMK, producing phosphatidylinositol (3,4,5)-triphosphate [$PtdIns(3,4,5)P_3$ or PIP_3], was subsequently identified. Through PIP_3 signaling, IPMK is a major regulator of Akt activation (7, 8). More recently, various kinase-independent functions of IPMK were elucidated, including its roles in mammalian target of rapamycin (mTOR) signaling, 5' AMP-activated protein kinase (AMPK) regulation, p53-mediated cell death, and cAMP response element-binding protein (CREB)-mediated immediate early gene (IEG) induction (9-12). The various functions of IPMK are described in more detail in this chapter

1.1.1 Inositol phosphate kinase activity

The inositol phosphate backbone, *myo*-inositol, consists of a cyclohexanol with a 2-hydroxyl group in the axial position while the remaining five hydroxyl groups are equatorial (1). Phosphorylation of different hydroxyl groups generates different members of the inositol polyphosphate pathway, which is involved in various cellular functions.

Inositol polyphosphate pathway

Ins(1,4,5)P_3 or IP_3 is involved in a myriad of cellular functions, the most extensively studied function being intracellular calcium (Ca^{2+}) signaling (13). IP_3 also gives rise to additional inositol phosphates, including the inositol tetrakisphosphates Ins(1,3,4,5)P_4 and Ins(1,4,5,6)P_4 (both known as IP_4), the inositol pentakisphosphate Ins(1,3,4,5,6)P_5 (IP_5), the inositol hexakisphosphate Ins(1,2,3,4,5,6)P_6 (IP_6), and the higher inositol polyphosphates, which are discussed later (6) (Figure 1.1). IP_3 is generated by the activation of phospholipase C (PLC) in response to ligand-receptor interactions. PLC hydrolyzes the lipid phosphatidylinositol-4,5-bisphosphate [PtdIns(4,5)P_2 or PIP_2] to produce IP_3 and the lipid-soluble diacylglycerol (DAG). IP_3 is phosphorylated by IPMK or IP_3K to generate IP_4, which is subsequently phosphorylated by IPMK to produce IP_5. Thus, IPMK is an inositol trisphosphate and tetrakisphosphate 6/5/3-kinase. Although there is some redundancy in the inositol polyphosphate pathway, IPMK is the only enzyme that can produce Ins(1,4,5,6,)P_4 and IP_5 (14). Interestingly, IP_3K null mouse embryonic fibroblasts (MEFs) still produce IP_5 and IP_6, indicating that IPMK is crucial in the metabolism of IP_3 (15). The roles of IP_4 and IP_5 are described below.

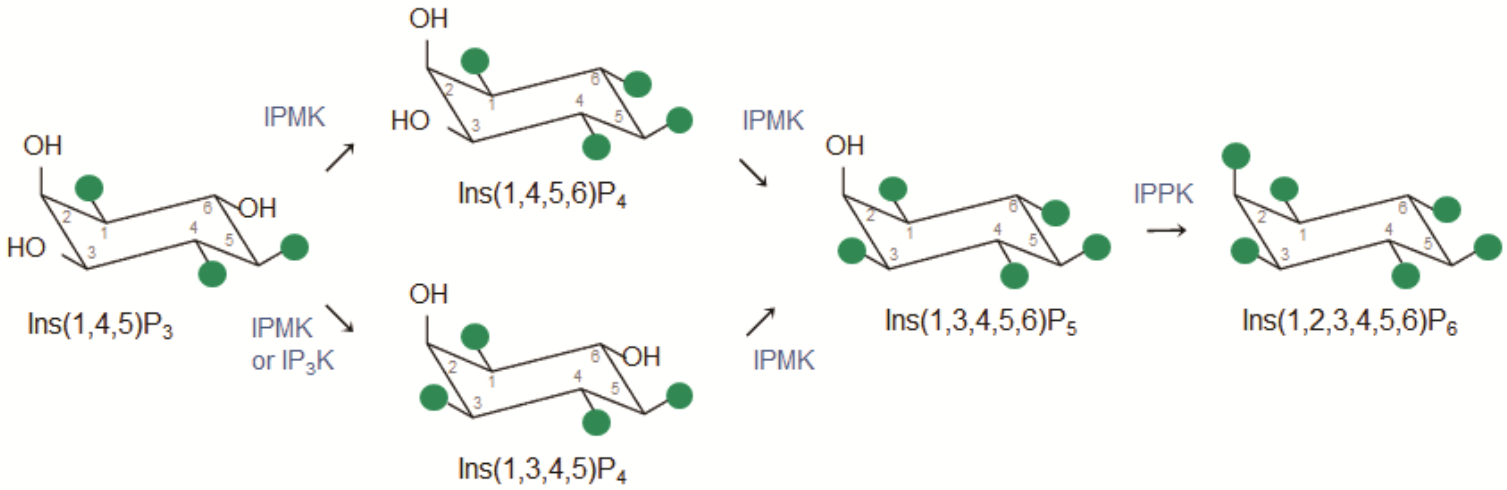

Figure 1.1. Soluble inositol polyphosphate kinase activity of IPMK

IPMK phosphorylates IP_3 to produce Ins(1,4,5,6)P_4 and Ins(1,3,4,5)P_4 both known as IP_4. Ins(1,3,4,5)P_4 also results from the catalytic activity of IP_3K. IPMK phosphorylates IP_4 to produce Ins(1,3,4,5,6)P_5, which is subsequently phosphorylated by inositol 1,3,4,5,6-pentakisphosphate 2-kinase (IPPK or IPK1) to produce Ins(1,2,3,4,5,6)P_6. The higher inositol phosphates, containing pyrophosphate moieties, are not shown. Circles indicate phosphate groups.

IPMK in yeast

IPMK was first identified as the *Saccharomyces cerevisiae* homolog, Arg82. Within yeast, the inositol phosphate kinase activity of Arg82 is required for numerous cellular functions including the yeast transcriptional response to arginine (16), nucleosome mobilization and chromatin remodeling (17, 18), and the cellular response to nitrogen source quality and phosphate availability (19).

The ArgR-Mcm1 complex, consisting of Arg80, Arg81, Arg82, and minichromosome maintenance protein 1 (Mcm1), is an arginine-responsive transcription complex. Arg82 is required for the formation of this complex independent of its soluble inositol phosphate kinase activity. However, IP_4 and possibly IP_5 are essential for the ArgR-Mcm1 complex-mediated transcriptional regulation of target genes as demonstrated by growth on ornithine as the only source of nitrogen (16). Interestingly, other studies focusing specifically on genes that regulate arginine metabolism indicate a role for a non-catalytic activity of Arg82 (20). Specifically, Arg82 represses ornithine carbamoyltransferase (OTCase) induction and enhances arginase induction by arginine independently of IP_4 and IP_5 production. The non-catalytic functions of Arg82 are described in section 1.1.3.

Arg82 is also involved in chromatin remodeling in yeast. IP_4 and IP_5 regulate the SWI/SNF (SWItch/Sucrose Non-Fermentable) complex, a nucleosome-remodeling complex that enhances transcription in an ATP-dependent manner (17). In addition to regulation of the SWI/SNF complex, the inositol polyphosphates regulate Ino80, another ATP-dependent chromatin-remodeling complex (18). Recruitment of these chromatin-

remodeling complexes to phosphate-responsive promoters and the subsequent induction of genes such as *PHO5* relies on IP_4 and possibly IP_5. Although the exact mechanism is unknown, the inositol phosphates may act by regulating the interaction between the SWI/SNF or Ino80 complexes with chromatin. Furthermore, IP_4 and IP_5 may contribute to the combinatorial signaling pathways regulating the activation of specific complexes.

The soluble inositol phosphate kinase activity of Arg82 was also demonstrated to be required for the induction of nitrogen-regulated genes and the repression of phosphate-regulated genes (19). Although the mechanism and the specific inositol polyphosphate products of Arg82 required for nitrogen and phosphate sensing are not known, the inositol polyphosphates may be acting through the regulation of chromatin-remodeling complexes.

Several other Arg82-dependent processes in yeast have been described including activation of macroautophagy, a complex lysosome-dependent process of degradation (21) and mRNA export (22). However, the mechanisms for these processes are unknown. In nitrogen-deprived conditions, yeast requires both Arg82 and KCS1 (the yeast homolog of IP6K1) for vacuolar processing, an essential step in autophagy (21). As described earlier, Arg82 produces IP_4 and IP_5, while KCS1 phosphorylates IP_6 to generate the higher inositol polyphosphate 5-PP-Ins(1,2,3,4,6)P_5 or 5-IP_7. The involvement of several enzymes of the inositol polyphosphate pathway in autophagy suggests that this cellular process may be dependent on the production of inositol phosphates in yeast. The physiologic functions of Arg82 are listed in Table 1.1.

Table 1.1. Physiologic roles of IP_4 and IP_5 in yeast

Process	IP_x	References
Chromatin remodeling	IP_4 (and IP_5)	(17, 18)
Regulation of gene expression	IP_4 and IP_5	(16)
Phosphate and nitrogen sensing	Unknown	(19)
Autophagy	Unknown	(21)
mRNA export	Unknown	(22)

IPMK in mammalian cells

In mammalian cells, IP_4 and IP_5 regulate several enzymes, signaling pathways, and cellular processes. Numerous crucial signaling proteins contain a pleckstrin homology (PH) domain, a 120-amino acid stretch comprised of seven β strands and a C-terminal α helix. These PH domains influence cellular localization by binding to inositol phosphates and phosphatidyl inositols (23). Interestingly, different pleckstrin homology domains display specificity for distinct inositol phosphates and phosphoinositides, such as PIP_2 and PIP_3. Pyruvate dehydrogenase kinase, isozyme 1 (PDK1) contains a PH domain that binds to PIP_3 and PIP_2 thereby allowing for membrane targeting and subsequent activation of the Akt/protein kinase B (PKB) signaling pathway described in section 1.1.2. This PH domain can also bind IP_5 and IP_6, allowing for cytoplasmic retention of PDK1 and activation of non-membrane targets (24). IP_5 also binds the PH domain of Akt, inhibiting membrane translocation and the subsequent phosphoinositide 3-kinase (PI3K)/Akt signaling pathway (24-26). Thus, IP_5 affects numerous cellular pathways requiring Akt activation. For instance, in endothelial cells, IP_5 inhibits basic fibroblast growth factor (FGF-2)-induced survival, cell migration, and angiogenesis as demonstrated by impaired capillary tube formation (26). Through the inhibition of Akt, IP_5 also exerts a pro-apoptotic effect in various cancer lines, including ovarian, breast, and lung cancer cells (27). Thus, one of the unique catalytic products of IPMK, IP_5, might act as a molecular switch regulating the activation of Akt.

Similarly, Bruton's tyrosine kinase (BTK), a cytoplasmic tyrosine kinase involved in B lymphocyte activation and development, contains a PH domain that binds Ins(1,3,4,5)P_4,

IP_5, and IP_6. X-linked agammaglobulinemia (XLA) and murine X-linked immunodeficiency (Xid) contain mutations in the PH domain of BTK resulting in decreased IP_4 binding and altering hematopoietic cell differentiation (28). Ins(1,3,4,5)P_4 is also involved in the development of T lymphocytes by binding interleukin-2-inducible T cell kinase (ITK). ITK is subsequently recruited to PIP_3 at the cell membrane where ITK phosphorylates PLC-γ1 (29). This mechanism is crucial for T cell receptor signaling during thymocyte positive selection. Other PH domain-containing proteins have been shown to interact with inositol phosphates, including $Gap1^{m}$ (30), and $Gap1^{IP4BP}$ (31), both members of the Ras GTPase-activating protein family. These studies implicate the inositol phosphates in an additional layer of complexity in phosphoinositide signaling resulting from the role of the inositol phosphates in modulating the affinity of various PH domains to PIP_3.

The soluble inositol phosphate kinase activity of IPMK modulates additional signaling pathways that do not involve PH domains. In the canonical Wnt/β-catenin signaling pathway, Wnt ligand binds Frizzled (Fz) and its co-receptor low-density lipoprotein receptor related protein 6 (LRP6). Interaction of this complex with the scaffolding protein Dishevelled (Dvl) recruits the Axin complex, which is subsequently phosphorylated by LRP6. In the absence of Wnt, the Axin complex, consisting of the scaffolding protein Axin, adenomatous polyposis coli protein (APC), casein kinase 1 (CK1), and glycogen synthase kinase 3β (GSK3β), phosphorylates β-catenin, targeting it for ubiquitination and subsequent degradation. In the presence of Wnt, phosphorylation of β-catenin is inhibited, allowing nuclear translocation of β-catenin, where it binds the

LEF/TCF (lymphoid enhancing factor/T-cell factor) transcription factors and induces Wnt-responsive genes (32).

In addition to the canonical pathway, Wnt3a stimulation results in Dvl3-mediated translocation of IPMK to the cell membrane through the interaction of Dvl3 with the N-terminal region of IPMK (33). The subsequent IP_5 generation is required to inhibit GSK3β and stimulate casein kinase 2 (CK2) collectively resulting in β-catenin stabilization and enhanced LEF/TCF activation (34). The inositol polyphosphates, specifically Ins(1,3,4,5)P_4 and IP_5 have also been shown to directly activate casein kinase 2 (35), a ubiquitously expressed serine/threonine kinase involved in numerous cellular processes ranging from cell cycle progression and transcription to apoptosis. (36).

The inositol polyphosphates also regulate global transcription through histone deacetylase enzymes (HDAC). HDAC inhibits transcription by removing acetyl groups from histone tails resulting in heterochromatin formation. Ins(1,4,5,6)P_4 promotes the assembly of HDAC3 to the deacetylase-activation-domain (DAD) of the SMRT/NCoR (silencing mediator for retinoid and thyroid receptors/nuclear receptor co-repressors) co-repression complex (37) . This interaction enhances HDAC3 activation. Thus, this pathway provides a likely mechanism for the role of IPMK and IP_4 in chromatin remodeling. Additional roles for IP_4 and IP_5 include the regulation of L-type calcium channels in vascular smooth muscle cells (38), IP_3 metabolism (39), and hemoglobin (Hb) affinity for oxygen (O_2) (40). The physiologic roles of the inositol phosphate kinase activity of IPMK in mammalian cells are listed in table 1.2.

Table 1.2. Physiologic roles of IP_4 and IP_5 in mammalian cells

Protein	Effect of IP_x	IP_x	References
Akt	Inhibition of PH domain and Akt signaling	IP_5	(24-27)
PDK1	Inhibition of PH domain and cytoplasmic retention of PDK1	IP_5	(24)
BTK	B cell activation and development	Ins(1,3,4,5)P_4	(28, 29)
ITK	T cell development (thymocyte positive selection)		(32)
$GAP1^{IP4BP}$	Enhanced Ras GAP activity	Ins(1,3,4,5)P_4	(30, 31)
$GAP1^{m}$	Enhanced Ras GAP activity	Ins(1,3,4,5)P_4	(34)
Wnt	GSK3β inhibition and β-catenin-induced LEF/TCF activation	IP_5	(33, 34)
CK2	Enhanced catalytic activity	Ins(1,3,4,5)P_4, IP_5	(35)
HDAC	HDAC-co-repressor assembly and chromatin remodeling	Ins(1,4,5,6)P_4	(37)
Ca^{2+} channel	L-type Ca^{2+} channel stimulation in vascular smooth muscle cells	IP_5	(38)
IP_3 5-phosphatase	Inhibition of IP_3 hydrolysis	Ins(1,3,4,5)P_4	(39)
Hb-O_2	Reduced affinity of Hb for O_2	IP_5	(40)

The production of IP_5 is the rate-limiting step for the production of the highly-energetic diphosphoinositol phosphates, also known as the higher inositol polyphosphates or inositol pyrophosphates. IP_5 is phosphorylated by IP_5 2-kinase (IPPK) to produce IP_6 (Figure 1.1), one of the starting products for the generation of the higher inositol polyphosphates, which include 5-PP-IP_4, 1-IP_7, 5-IP_7, and 1/5-IP_8 (6, 41). In fact, IPMK deletion in MEFs abolished the synthesis of IP_5, as well as the higher inositol polyphosphate IP_7 (42). These inositol pyrophosphates are involved in various cellular functions including the regulation of telomere length (43, 44), insulin secretion (45), endocyte trafficking (46), and homologous recombination repair of damaged DNA (47). The inositol pyrophosphates also contribute to post-translational modifications through the addition of a phosphate group onto phosphorylated residues (48, 49). Thus, IP_5 is also indirectly involved in numerous cellular processes through the production of IP_6 and the higher inositol polyphosphates.

1.1.2 Lipid kinase activity

Phosphatidyl Inositol 3-kinase

Class I PI3K, which phosphorylates the 3-hydroxyl group of the inositol ring of phosphoinositides, is the main player in the canonical lipid kinase signaling pathway (50). Class I PI3K consists of a p85-p110 complex. Receptor activation and autophosphorylation of tyrosine residues promotes receptor interaction with p85, which subsequently activates p110, the catalytic subunit. Class I PI3Ks produce PI(3)P, $PI(3,4)P_2$, and $PI(3,4,5)P_3$ (51). Class II PI3Ks are thought to specifically produce PI(3)P

while the Class III PI3K is a PtdIns-specific vacuolar protein sorting-associated protein 34 (VPS34) involved in various cellular processes including autophagy and amino acid sensing (50, 52).

Lipid kinase activity of IPMK

IPMK displays a lipid kinase or PI3-kinase activity similar to Class I PI3Ks (51) (Figure 1.2). Interestingly, IPMK is more selective than PI3K since it only produces PIP_3 whereas PI3K produces PI(3)P, $PI(3,4)P_2$, and $PI(3,4,5)P_3$. Although IPMK is not directly inhibited by wortmannin (51), wortmannin prevents IPMK phosphorylation and activation (7). Wortmannin inhibits PI3Ks. Therefore, PI3K-mediated PIP_3 production is thought to activate specific kinases that subsequently phosphorylate and activate IPMK, creating a feed-forward loop amplifying PIP_3 production (7). The proposed kinases and phosphorylation sites regulating IPMK remain to be identified. *In vitro* competition assays using IP_3 and $Ins(1,3,4,6)P_4$ in the presence of PIP_2 indicate that PIP_2 competes successfully with the inositol phosphates as IPMK substrates (51). Phosphorylation of IPMK may add another level of regulation enhancing the lipid kinase activity of IPMK.

As described earlier, the PH domain is a loosely conserved stretch of 120 amino acids, which recognizes PIP_2 and PIP_3 and promotes the recruitment of proteins to the cell membrane (50). Through the production of PIP_3, PI3K leads to the activation of various PI3K effectors containing PH domains, including Akt, PDK1, PLCγ, BTK, ITK, and GAPs among others (53). Collectively, these effector molecules influence numerous cellular processes ranging from actin rearrangement and vesicular trafficking to gene

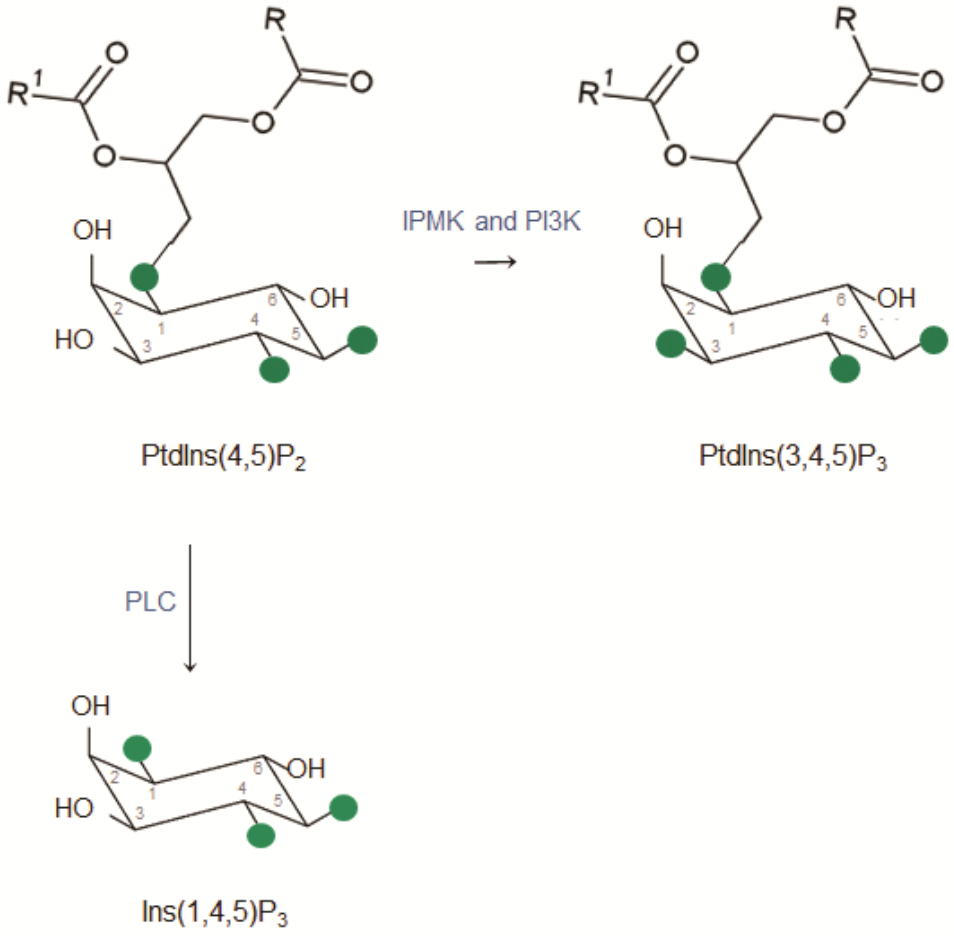

Figure 1.2. Lipid kinase activity of IPMK

IPMK and the p110 PI3-kinase (PI3K) both phosphorylate PtdIns(4,5)P_2 (or PIP_2) to produce PtdIns(3,4,5)P_3 (or PIP_3). PtdIns(4,5)P_2 can also be cleaved by phospholipase C (PLC) thereby generating Ins(1,4,5)P_3, the starting product of the inositol polyphosphate pathway. Circles indicate phosphate groups.

expression and cell growth. Several effector proteins, including Akt, are discussed next.

Downstream signaling pathways

Akt/PKB, a serine/threonine kinase, is involved in a myriad of cellular functions such as proliferation, survival, growth, and metabolism through the inhibition of various substrates. The substrates include Bcl-2-associated death promoter (BAD), tuberous sclerosis 2 (TSC2), forkhead box protein O1 (FOXO1), and p21 among others (50). Akt localizes to the membrane through the interaction of its PH domain with PIP_3. The subsequent phosphorylation of Akt at the T308 and the S473 sites by PDK1 and mTORC2 (mTOR complex 2), respectively, results in the activation of the Akt signaling pathway (54). The mTORC2 complex consists of mTOR associated with rapamycin-insensitive companion of mTOR (rictor). An RNAi-based screen designed to identify modulators of Akt activation revealed that IPMK influences the phosphorylation status of Akt (8). This observation was further confirmed in IPMK null MEFs, which display decreased phosphorylation of Akt at both the T308 and S473 sites (7). T308 phosphorylation reflects IPMK-mediated PIP_3 production. IPMK also acts as a co-factor for mTORC2 possibly promoting S473 phosphorylation; however, the mechanism remains unknown (10). Therefore, through its regulation of Akt, IPMK influences numerous pathways affecting cell survival, growth, proliferation, and migration (54).

The lipid kinase activity of IPMK also regulates additional proteins. Steroidogenic factor-1 (SF-1) regulates the transcription of endocrine-associated genes including various steroidogenic enzymes and peptide hormones. SF-1 contains a deep hydrophobic ligand-

binding domain (LBD) allowing for binding with PIP_2 such that the acyl chains are buried in the LBD. The inositol polyphosphate head is exposed at the surface of this non-membrane protein/lipid complex. IPMK, but not PI3K, interacts with and phosphorylates PIP_2 to produce SF-1/PIP_3, which is required for the transcriptional activity of SF-1 (55).

The lipid kinase activity of IPMK is also involved in mRNA export. Specifically, IPMK is required for ALY mediated mRNA recognition at the 3' untranslated region (UTR) and release from nuclear speckle domains. Through this mechanism, IPMK selectively regulates the export of transcripts involved in genome duplication and repair (56). Interestingly, like SF-1, ALY is also known to form a complex with PIP_2 or PIP_3, which regulates the mRNA export activity of this non-membrane protein/lipid complex (57). The lipid kinase activities of IPMK are summarized in Table 1.3.

1.1.3 Non-catalytic activities

The non-catalytic roles of IPMK were first identified using the yeast homolog Arg82. The regulation of arginine metabolism in yeast requires Arg82, Arg80, Arg81, and Mcm1, and results in arginine-induced anabolic gene repression and catabolic gene induction (58). The aspartate stretch of Arg82 is sufficient to stabilize members of the MADS-box (Mcm1, agamous, deficiens and serum response factor [SRF]) family of transcription factors, Arg80 and Mcm1, by preventing their degradation and promoting their nuclear localization (19, 58) (Figure 1.3A). In fact, the stability of both Arg80 and Mcm1 was impaired in Arg82 null *S. cerevisiae* yeast supplemented with the *S. pombe*

Table 1.3. Summary of lipid kinase activity of IPMK

Protein	Cellular processes	References
Akt	Cell survival, growth, proliferation	(7, 8)
SF-1	Endocrine transcriptionl network	(55)
ALY	mRNA export	(56)

ortholog of Arg82, which lacks the aspartate stretch (19, 20). Furthemore, catalytically inactive Arg82 does not impair the regulation of arginine metabolism (59).

IPMK is similarly a key regulator of metabolism signaling networks in mammalian cells through its regulation of mTOR and AMPK. mTORC1 (mTOR complex I) exists in a complex with raptor (regulatory associated protein by mTOR) and is crucial for nutrient amino acid-mediated regulation of protein synthesis and cell growth. Through its N-terminal domain, IPMK interacts with and stabilizes mTORC1 specifically enhancing mTOR-raptor interaction (10) (Figure 1.3B). AMPK is an energy sensor that promotes catabolic pathways while inhibiting anabolic pathways such as fatty acids synthesis and mitochondrial biogenesis (60). Glucose promotes IPMK-AMPK binding in the hypothalamus and prevents liver kinase B1 (LKB1)-mediated phosphorylation of AMPK at the T172 residue thereby preventing AMPK activation. This interaction requires the tyrosine phosphorylation of IPMK at the Y174 residue (9) (Figure 1.3B). Through its regulation of mTOR and AMPK, IPMK appears to regulate both cellular metabolism as well as central metabolism.

More recent studies have also demonstrated a kinase independent role for IPMK as a transcriptional co-activator in mammalian cells (Figure 1.3B). IPMK binds p53 thereby enhancing its interaction with p300. The subsequent acetylation of p53 promotes the expression of various downstream targets including Puma, resulting in decreased cell viability (12). In addition to its role in modulating cell death, IPMK influences the induction of immediate early genes (IEGs), which play a role in synaptic plasticity and

long-term memory (61). IPMK interacts with CREB-binding protein (CBP), increasing its function as a transcriptional co-activator of CREB and leading to IEG induction (11). IPMK also binds directly with SRF, enhancing its interaction with serum response elements (SRE) and promoting IEG expression among other target genes (62). As a result, conditional deletion of IPMK in neurons cause spatial learning and memory deficits *in vivo* (11). The non-catalytic activities of IPMK are summarized in Figure 1.3.

Given the pleiotropic roles of IPMK, this enzyme is crucial for the development and survival of organisms. In fact, yeast mutants lacking IPMK demonstrate sporulation, mating, and stress response deficits (51). IPMK knockout mice die at embryonic age 9.5 due to morphological defects including impaired neural tube formation (42). Furthermore, neurotrophic factors, which promote neuronal survival and differentiation, alter IP_5 levels (63). Therefore, it is essential to understand the regulation of IPMK.

Figure 1.3. Non-catalytic activities of Arg82 and IPMK

(Figure on following page)

(A) The aspartate stretch of Arg82 stabilizes Arg80 and Mcm1, enabling assembly with Arg81 and induction of arginine metabolizing enzymes. Essential domains in Arg82 are indicated, specifically the inositol phosphate binding site (IP), the SSLL (ser-ser-leu-leu) site is catalytically important, and the aspartate stretch. (B) The various non-catalytic activities of mammalian IPMK include its role in mTOR and AMPK signaling, as well as its function as a transcriptional co-activator for CBP, SRF, and p53. The interaction sites of IPMK with its binding partners specifically involve IPMK exon 1 (mTOR, Dvl3, CBP), exon 3 (SRF), exon 4 (AMPK, p53, SRF), and exon 6 (AMPK, SRF). Essential domains in IPMK include the IP site, ATP-binding site (ATP), and SSLL site, which are all required for the catalytic activity of IPMK. The nuclear export signal (NES) and nuclear localization signal (NLS) are also shown. The start sites and sequences for these essential domains of IPMK are as follows: IP (139-KPCIMDVKIGQKSYDPFASSEK), NES (170-LMEEIGFLVL), SSLL (249-YASSLLFVYEG), NLS (320-RHRKIYTKKHH), and ATP (380-EVRMIDFAH).

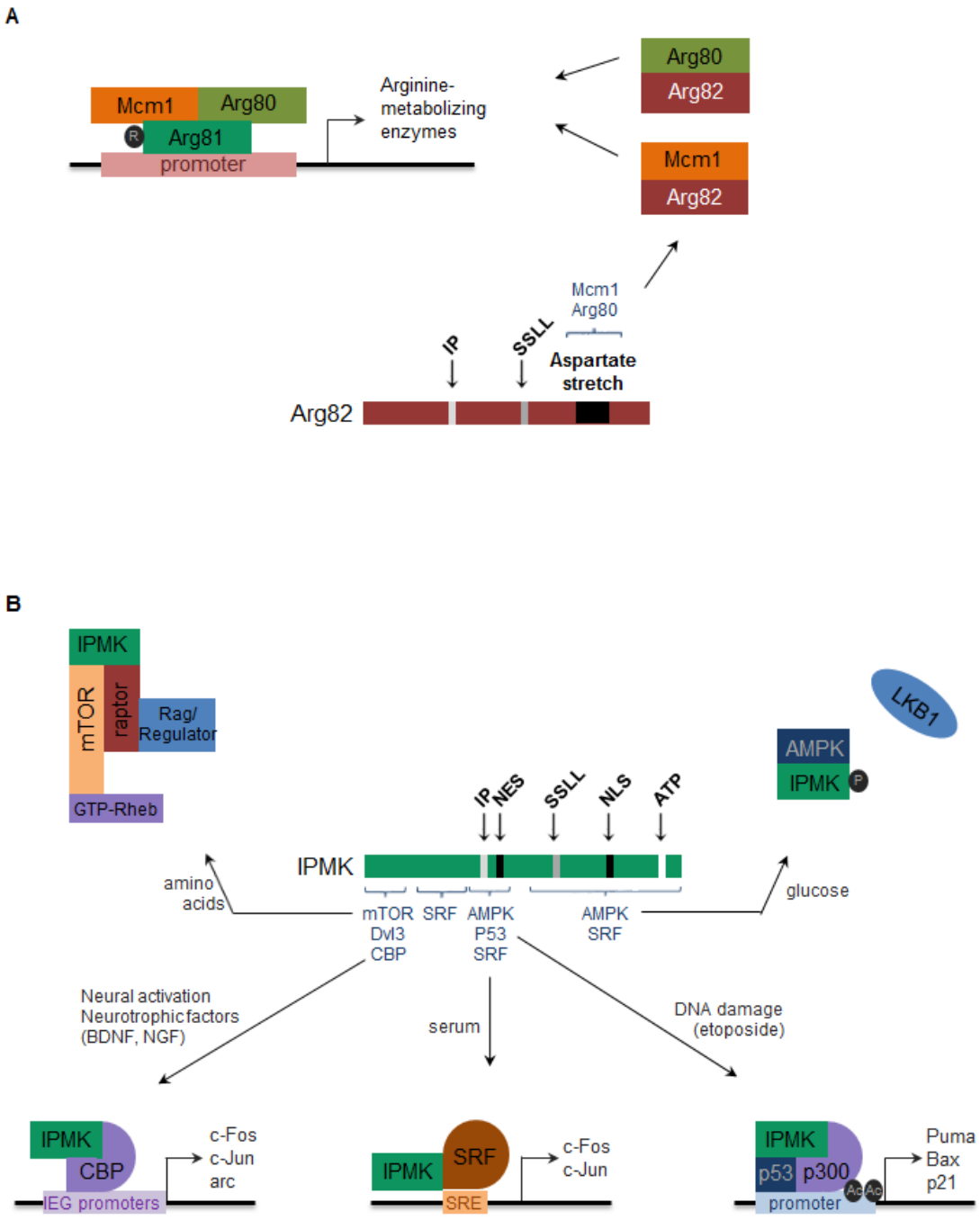

Figure 1.3. Non-catalytic activities of Arg82 and IPMK

(Figure legend on previous page)

1.2 Regulation of IPMK

Given the diverse and sometimes polar physiologic functions of IPMK, it is necessary to understand the regulation of the catalytic and non-catalytic activities of IPMK. Cellular localization, post-translational modifications, transcriptional regulation, binding affinity of the catalytic sites, and the availability of interaction partners all contribute to the specific pathway or pathways activated by IPMK.

1.2.1 Cellular localization

The subcellular localization of IPMK might influence the specific activity required within a particular context. IPMK contains a nuclear localization signal (NLS) and is mainly located in the nucleus as demonstrated by GFP-tagged IPMK (2). Nuclear localization of IPMK partly requires the conventional pathway involving the interaction of importin α/β with the NLS. However, NLS inactivation does not completely abrogate nuclear localization, suggesting that non-conventional nuclear shuttling pathways exist (64).

The nuclear export receptor chromosomal maintenance 1 (CRM1), which recognizes the nuclear export signal (NES), regulates the cytoplasmic localization of IPMK (65). Additional proteins influence the nucleocytoplasmic shuttling of IPMK. For example, CK2 binds and phosphorylates IPMK at the S284 site promoting nuclear uptake of IPMK (65). The domains for the nuclear import and export of IPMK, as well as its catalytic activities are provided in Figure 1.3. The membrane localization of IPMK also

modulates signaling pathways. IPMK is required for the cellular response to Wnt3a. Wnt3a stimulation leads to IPMK docking onto disheveled and thereby localizes it to the cell membrane. This interaction relies on the PDZ domain and C-terminal tail of Dvl3, as well as the N-terminal region of IPMK (33).

1.2.2 Post-translational modification

Post-translational modifications of IPMK are not well understood. CK2 phosphorylates IPMK, which regulates localization as described in section 1.2.1 (65). Furthermore, IPMK is phosphorylated in the presence of glucose (9). This modification is required for IPMK-mediated inhibition of AMPK as discussed in section 1.1.3. However, the kinase that phosphorylates IPMK remains to be identified. Given the various functions of IPMK, elucidating the post-translational modifications of IPMK, including but also extending beyond phosphorylation, is required to understand the regulation of its functions.

1.2.3 Binding affinity

The soluble inositol phosphate kinase and lipid kinase activities of IPMK both require the same catalytic site. Competition assays described in section 1.1.2 indicate that the lipid kinase activity of IPMK competes successfully with the substrates of its soluble inositol phosphate kinase activity, IP_3 and IP_4 (51).

1.2.4 Transcriptional regulation

The transcriptional regulation of IPMK also remains to be further investigated. Chicken ovalbumin upstream promoter transcription factor-interacting protein 2 (Ctip2), also known as B cell lymphoma/leukemia 11B (Bcl11b), is a C_2H_2 zinc finger transcription factor. It was recently identified as a putative transcription factor for IPMK in a screen (66). Ctip2 was initially studied for its role in T lymphocyte differentiation and maintenance (67). Mutations in Ctip2 are also associated with numerous malignancies, including T-acute lymphoblastic leukemia (T-ALL) and Ewing's sarcoma (68). The central nervous system roles of Ctip2 are further described in section 2.5.2.

Understanding the temporal and spatial regulation of IPMK at the cellular and organ systems levels are crucial. Furthermore, the regulation and role of IPMK in pathogenic processes remain to be investigated.

CHAPTER 2

HUNTINGTON'S DISEASE

2.1 Clinical manifestation and epidemiology

Huntington's disease is a progressive neurodegenerative disorder first described in 1872 by George Huntington who reported the prominent motor deficits and personality changes present in adult-onset HD (69). HD is characterized by a gradual decline in cognitive and motor function, as well as the presence of psychiatric symptoms and motor signs. Although subtle signs are present during the pre-symptomatic stage of the disease, the clinical diagnosis is based on extrapyramidal motor signs, such as chorea, an involuntary and abnormal dance-like movement (70). Approximately 90% of HD patients experience chorea (71). Additional motor signs during early stages of the disease include dyskinesia. As the disease progresses, patients exhibit more debilitating motor signs, such as rigidity, dystonia and bradykinesia. It is also essential to consider the impairment of fine motor control resulting in dysarthria and dysphagia, or speech and swallowing difficulties. The progressive impairment of gross and fine motor functions is associated with a concomitant decline in function and quality of life (72).

The cognitive decline and psychiatric symptoms also contribute substantially to the loss of quality of life of HD patients and often begin early prior to a formal diagnosis. Cognitive dysfunction includes impaired executive function such as planning, altered memory and learning, and diminished attention, language-related functions, and visuospatial functions (73). There is also a lack of awareness of deficits, as well as disinhibition. Psychiatric symptoms include anxiety, irritability, impulsivity, aggression, apathy, and depression (70). Delusions, hallucinations, and psychoses have also been

detected in approximately 50% of patients (74). These psychiatric symptoms are thought to contribute to the high suicide rate of HD patients, which was also described by George Huntington (69).

Although HD is mainly characterized by the triad of motor, cognitive and psychiatric symptoms, additional systems are also affected. There is evidence of weight loss, muscle wasting, metabolic dysfunction, endocrine disturbance (75), as well as sleep and circadian disturbances in HD patients (76).

2.2 Brain pathology

2.2.1 Neuropathology

Histopathologically, HD is characterized by striatal atrophy resulting from the selective loss of medium spiny neurons (MNSs), whereas the striatal interneurons remain largely unaffected. MSNs comprise 90-95% of striatal neurons (77-79). As the disease progresses, other brain regions become affected including the cerebral cortex, subcortical white matter and thalamus (80). Within the cerebral cortex, the pyramidal neurons of the middle and deeper cortical layers are specifically affected (81, 82). At the cellular level, inclusions containing insoluble mHtt aggregates are present in the nucleus, cytoplasm, and neurites of affected MSNs (83). The neuropathological changes in the striatum, as well as the other subcortical nuclei that comprise the striatum, are classified according to severity (84) (Table 2.1).

2.2.2 Basal ganglia

The basal ganglia is a complex series of circuits connecting the striatum, which receives excitatory input from the cortex, to the internal or external segment of the globus pallidus (GPi or GPe), the substantia nigra *pars reticulata* (SNr), and the subthalamic nucleus (STN). Projections from these nuclei converge on the ventral anterior (VA) and ventral lateral (VL) nuclei of the thalamus, which sends excitatory projections back to the cerebral cortex. The projections of the basal ganglia are all inhibitory projection except

Table 2.1. Classification of HD striatal pathology

Grade	*Striatal neuropathological features*
0	Normal
1	Mild neuronal death and fibrillary astrocytosis
2	Mild striatal atrophy, neuronal death and fibrillary astrocytosis
3	Moderate striatal atrophy, neuronal death and fibrillary astrocytosis
4	Severe striatal atrophy, neuronal death and fibrillary astrocytosis

the STN, which sends excitatory glutamatergic efferents to the GPi. Depending on the cortical area involved, the basal ganglia can modulate various functions ranging from motor functions to executive and limbic functions. The motor functions include the planning, initiation, and execution of movements, as well as motor learning (85).

The motor circuit originates in the pre- and postcentral sensorimotor fields and the motor areas of the cortex. It consists of two main pathways with polar effects: the direct and the indirect pathways, which project to two distinct populations of MSNs (figure 2.1). Both MSN populations release the inhibitory neurotransmitter γ-aminobutyric acid (GABA). In the direct pathway, the cortex sends excitatory projections to striatal MSNs, which send inhibitory projections to the GPi and SNr. The GPi/SNr send inhibitory signals to the VA/VL complex of the thalamus, thus the thalamus is disinhibited in the direct pathway and provides excitatory efferents to the cortex. Overall, the direct pathway facilitates movement.

In the indirect pathway, a second population of striatal MSNs send efferent inhibitory signals to the GPe, which subsequently sends inhibitory projections to both the GPi and the STN. The disinhibited GPi projects inhibitory efferents to the VA/VL complex of the thalamus thus reducing thalamocortical input. The STN, which is also disinhibited, sends excitatory projections further activating the GPi. The resulting inhibition of the thalamus suppresses movement.

Dopaminergic efferents from the substantia nigra *pars compacta* (SNpc) also modulate the direct and indirect pathways with the net effect of decreasing the inhibitory transmission of the basal ganglia and promoting movement. The excitatory D1 receptors expressed in direct pathway MSNs stimulate the direct pathway thereby enhancing movement. The inhibitory D2 receptors of the indirect pathway MSNs inhibit the indirect pathway thereby also facilitating movement.

Huntington's disease is a hyperkinetic disorder involving excessive movements, such as chorea and dyskinesia during the early stages of the disease. This excessive movement reflects impaired inhibitory basal ganglia transmission due to the loss of indirect pathway medium spiny neurons, resulting in the disinhibition of the thalamus and facilitation of movement early in HD (86). The later loss of direct pathway MSNs is associated with impaired movement characteristic of late-stage HD, including bradykinesia and dystonia (87). The differences between these MSN subtypes may account for their different vulnerability in HD. The direct pathway MSNs express Substance P, dynorphin, and D1 dopamine receptors while the indirect pathway MSNs express enkephalin and D2 dopamine receptors. Furthermore, the direct and indirect pathway MSNs display different morphological and electrophysiological properties (88, 89).

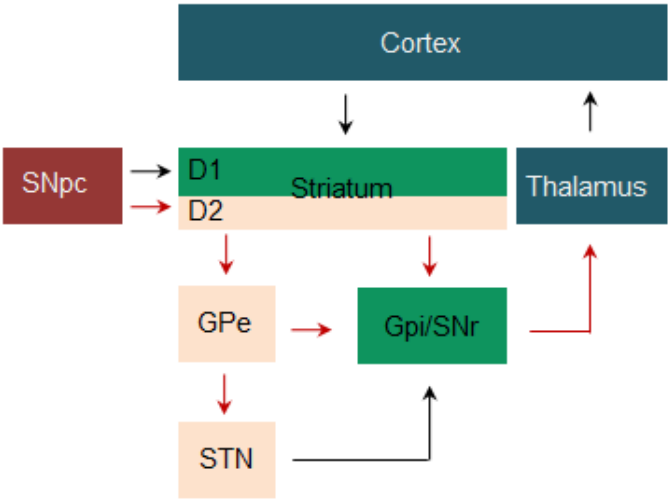

Figure 2.1. Basal ganglia circuitry

In a healthy brain, the direct pathway (cortex, striatum, GPi/SNr, and thalamus) facilitates movement whereas the indirect pathway (cortex, striatum, GPe, STN, GPi/SNr, and thalamus) inhibits movement. Dopaminergic projections from the SNpc enhance the direct pathway while inhibiting the indirect pathway thereby facilitating movement. Black arrows and red arrows indicate excitatory and inhibitory projections, respectively. Components of the basal ganglia represented in beige are part of the indirect pathway, which is altered early in HD. Components shown in green are part of the direct pathway.

2.3 Genetics

The discovery of the genetic cause of HD, a mutation in the huntingtin gene, has led to significant advances in the understanding of HD pathogenesis (90). A large collaborative effort involving the scientific community, specifically the HD Collaborative Research group (HDCR) and a Venezuelan community with a high rate of HD cases, led to mapping the mutation to chromosome 4p in 1983. Ten years later, the polyglutamine repeat expansion in the N-terminus of the huntingtin gene was identified (69).

HD is a monogenic autosomal dominant disorder. In fact, 90% of HD is hereditary (91). HD is caused specifically by a poly-glutamine (CAG) triplet repeat expansion in the N-terminus of the huntingtin gene. Individuals with 6-35 glutamine repeats are asymptomatic although CAG repeats between 27 and 35 can be unstable during transmission. Expansions greater than 35 repeats generally cause HD and longer repeats correlate with earlier disease onset (69). In fact, juvenile-onset HD is associated with more than 70 repeats, as well as anticipation, which consists of polyglutamine repeat expansion during paternal inheritance (92). CAG repeat lengths account for 50-70% of variance of age of onset. Other factors affecting age of onset include genetic modifiers, such as glutamate receptor ionotropic, kainate 2 (GluR6) discussed in section 2.5.2 (72).

Huntingtin is a 348-kDa protein consisting of several domains (Ross and Tabrizi, 2011). The N-terminal begins with a 17-amino acid stretch, also known as the N17 domain, which is highly susceptible to post-translational modifications. The polyglutamine region

begins at the 18th amino acid and is followed by a proline-rich region, which is involved in protein-protein interactions and also modulates mHtt toxicity (93-95). The remaining huntingtin sequence contains several interspersed HEAT repeats (huntingtin, elongation factor 3, protein phosphatase 2A, and yeast kinase TOR1), which form a superhelical structure. These HEAT domains are also thought to be involved in protein interactions. The C-terminus contains the nuclear export and nuclear localization signals (72).

Huntingtin undergoes several post-translational modifications. The N17 domain is phosphorylated at several sites (T3, S13, and S16) modulating mHtt (96, 97). This domain is also ubiquitinated and sumoylated at K6/9 and K15 (72, 98). These modifications occur at the same lysine residues and are thought to compete with each other. Ubiquitination promotes the ubiquitin-proteasome system-mediated degradation of mHtt (99) whereas sumoylation enhances toxicity (98).

Additional modifications are present outside the N17 domain. Huntingtin is palmitoylated by huntingtin-interacting protein HIP14 at the C214 site, resulting in the membrane localization of huntingtin (100). Huntingtin is also phosphorylated at the S421 site by Akt (101) and serum- and glucocorticoid- induced kinase (SGK) (102), resulting in decreased aggregation and neuroprotection. Lastly, huntingtin is acetylated at K444 by CBP, which improves clearance of mHtt by targeting it to autophagosomes (103).

2.4 Cellular dysfunction

HD symptoms are evident prior to neuronal death, indicating that neuronal dysfunction contributes to the psychiatric, cognitive, and motor deficits characteristic of HD. Mechanisms associated with the loss of function of Htt and gain of function of mHtt are thought to contribute to neuronal dysfunction in HD

2.4.1 Loss-of-function mechanisms

Wild type Htt is expressed ubiquitiously in the organism. Although it is also expressed through the cell, Htt is mainly localized within the cytoplasm where it associates with vesicles (104). At the cellular level, a greater than 50% decrease in Htt expression results in impaired neurogenesis, neuronal dysfunction and death, abnormal morphology of cellular organelles, and impaired transport of mitochondria and vesicles containing brain-derived neurotrophic factor (BDNF) (95, 105). Given these various cellular roles, Htt is crucial for several developmental processes, including gastrulation and brain development (106). In fact, Htt null mice are embryonic lethal at E8.5 (107). Interestingly, mHtt can compensate for the loss of Htt during development. However, these MSNs containing mHtt may be more vulnerable to cellular stressors (108).

2.4.2 Gain-of-function mechanisms

Pathogenic forms of mHtt

Several pathologic forms of mHtt have been described including compact β configurations, toxic N-terminal cleavage products, and post-translational modifications. These forms of mHtt alter its localization, aggregation, and clearance resulting in neuronal dysfunction through several cell-autonomous mechanisms (72). Two main subtypes of inclusions have been identified. The tightly-packed fibrillary form, which can be phosphorylated in the N17 domain, is less cytotoxic than the loosely-packed globular form (109). Furthermore, although mHtt aggregates cause cytoplasmic and nuclear inclusion bodies, the toxic forms consist mainly of mHtt oligomers and fragments (110). These pathogenic forms of mHtt alter numerous cellular processes.

Transcriptional dysregulation

Transcriptional dysregulation may be an important pathogenic mechanism in HD (111). The polyglutamine rich expansion of mHtt can interact directly with DNA (112) and also with glutamine-rich domains on transcription factors thereby inhibiting them (111). These transcription factors include Ctip2 (113), as well as specificity protein 1 (Sp1) (114), TAFII130 (115), nuclear receptor co-repressor (N-CoR) (116), CBP (117), and p53 (118). mHtt may also influence transcription at a global level through interactions with the histone acetyltransferase domain of CBP (119, 120).

Additional mHtt-mediated nuclear impairments have also been identified. Perinuclear inclusions disrupt the nuclear envelope. Neurons containing these types of inclusions display markers associated with cyclin-dependent kinase 5 (CDK5)-induced cell cycle re-entry, and were more susceptible to death (121).

Impaired protein degradation

The ubiquitin-proteasome system (UPS) and the lysosomal pathway are the two main intracellular degradation pathways. mHtt impairs both proteasomal and autophagic degradation resulting in the presence of additional abnormally folded proteins (122).

Proteasomal degradation mainly targets cytosolic and misfolded proteins. It requires a multi-step process whereby ubiquitin-activating enzyme (E1) activates ubiquitin in an ATP-dependent step followed by the transfer of ubiquitin to the ubiquitin-conjugating enzyme (E2). E2 acts in concert with ubiquitin ligase (E3) to transfer ubiquitin to the substrate resulting in a polyubiquitin chain linked at the K48 residue (123). The accumulation of K48-linked polyubiquitin chains in R6/2 mice and HD patients indicates loss of UPS function in HD (122).

Lysosomal degradation, which includes macroautophagy and chaperone-mediated autophagy (CMA) involves the degradation of bulk cytoplasmic content (124). Macroautophagy requires the formation of a double-membrane vesicle around the content marked for degradation by K63-linked polyubiquitin (125). These vesicles subsequently fuse with lysosomes resulting in the degradation of vesicular contents. Macroautophagy impairment results in the accumulation of ubiquitinated aggregates (126). K63-linked polyubiquitin chains also accumulate in HD patients and animal models (122). Furthermore, autophagy induction by rapamycin in fruit fly and murine models of HD protected against neurodegeneration by reducing aggregate formation and toxicity (127).

Chaperone-mediated autophagy specifically requires substrate recognition by heat-shock cognate 70 (HSC70), which binds to the lysosome-associated membrane protein 2A (LAMP2A) receptor and transfers the substrate to the lysosome (123). CMA is thought to be up-regulated in early HD to compensate for the loss of the UPS and macroautophagy (128).

Mitochondrial dysfunction

Mitochondrial dysfunction is a common feature in neurodegenerative disorders. Fewer mitochondria, corresponding with disease severity, have been detected in HD brain tissue. Altered expression of proteins involved in mitochondrial regulation have also been implicated in HD. Elevated dynamin-related protein 1 (Drp1) with concomitant mitofusin (MFN) depletion enhance mitochondrial fission (129). The transcriptional co-activator peroxisome proliferator-activated receptor γ coactivator-1 α (PGC-1α) regulates mitochondrial biogenesis and respiration. Impaired transcription of PGC-1α in HD also results in reduced neuronal size, neurodegeneration and motor deficits (130).

Mitochondrial damage has been linked to altered calcium (Ca^{2+}) homeostasis. In fact, elevated cytosolic Ca^{2+} levels cause excess mitochondrial calcium loading resulting in superoxide generation, oxidative damage, and also the loss of mitochondrial membrane potential (131). Mitochondrial depolarization subsequently leads to cytochorome c release and cell death (132). The various effects of mHtt in HD collectively alter cellular metabolism and increase neuronal vulnerability to cellular stressors, such as a reactive oxygen species (ROS), leading to neuronal death.

2.5 Striatal selectivity

2.5.1 Non-cell autonomous mechanisms

Similar to other progressive neurodegenerative disorders, HD targets a particular neuronal population, specifically the striatal MSNs. Since mHtt is ubiquitously expressed, numerous cell-autonomous and non-cell autonomous hypotheses have been proposed to explain the striatal selectivity of HD.

Excitotoxicity

Corticostriatal excitotoxicity was one of the earliest mechanisms posited for the striatal selectivity observed in HD. Intrastriatal glutamate injections resulting in excitotoxicity demonstrated the increased vulnerability of MSNs compared to the interneurons (133). The receptor composition and localization of MSNs contribute to their susceptibility. Synaptic N-methyl-D-aspartate receptor (NMDAR) activate CREB, resulting in neuroprotection. However, the stimulation of extrasynaptic NMDAR inhibit the pro-survival effects of CREB (134, 135). Polymorphisms of the GluR6 kainate receptor also contribute to age of onset of HD (136).

Excitotoxicity is linked to altered calcium homeostasis and mitochondrial dysfunction (discussed in section 2.4.2). Several types of glutamate receptors, including mGluR1/5 and NR2B, appear to mediate the increase in cytosolic calcium levels in HD. Elevated cytosolic calcium results in excess cytochrome c release and apoptosis (137).

Neurotrophic factors

Neurotrophic factors are required for neuronal survival. Decreased transcription of neurotrophic factors, impaired transport of these factors, loss of cortico-striatal projections, and altered receptor signaling all contribute to reduced neurotrophic factor signaling.

The cortex supplies much of the BDNF required for the development, maintenance, and plasticity of MSNs through anterograde transport (138). BDNF specifically binds to the receptor tyrosine kinase tropomyosin receptor kinase B (TrkB), resulting in receptor dimerization and autophosphorylation. The subsequent phosphorylation of additional tyrosine residues creates docking sites for adapter proteins thereby coupling TrkB to intracellular signaling cascades, which include the PI3K/Akt, Ras/ERK, and PLCγ1 pathways (139). The two main isoforms of TrkB include the full-length isoform, which contains a tyrosine kinase domain and a truncated isoform lacking the catalytic domain. This truncated isoform can act as a dominant negative, adding another layer of complexity to this signaling pathway (140).

mHtt-mediated transcriptional dysregulation results in decreased production of cortical BDNF (141). mHtt also impairs the anterograde transport of BDNF vesicles (142). More recently, impaired TrkB signaling, independent of BDNF alterations, has been demonstrated in HD (143). Thus, the BDNF-TrkB signaling pathway is severely diminished and contributes to the increased vulnerability of MSNs in HD.

Inflammation

Several non-neuronal mechanisms of MSN-selectivity have also been suggested. Microglial activation begins during the prodromal stages of HD and correlates with disease severity (144, 145). In fact, mHtt expression in glial cells causes neuronal excitotoxicity in a co-culture model (146). The release of cytokines is also thought to contribute to neuronal death (147). Similarly, mHtt expression in astrocytes cause motor deficits and reduced survival *in vivo*. One possible mechanism involves the mHtt-mediated inhibition of Sp1 thereby impairing glutamate transporter expression in astrocytes (148).

Thus, numerous non-cell autonomous mechanisms involving corticostriatal projections, astrocytes, and microglia contribute to the complex network that results in neuronal dysfunction and death. These mechanisms also account for the striatal selectivity of HD.

2.5.2 Cell autonomous mechanisms

Altered expression or activity of striatal-enriched proteins may provide additional clues to the cell-autonomous mechanisms contributing to the striatal selectivity of HD. Numerous striatal-enriched genes have been identified and the majority are decreased in R6/1 mice. These genes belong to specific functional groups, including proteins involved in transcription, excitotoxicity, axon growth and guidance, synaptic function, neurotransmitter receptors, and G-protein signaling (149). Two striatal-enriched proteins, Ctip2 and Ras homolog enriched in striatum (Rhes or Rasd2) are discussed in this section.

Ctip2

The transcription factor Ctip2 is enriched in the striatum and is also expressed in other regions of the brain such as the cortex and hippocampus (150). Within the striatum, Ctip2 is specifically expressed in MSNs and is required for the differentiation of MSNs as well as the patch-matrix organization of the striatum (151). Ctip2 is also expressed in the anterior neocortex throughout the cortical plate during development (152) where it is involved in corticospinal motor neuron axon growth and fasciculation (150, 153).

Interestingly, Ctip2 is depleted in the R6/1 animal model of HD and in post-mortem striatal samples from HD patients (113, 149). Furthermore, over-expression of Ctip2 in a cellular model of HD appears to rescue the metabolic activity deficit in these cells (113). Thus, Ctip2 and its downstream targets could also account for the striatal and MSN-specific disease pathology in HD.

Ctip2 generally results in transcriptional repression when interacting with COUP-TF family members (154). However, it can also act as a transcriptional co-activator. A genome-scale chromatin immunoprecipitation followed by massively parallel sequencing (ChIP-Seq) and genome-wide expression profiling led to the identification of several putative targets of Ctip2 in immortalized wild-type striatal cells over-expressing Ctip2. IPMK was identified as a potential target of Ctip2 in this screen (66).

Given the various targets of Ctip2 and its functions as a transcriptional repressor and transcriptional co-activator, it is necessary to understand the regulation of Ctip2

expression and activity. The histone deacetylase sirtuin 1 (SIRT1) interacts with Ctip2 and specifically enhances transcriptional repression mediated by Ctip2 (155). In addition, Ctip2 is a substrate for sumoylation (156). However, the effect of this modification remains to be investigated.

Rhes

Rhes was first identified as a guanosine triphosphate (GTP)-binding protein (157). In addition to this function, Rhes is involved in sumoylation, a process similar to ubiquitination, in which small ubiquitin-like modifier (SUMO) is conjugated to a substrate (158). Sumoylation is involved in numerous neuronal functions ranging from synapse formation to neurotransmitter release and synaptic scaling (158).

Aberrant sumoylation has been implicated in several diseases, including HD. Rhes has been shown to enhance cytotoxicity in cellular models of HD (157, 159). Furthermore, Rhes knockout mice are protected from 3-nitroproprionic (3-NP)-induced striatal degeneration (160) and Rhes-deleted transgenic HD mice also show a delayed onset of behavioral symptoms (161). At the molecular level, Rhes acts as an E3 ligase for the sumoylation of mHtt resulting in decreased protein aggregation, increased levels of soluble mHtt, and cytotoxicity (159). Interestingly, mutant Htt is ubiquitinated and sumoylated at the same lysine residue resulting in neuroprotection and enhanced neurodegeneration, respectively (98).

2.6 Animal models

Early models of HD involve neurotoxin-based striatal lesions. The glutamate agonists, kainic acid and quinolinic acid, both result in glutamatergic excitotoxity (162-164). Mitochondrial toxins such as 3-NP, also cause bilateral striatal lesions (165). 3-NP inhibits complex II of the mitochondrial electron transport chain (166). These neurotoxin-mediated models of HD have helped elucidate several mechanisms contributing to the striatal pathology of HD, specifically excitotoxicity and mitochondrial dysfunction. However, these models are incomplete due to the acute nature of the lesion (167).

The discovery of mHtt led to the generation of numerous rodent models of HD. These models differ based on several features including: 1) full length mHtt versus mHtt fragment, 2) length of CAG repeats, 3) transgene versus knock-in into endogenous Htt locus, 4) human or mouse Htt, 5) cDNA versus genomic DNA which carries introns and regulatory sequences, and lastly, 6) endogenous Htt promoter versus another promoter. The different features of these models influence neuropathological changes in the animal, as well as motor deficits and survival. Various behavioral tests are used to assess the severity of motor dysfunction, which include locomotor activity deficit, progressive decline in rotarod activity, lengthened time to cross balance beam, and gait abnormalities (167). The R6/2 transgenic model and the zQ175 knock-in model are described below.

The R6/2 transgenic model of HD involves the expression of the N-terminal fragment of mHtt, specifically exon 1, downstream of a human Htt promoter. This is the most severe model of HD with a lifespan of approximately 13 weeks due to the large repeat number and the use of the N-terminal fragment, which is more toxic than full-length mHtt. In fact, neuropathological changes such as striatal atrophy are detected as early as six weeks of age in this model (168). Several motor deficits such as rotarod and open field performance are evident even earlier, at approximately five weeks of age (169).

The zQ175 knock-in model consists of full-length human mHtt downstream of the endogenous mouse Htt promoter (170). These mice have a longer survival period ranging from 76-104 weeks, reflecting the milder genetic modifications used to generate this model. Behavioral deficits are also more progressive in this model of HD. In fact, impaired rotarod performance is detected at approximately 30 weeks.

There are also several non-rodent models of HD, which present several advantages and disadvantages. Invertebrate models of HD, specifically *Caenorhabditis elegans* and *Drosophila melanogaster*, allow for rapid initial studies. However, findings from these models require further testing in mammalian models of HD. Non-human primate models and larger mammalian models such as pigs and sheep facilitate the study of drug delivery mechanisms, including the delivery of viral vectors and anti-sense oligonucleotides. However, these models take longer to generate and study due to the more gradual neuropathologic changes (72, 167).

2.7 Therapeutic directions

Knowledge of the genetic mutation causing HD, as well as the correlation between repeat number and age of onset, has allowed for predictive genetic testing. Therefore, abolishing mHtt pathology prior to disease onset could potentially cure HD patients. Furthermore, HD therapies might not only delay disease progression, but could also reverse symptoms. Blocking mHtt expression in a tetracycline-regulated HD model eliminated inclusions and rescued motor phenotype (171).

Potential drugs targeting huntingtin aggregation, mitochondrial dysfunction, excitotoxicity, transcriptional impairment, inflammation and oxidative stress appear to increase survival in animal models of HD and reduce neuropathological changes (120, 172-175). However, human clinical trials will ultimately determine the efficacy of these drugs. More recent studies have focused on developing mHtt-lowering therapies, such as the mHtt allele specific anti-sense oligonucleotides (ASOs) (176). Lastly, the potential benefits of endogenous stem cells, as well as their differentiation and integration are being investigated (177). However, further research is needed to assess potential neuropathologic changes in the newborn neurons over time.

The discovery of the genetic cause of mHtt has led to the elucidation of a vast network of signaling pathways and cellular processes that contribute to the pathophysiology of HD. Understanding the central players in this network and the striatal selectivity of HD will ultimately pave the way towards a cure for this disease.

CHAPTER 3

ROLE OF IPMK IN HUNTINGTON'S DISEASE

3.1 Objectives

Various processes are thought to contribute to the selective dysfunction and death of MSNs in Huntington's disease. Given the mHtt-mediated alterations in the expression and function of the striatal-enriched protein Ctip2, which has been identified as a putative transcription factor for IPMK, we hypothesized that IPMK might also play a role in the pathophysiology of HD. IPMK has been shown to exert pro-survival and pro-death effects through its numerous catalytic and non-catalytic functions, suggesting that it could be a central component in the vast signaling network contributing to cellular dysfunction in HD. Thus, we sought to elucidate the role of IPMK in neurodegeneration. The main objectives of this study include the following: 1) characterize the expression of IPMK in HD, 2) identify the molecular mechanisms regulating IPMK expression, 3) determine the signaling targets of IPMK involved in HD, and 4) study the therapeutic potential of IPMK *in vivo*.

3.1.1 Characterization of IPMK expression in HD

Since IPMK is likely regulated by Ctip2, which is depleted in HD, IPMK expression is also expected to be altered in HD. IPMK expression was characterized in cell models of HD, animal models of the disease, and post-mortem tissue samples from HD patients. Furthermore, catalytic activities unique to IPMK were investigated to further confirm alterations in IPMK protein.

3.1.2 Identification of molecular mechanisms regulating IPMK

We sought to confirm whether IPMK is indeed a transcriptional target of the striatal-enriched transcription factor Ctip2. Furthermore, since numerous cellular mechanisms are altered in HD, we also examined whether IPMK protein stability is altered.

3.1.3 Identification of the role of IPMK in neuronal dysfunction

IPMK is involved in numerous cellular functions yielding pro-apoptotic and pro-survival effects depending on the signaling pathways activated. Thus, it was necessary to determine whether alterations in IPMK expression are pathogenic or compensatory. Given the multi-functional nature of IPMK, the specific downstream signaling pathways involved in HD pathogenesis were also examined.

3.1.4 Investigation of the effect of IPMK in an animal model of HD

The cellular model of HD indicated that loss of IPMK is pathogenic in HD. Furthermore, restoration of IPMK improved cellular metabolism. Thus, we investigated whether down-regulation of IPMK, and conversely, intrastriatal delivery of IPMK in an animal model of HD modify striatal pathology and behavioral deficits.

3.2 Materials and methods

Cell cultures

The immortalized striatal cell lines STHdh$^{Q7/Q7}$ (Q7), STHdh$^{Q111/Q111}$ (Q111), and STHdh$^{Q7/Q111}$ (Q7/Q111) express endogenous wild type huntingtin (Htt) and mutant huntingtin (mHtt) with 7 or 111 polyglutamine repeats, respectively. These cell lines were provided by M. MacDonald (Department of Neurology, Massachusetts General Hospital, Boston). The cells were maintained at 33ºC in Dulbecco's modified Eagle's medium (DMEM) supplemented with 10% fetal bovine serum, 2mM L-glutamine, 400 µg/ml geneticin, and antibiotics (penicillin and streptomycin). Experiments were performed without geneticin. Cells beyond passage 15 were not used for experiments. HEK293 cells were grown at 37ºC in DMEM supplemented with 10% fetal bovine serum, 2mM L-glutamine, and antibiotics.

Reagents

The Q7 and Q111 cells were transfected using Lipofectamine 2000 (Invitrogen). HEK293 cells were transfected with Polyfect (Qiagen). Ctip2 siRNA and scrambled siRNA (Santa Cruz) were used at a concentration of 50 pmol and 100 pmol. For translational blocking, cells were treated with 30 µg/ml cycloheximide (Sigma). Q7 and Q111 cells were treated with MG132 (carbobenzoxy-Leu-Leu-leucinal) and bafilomycin, inhibitors of proteasomal degradation and lysosomal degradation, respectively, for 13 h at the indicated concentrations.

Animals

Animals were housed and cared for in accordance with the National Institutes of Health guide for the Care and Use of Laboratory Animals and approved by the Johns Hopkins University Animal Care and Use Committee (JHU ACUC). Animals were kept on a 12 h light/dark cycle and provided food and water *ad libitum*. The R6/2 mice (B6CBA-Tg(HDexon1)62Gpb/1J), a transgenic model of HD which expresses exon 1 of human Htt, were purchased from Jackson Laboratory. This line carries approximately 150 polyglutamine repeats. The breeding strategy involved ovarian transplant hemizygous females and B6CBAF/1J males. Only F1 R6/2 and non-carrier sibling males were used for the experiments. The zQ175 mice, obtained from the CHDI foundation, is a knock-in model of Huntington's disease and contains one chimeric human/mouse exon 1 allele with approximately 190 polyglutamine repeats (170). IPMK gene knockout is embryonic lethal in mice (42).

IPMK floxed ($IPMK^{fl/fl}$) mice, in which the loxP sites flank exon 6 of IPMK, were generated by Ozgene. Neuron-specific conditional IPMK knockouts were generated by breeding the $IPMK^{fl/fl}$ animals with Nestin-cre, producing Nestin-cre; $IPMK^{fl/fl}$ animals with littermate $IPMK^{fl/fl}$ controls. Animals heterozygous for IPMK (IPMK Het) were also generated by Ozgene. Male IPMK Het animals were bred with ovarian transplant R6/2 hemizygous females to produce HD animals heterozygous for IPMK.

Post-mortem brain tissues

Striatal tissues from control and HD patients were obtained from J. Troncoso and O. Pletnikov (Brain Resource Center, Johns Hopkins University). Information on patient age at death, gender, HD grade and post-mortem delay (PMD) are provided in Table 3.1.

Plasmids

The plasmids encoding wild type IPMK (IPMK WT), kinase dead IPMK (KASA), and the *Arabidopsis thaliana* ortholog atIPK2β, as well as the wild type IPMK fragments were previously described (7, 10, 12). IPMK displays a soluble inositol phosphate kinase (IPK) activity, which is present in mammalian IPMK as well as atIPK2β. Only mammalian IPMK exhibits a lipid kinase (PI3K) activity. Furthermore, mammalian IPMK interacts with various proteins resulting in non-catalytic activities. Mutation of IPMK at K129A-S235A (IPMK KASA) abolishes both catalytic activities of IPMK, while retaining its non-catalytic activities. The activities of IPMK WT, IPMK KASA, and atIPK2β are summarized in Table 3.2. The CTIP2 plasmid was purchased from Origene. The N-terminal fragments of wild type Htt (N171-18Q) and mHtt (N171-82Q) were previously described (159). pcDNA3-AKT-PH-GFP was a gift from Craig Montell (Addgene plasmid #18836) (178).

Table 3.1. Post-mortem control and HD striatal tissues

Sample	*Grade*	*Gender*	*Age (yrs)*	*PMD (hrs)*
1	Control	Male	60	6
2	Control	Female	68	11
3	Control	Male	64	12
4	Control	Male	42	19
5	Control	Female	46	24
6	HD Grade 4	Male	63	5
7	HD Grade 4	Male	63	15
8	HD Grade 4	Male	41	21
9	HD Grade 4	Male	41	8
10	HD Grade 3	Female	50	4
11	HD Grade 3	Male	43	23
12	HD Grade 3	Female	45	24

Table 3.2. Catalytic and non-catalytic activities of IPMK mutant and ortholog

	IPMK WT	*IPMK KASA*	*atIPK2β*
IPK activity	+	-	+
PI3K activity	+	-	-
Non-catalytic	+	+	-

Quantitative real-time PCR

RNA was isolated from Q7 and Q111 cells using the RNEasy mini kit (Qiagen). Quantitative real-time PCR was performed in quadruplicates using the TaqMan RNA-to-Ct 1-step kit and the StepOnePlus real-time PCR system (Life Technologies). TaqMan probes for mouse IPMK and mouse Ctip2 were used. Data were normalized to β-actin. n = 3 for all real-time PCR experiments.

Western blotting

Q7 and Q111 cells were lysed in a buffer containing 50mM Tris HCl (pH 7.5), 150mM NaCl, 1% triton x-100,10% glycerol and protease and phosphatase inhibitors (standard lysis buffer). Animals were euthanized with CO_2 in accordance with JHU ACUC protocol. The striatum of wild type (WT) and R6/2 mice were collected at 13 weeks. The striatum of WT and zQ175 mice were harvested at 12 months. These were homogenized in standard lysis buffer using a hand-held homogenizer. Post-mortem human tissue was homogenized in RIPA lysis and extraction buffer. Cell lysates and brain homogenates were centrifuged at 14,000 rpm for 30 min and the supernatant was collected for Western blotting. Mouse IPMK antibody, which detects a 47-kDa band, was produced in-house (Covance), and was previously described (7). This antibody also binds non-specifically thereby generating several additional bands, including a yet unidentified 49-kDa protein. Additional antibodies used include human IPMK (Genetex), total Akt, phospho-Akt (T308) and phospho-Akt (S473) (Cell Signaling Technology), and IPPK, GAPDH and β-actin (Santa Cruz). The secondary anti-rabbit and anti-mouse antibodies were purchase from GE Healthcare. Densitometric analysis of

Western blot bands was performed using ImageJ and normalized to β-actin, GAPDH, or total Akt. n = 4 for the cycloheximide studies and IPMK overexpression studies. n = 3 for all experiments.

Co-Immunoprecipitation

Cells were lysed in standard lysis buffer 24 h after transfection. Lysates were further homogenized using a 25-gauge needle and then centrifuged. Samples were pre-cleared using rabbit IgG-agarose (Sigma) for 1 h. Following protein measurement, supernatant containing 500 μg of protein were incubated overnight with EZview Red c-myc-agarose (Sigma). The beads were washed five times with wash buffer (50mM Tris HCL [pH 7.5], 300mM NaCl, 1% Triton X-100 and 10% Glycerol). Protein was eluted by boiling in 2x LDS sample buffer (Invitrogen) with 5% 2-mercaptoethanol. n = 3 for all co-immunoprecipitation assays.

MTT assay

The MTT [3-(4,5-dimethylthiazol-2-yl)-2,5-diphenyltetrazolium bromide] assay, which measures mitochondrial succinate dehydrogenase activity, was used to assess mitochondrial metabolic activity. Q7 and Q111 cells were plated at a density of $2x10^5$ cells/well and transfected in triplicates after 16 h. After 48 hours, cells were treated with 250 μg/ml MTT and incubated at 33ºC for 1.5 hours. After removal of the media, 2 ml DMSO was added to each well to dissolve the formazan crystals. The absorbances at 570 nm and 630 nm were determined using a SpectraMax M3 plate reader (Molecular Devices) and Softmax Pro software. n = 4-6 for MTT experiments.

Inositol polyphosphate measurement

Q7 and Q111 cells were plated in 6-well dishes. After reaching 60% confluence, the cells were labeled with 200 μCi [^{3}H]inositol (Parkin Elmer) for three days. Soluble inositol phosphates were extracted using an acid lysis (0.6M perchloric acid and 2mM EDTA), neutralized with 1M K_2CO_3, and then centrifuged. 1mM EDTA was added to the supernatant. Following extraction, the inositol phosphates were resolved by anion-exchange HPLC as previously described (51). The soluble inositol phosphates were detected using a scintillation counter. IP_4, IP_5, and IP_6 levels were normalized to *myo*-inositol levels in each sample. n = 6 for all inositol phosphate quantitation experiments.

Cloning Strategy

The myc-tagged IPMK sequence was cloned into the pAAV-SYN-EGFP-T2A vector (provided by Vector Biolabs) (Figure 3.1A) and subsequently subcloned into the pAAV-E/SYN-WPRE vector (provided by Vector Biolabs) (Figure 3.1B). Primers containing the EcoRV and XbaI restriction sites in the 5' and 3' primers, respectively, were used to amplify IPMK (Table 3.3). Following EcoRV and XbaI digestion of the insert and the pAAV-SYN-EGFP-T2A vector, the insert was ligated downstream of the EGFP-T2A sequence (Figure 3.1A). The T2A linker is a self-cleaving peptide that enables separation of EGFP from IPMK; thus enabling visualization of cell transduction without altering IPMK function.

The E/SYN hybrid promoter consists of a 400-bp CMV enhancer (designated as E) and 450-bp human Synapsin I promoter fragment (SYN), which results in approximately 2-4

fold higher expression than the parental SYN promoter. In fact, the pAAV-SYN-EGFP-T2A vector takes about four weeks to express when injected in mouse brain, whereas the pAAV-E/SYN-WPRE vector requires about two weeks for expression post-injection (data not shown). Therefore, the EGFP-T2A-IPMK sequence was subcloned into the pAAV-E/SYN-WPRE vector using the NheI and AgeI restriction sites (Figure 3.1B). Correct insertion of IPMK was verified at all stages of cloning using the IPMK forward and reverse sequencing primers (Table 3.3). The E/SYN forward, EGFP forward and WPRE reverse sequencing primers confirmed correct insertion of the EGFP-T2A-IPMK sequence in the final vector. Vector Biolabs generated the adeno-associated virus serotype 2 (AAV2) expressing the gene of interest.

Figure 3.1. AAV vector cloning strategy

(Figure on following page)

(A) IPMK was inserted within the multiple cloning site of pAAV-SYN-EGFP-T2A using the EcoRV and XbaI restriction enzyme sites. (B) EGFP and IPMK were subcloned into a second vector, pAAV-E/SYN-WPRE, using the NheI and AgeI restriction enzyme sites.

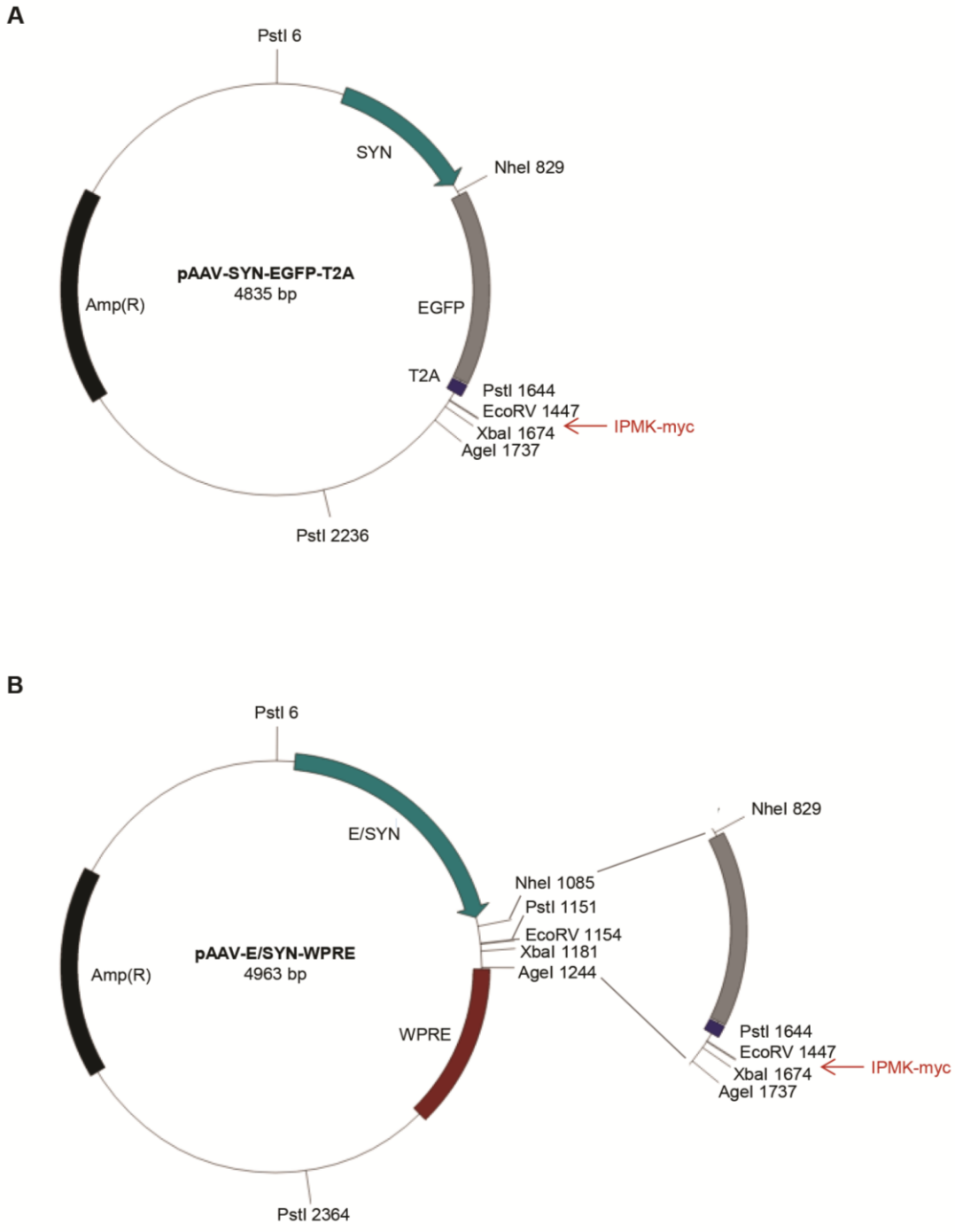

Figure 3.1. AAV vector cloning strategy

(Figure legend on previous page)

Table 3.3. PCR primers and sequencing primers

Primer	*Sequence*
PCR primers	
IPMKmyc-EcoRV	AAATTTGATATCCAATGGCATCAATGCAGAAGCTGATCT
IPMKmyc-XbaI	AAATTTTCTAGATCAACTGTCTAAAATACTCCG
Sequencing primers	
IPMK forward	CCTGGCCCAAGATCTGAAT
IPMK reverse	AGACCGAGGAGAGGGTTAGG
E/SYN forward	ACTCAGCGCTGCCTCAG
WPRE reverse	AGCAATAGCATGATACAAAGGCA
EGFP forward	CAT GGTCCTGCTGGAGTTCGTG

Stereotaxic Surgery

AAV2 containing either a control empty vector or IPMK were generated by Vector BioLabs at a titer of $3.1x10^{12}$ GC/ml. IPMK is expressed downstream of an E/SYN promoter and an EGFP cassette followed by a T2A linker. EGFP is cleaved from IPMK once the proteins are expressed. Three-week-old male mice were anesthetized using 300 µl avertin (20 mg/ml solution). The zero coordinates were set at Bregma. Two holes were drilled and the virus was delivered using a Hamilton syringe with a 33-gauge blunt-tip needle bilaterally. The needle was lowered at a rate of 1 mm/min into the striatum (anterior (A) -0.8, lateral (L) 2, ventral (V) -3.7), pulled back to (A -0.8, L 2, V -3.5), and left in place for 2 min. One µl virus was injected at this site and three additional sites along the Z-axis (A -0.8, L 2, V -3.3), (A -0.8, L 2, V -3.1), (A -0.8, L 2, V -2.9) for a total of 4 µl virus in each striatum. After the last injection and 2-min hold, the needle was raised up 0.2 mm and left in place for 5 min. The needle was then withdrawn at 0.5 mm/min.

Immunofluorescence and immunohistochemistry

Male mice, which received AAV2 injections, were anesthetized with 100 mg/kg pentobarbital and perfused transcardially with 4% paraformaldehyde (PFA) at 5 weeks and 13 weeks of age. Brains were extracted, post-fixed overnight in 4% PFA, and cryo-protected in 30% sucrose. 40-µm thick free-floating sections were harvested with a microtome. EM48 (Millipore) and glial fibrillary acidic protein (GFAP) (Abcam) immunohistochemistry were detected using ABC vectastain (Vector Labs). The number and size of aggregates were quantified using ImageJ. Nissl staining was performed using

a previously described standard protocol (179). For immunofluorescence, the sections were mounted with ProLong Gold Antifade reagent with DAPI (Life Technologies) and visualized using a Zeiss LSM 510 confocal microscope.

Behavior assays

Animals were tested at 6, 8, and 10 weeks of age, except gait analysis, which was performed at 10 weeks of age only. Only male animals were used unless otherwise indicated. All behavior assays were performed blind to virus treatment. For body weights for IPMK down-regulation studies, n = 8 for wild type, n = 7 for IPMK Het, n = 6 for R6/2, and n = 5 for R6/2;IPMK Het animals. Male and female animals were included for survival: n = 18 for wild type, n = 11 for IPMK Het, n = 13 for R6/2, and n = 12 for R6/2;IPMK Het. For body weight in IPMK overexpression studies, n = 10 (wild type with control virus), n = 9 (wild type with IPMK virus), n = 17 (R6/2 with control virus), and n = 13 (R6/2 with IPMK virus). For survival, n = 10 (wild type with control virus), n = 11 (wild type with IPMK virus), n = 11 (R6/2 with control virus), and n = 11 (R6/2 with IPMK virus).

Open field

Locomotor activity was assessed during the wake cycle using open field activity chambers with infrared photo beams (San Diego Instruments). Data was collected over 1 h following a 30-min acclimatization period. Horizontal and vertical activities were automatically recorded as beam breaks. For open field, n = 9 (wild type with control

virus), n = 10 (wild type with IPMK virus), n = 11 (R6/2 with control virus), and n = 12 (R6/2 with IPMK virus). These tests were performed in the dark.

Balance beam and rotarod

Motor coordination and balance was assessed using rotarod and the balance beam task. For rotarod, mice were trained for 10 min at constant speed. An accelerating protocol was then used and repeated three times at each time point. For rotarod, n = 7 (wild type with control virus), n = 10 (wild type with IPMK virus), n = 11 (R6/2 with control virus), and n = 9 (R6/2 with IPMK virus). For the balance beam task, the time to traverse a 60 cm long wooden rod (50 cm above ground) away from a light source was recorded. Three measurments were taken for each animal. n = 7 (wild type with control virus), n = 10 (wild type with IPMK virus), n = 9 (R6/2 with control virus), and n = 9 (R6/2 with IPMK virus). The balance beam tests were performed in the dark. For IPMK down-regulation rotarod studies, n = 7 for wild type, n = 7 for IPMK Het, n = 5 for R6/2, and n = 5 for R6/2;IPMK Het.

Composite score

Mice were evaluated for hindlimb clasping, ledge walking, kyphosis, and gait to obtain a composite phenotype score (180). A score of three is given for the worst performance in each category (for a maximum total score of 12). The wild type mice received a perfect score of 0. n = 9 (wild type with control virus), n = 9 (wild type with IPMK virus), n = 10 (R6/2 with control virus), and n = 9 (R6/2 with IPMK virus).

Gait analysis

Gait analysis was performed using the footprint test. Hindpaws and forepaws were painted with blue and red, respectively. Animals walked on paper lining the floor of an elongated box starting from a light source at one end to a dark box at the other end. Three stride length measurements were taken for each animal. n = 6 (wild type with control virus), n = 9 (wild type with IPMK virus), n = 10 (R6/2 with control virus), and n = 7 (R6/2 with IPMK virus).

Statistical analysis

Statistical analysis was performed using Excel software (Analysis ToolPak). Student's t-test and single-factor ANOVA were performed. All error bars represent ± SEM. Significance was determined as $p < 0.05$.

3.3 Results

3.3.1 IPMK protein is depleted in HD striatum

A useful model of HD is the striatal progenitor cell line with 111 glutamine repeats ST*Hdh*$^{Q111/Q111}$ (Q111 or Q111/Q111) and the control cell line with 7 glutamine repeats ST*Hdh*$^{Q7/Q7}$ (Q7 or Q7/Q7) (181). IPMK protein is depleted by 75% in Q111 cells (Figure 3.2A). A similar loss of IPMK is also detected in ST*Hdh*$^{Q7/Q111}$ (Q7/Q111) heterozygous cells suggesting that one allele of mHtt is sufficient to deplete IPMK protein levels (Figure 3.2B). The deficit in IPMK expression appears to reflect, at least in part, defective transcription, as IPMK mRNA levels are reduced by 40% in Q111 cells (Figure 3.2C).

We next sought to determine whether the catalytic products of IPMK are altered in this cell model of HD. IPMK produces the soluble inositol phosphates IP_4 and IP_5, which are both depleted in Q111 cells by 75% and 85%, respectively (Figure 3.3A and Figure 3.3B). IP_5 production is entirely dependent on IPMK activity whereas IP_4 and PIP_3 can also be produced by IP_3K and the p110 PI3K, respectively. Thus, the reduction in IP_5 production is consistent with the loss of IPMK protein in Q111 cells. The IP_4 peak contains Ins(1,3,4,5)P_4 and Ins(1,4,5,6)P_4. Ins(1,3,4,5)P_4 is generated by IPMK, as well as IP_3K, which could account for the lower decrease in IP_4 levels relative to the reduction in IP_5 levels. The levels of inositol hexakisphosphate (IP_6), the catalytic product of

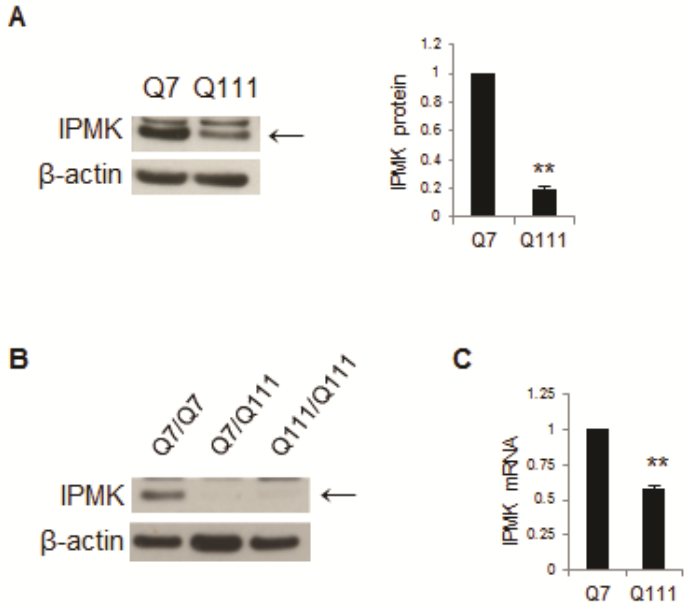

Figure 3.2. Loss of IPMK protein and mRNA in a cellular model of HD.

(A) IPMK protein levels are decreased in Q111 cells. Bars represent means ± SEM normalized to β-actin (n=3). **p<0.01 relative to Q7 cells. (B) IPMK protein levels are similarly decreased in Q7/Q111 cells. (C) IPMK mRNA levels are reduced in Q111 cells. Bars represent means ± SEM normalized to β-actin mRNA (n=3). **p<0.01 relative to Q7 cells.

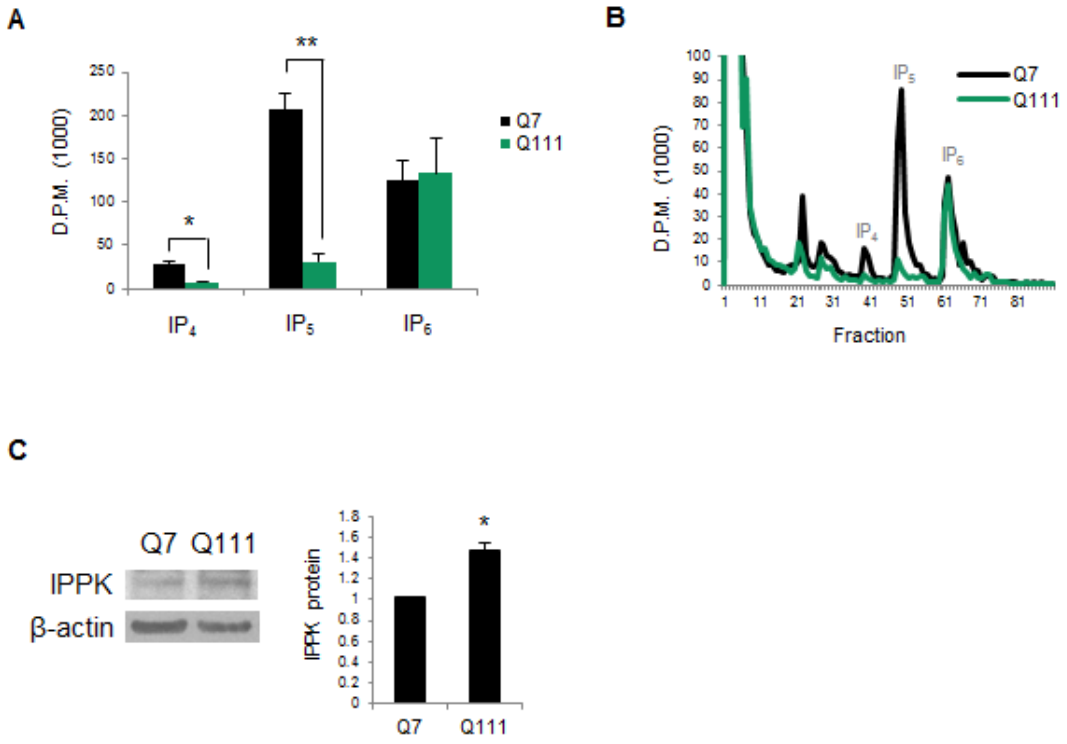

Figure 3.3. Inositol polyphosphate production in a cellular model of HD.

(A) IP_4 and IP_5 levels are depleted in Q111 cells while IP_6 levels remain normal. Bars represent means ± SEM disintegrations per min (D.P.M.) normalized to *myo*-inositol levels (n=6). *p<0.05 and **p<0.01 relative to Q7 controls. (B) Representative raw scintillation data showing D.P.M. per fraction. The IP_4, IP_5, and IP_6 peaks are indicated. (C) IPPK levels are elevated in Q111 cells. Bars represent means ± SEM normalized to β-actin (n=3). *p<0.05 relative to Q7 control.

IPPK, are unaltered. This is likely due to the 45% increase in IPPK protein expression in Q111 cells (Figure 3.3C).

The R6/2 transgenic murine model of HD involves about 150 glutamine repeats (168). We examined IPMK levels in the striatum of R6/2 mice, as this portion of the brain is most prominently affected in HD (182). Striatal IPMK protein levels are reduced about 65% in R6/2 striatum at 13 weeks of age (Figure 3.4A). The R6/2 mice are already symptomatic by 13 weeks. A similar loss is detected in the cortex and hippocampus of R6/2 mice, but not in the cerebellum, which remains largely unaffected in HD (Figure 3.4B). The zQ175 knock-in model of HD (170) displays a similar decrease in IPMK protein expression in the striatum (Figure 3.4C). Since the zQ175 model is a more slowly-progressing model of HD relative to the R6/2 model, changes in IPMK protein levels are not detectable until 12 months of age.

The IPMK antibody detects an undetermined band with an approximate molecular weight of 49 kDa. Interestingly, the expression of this unknown protein appears to be decreased in the cortex, hippocampus, and cortex of R6/2 animals, while remaining stable in the cerebellum (Figure 3.4A and Figure 3.4B).

Most importantly, IPMK levels are diminished by 75% in post-mortem HD striatal tissues relative to control (Figure 3.5). IPMK protein was similarly altered in stage III and stage IV HD striatal tissue.

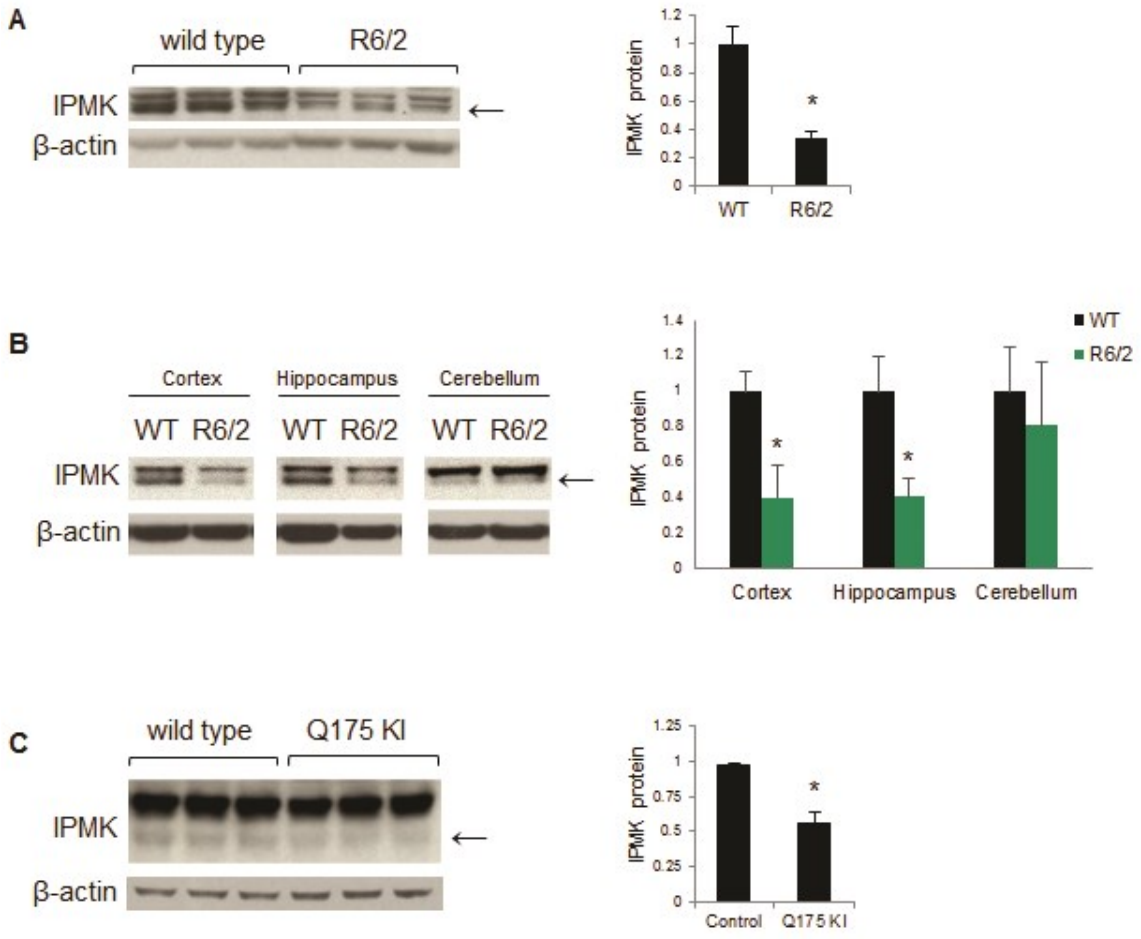

Figure 3.4. IPMK protein levels are reduced in murine models of HD

(A) 13-week-old R6/2 striatal samples contain less IPMK than littermate controls. Bars represent means ± SEM normalized to β-actin (n=3). *$p<0.05$ relative to wild type. (B) IPMK protein levels are depleted in the cortex and hippocampus of R6/2 mice, but not the cerebellum. Bars represent means ± SEM normalized to β-actin (n=4). *$p<0.05$ relative to wild type control. (C) IPMK levels are also decreased in the zQ175 knock-in mouse model of HD at 12 months of age. Bars represent means ± SEM normalized to β-actin (n=3). *$p<0.05$ relative to wild type control.

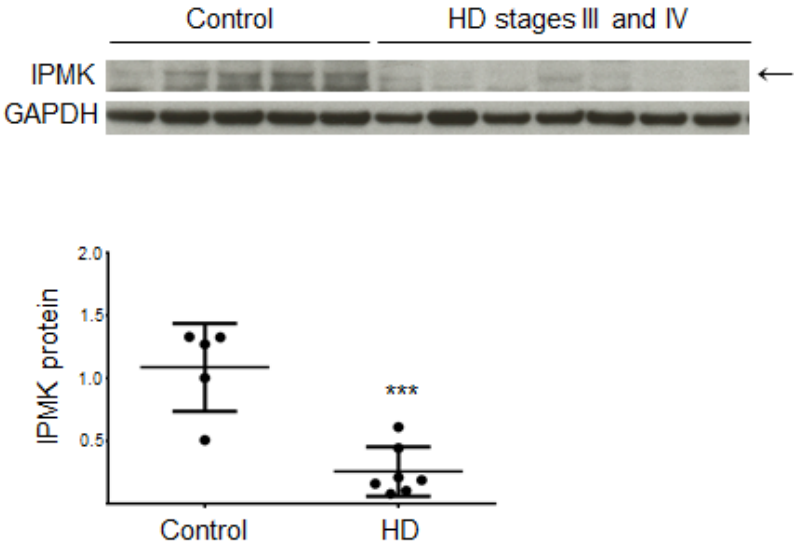

Figure 3.5. IPMK protein levels are decreased in post-mortem HD striatal tissues. IPMK protein is decreased in post-mortem HD striatum. The arrow points to the upper band. Bars represent means ± SEM normalized to GAPDH (n=5 for control group and n=7 for HD stages III and IV group). ***$p<0.001$ relative to normal control.

3.3.2 Regulation of IPMK at the transcriptional level

IPMK protein levels are significantly decreased in HD. Therefore, we sought to elucidate the molecular mechanisms regulating IPMK at the transcript and protein levels. The striatal-enriched protein Ctip2 was recently revealed as a putative transcription factor for IPMK (66). Accordingly, we explored its relevance to HD. We confirm the loss of Ctip2 in R6/2 striatum (Figure 3.6A). We also detect a similar decrease in the cortex and hippocampus of R6/2 mice, but not the cerebellum, which does not express Ctip2 (Figure 3.6B). These results are consistent with previous reports describing altered expression of Ctip2 in the R6/1 model of HD, as well as in HD patients (113).

We next sought to confirm whether Ctip2 is in fact a transcriptional regulator for IPMK. Depletion of Ctip2 in Q7 cells using 100 pmol Ctip2 siRNA for 96 h reduces IPMK levels by about 60% (Figure 3.7A). Due to the low baseline levels of IPMK in the Q111 cells, we were unable to detect the effect of Ctip2 down-regulation on IPMK expression in these cells (data not shown). Conversely, overexpression of Ctip2 for 48 h reverses the loss of IPMK protein in Q111 cells, restoring them to normal values, but does not alter IPMK levels in Q7 cells (Figure 3.7B). Interestingly, we also observed a similar increase in the 49-kDa unknown protein when overexpressing Ctip2 in Q111 cells. These experiments involving the down-regulation and up-regulation of Ctip2 in Q7 and Q111 cells are consistent with its role as a transcription factor for IPMK. Thus, IPMK depletion in this cellular model of HD occurs in part at the transcriptional level through Ctip2.

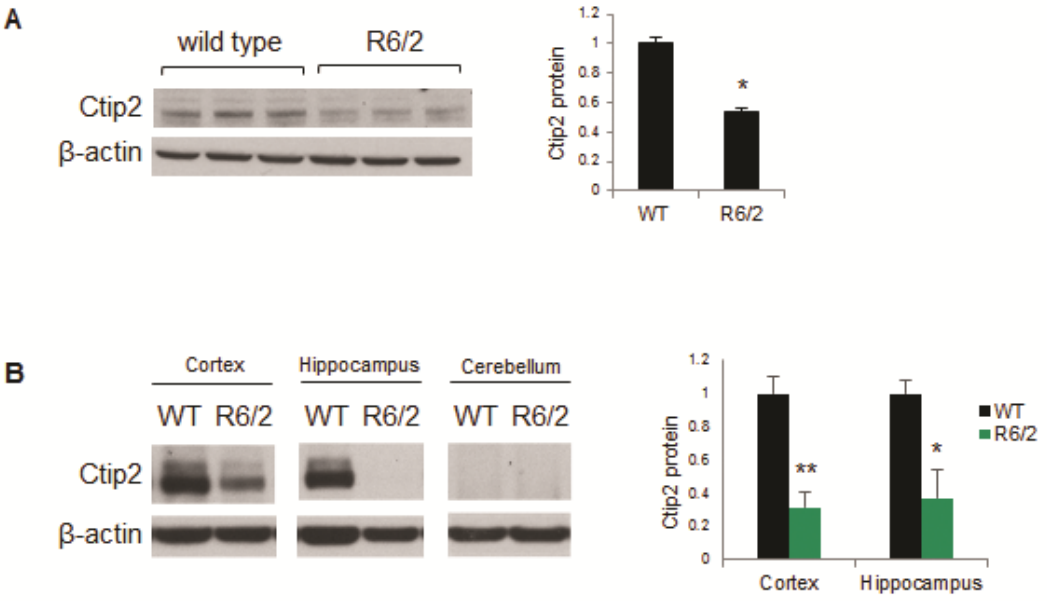

Figure 3.6. Transcription factor Ctip2 is depleted in HD

(A) Ctip2 protein levels are reduced in the R6/2 striatum relative to wild type (WT) mice. Bars represent means ± SEM normalized to β-actin (n=3). *p<0.05 relative to wild type. (B) Ctip2 protein levels are also reduced in the cortex and hippocampus of R6/2 mice. Ctip2 is not expressed in the cerebellum. Bars represent means ± SEM normalized to β-actin (n=3). *p<0.05 and **p<0.01 relative to wild type control.

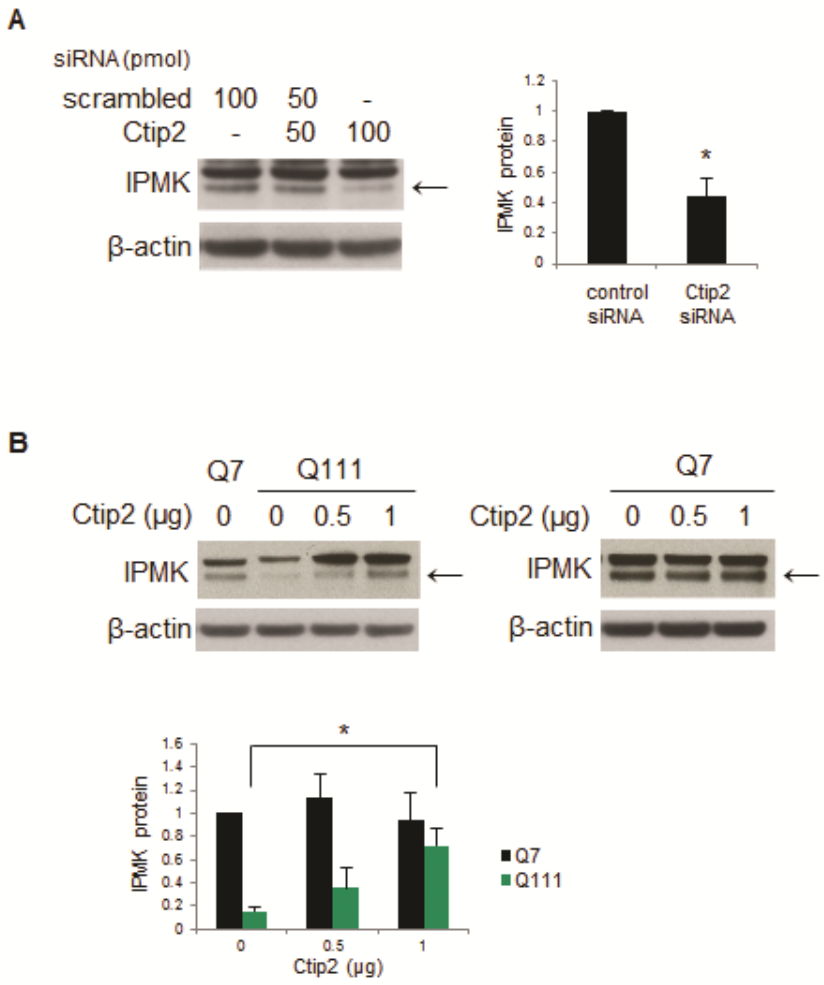

Figure 3.7. Ctip2 regulates IPMK expression

(A) Ctip2 knock-down resulted in decreased IPMK expression. Bars represent means ± SEM normalized to β-actin (n=3). *p<0.05 relative to scrambled siRNA control. (B) Overexpression of Ctip2 in Q7 and Q111 cells rescues IPMK protein levels. Bars represent means ± SEM normalized to β-actin (n=3). *p<0.05 relative to Q111 empty vector control.

Negative feedback regulation is a common feature of signaling pathways and is required to maintain the pathway at homeostatic levels. Since Ctip2 overexpression did not alter IPMK levels in Q7 cells, we wondered whether feedback inhibition is also involved in the Ctip2/IPMK signaling pathway. Ctip2 expression is upregulated by approximately 40% in the striatum of Nestin-cre; $IPMK^{fl/fl}$ animals compared to $IPMK^{fl/fl}$ controls (Figure 3.8A). This suggests that IPMK or other downstream components of this pathway, or other transcriptional targets of Ctip2 inhibit Ctip2 expression. Therefore, it is possible that proteins involved in the negative feedback regulation of the pathway act directly by altering Ctip2 expression and/or activity. When overexpressed in HEK293 cells, Ctip2 co-immunoprecipitates with IPMK (Figure 3.8B). These preliminary data suggest a potential role for IPMK as a negative feedback regulator of Ctip2. Furthermore, since Ctip2 is known to regulate several hundred proteins (66), IPMK might also indirectly be an important player in maintaining cellular homeostasis.

Thus far we describe the transcriptional regulation of IPMK by Ctip2. Furthermore, preliminary evidence suggests a role for IPMK in the negative feedback regulation of Ctip2 signaling.

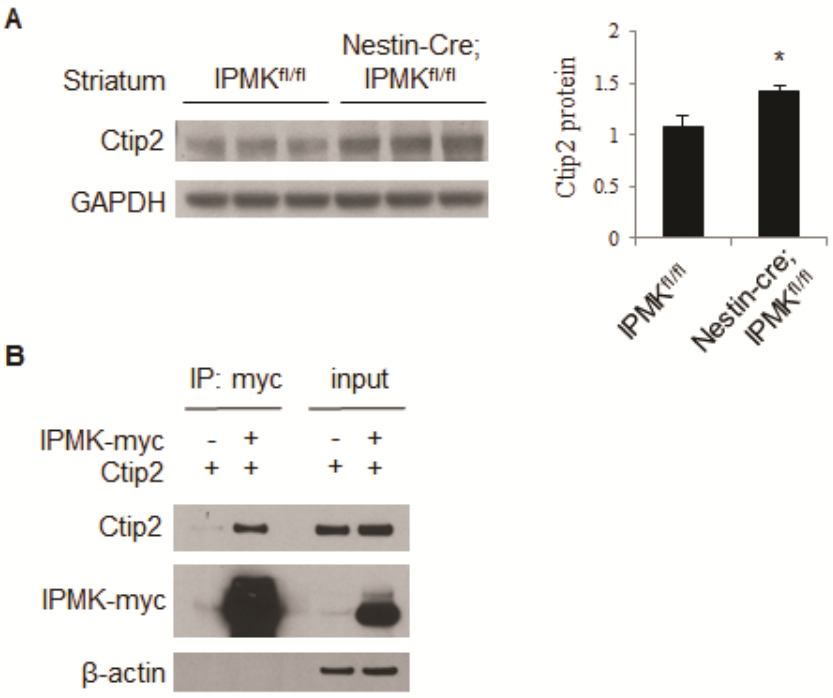

Figure 3.8. Role of IPMK in the negative feedback regulation of Ctip2.

(A) Ctip2 protein levels are elevated in adult Nestin-Cre; $IPMK^{fl/fl}$ striatum relative to $IPMK^{fl/fl}$ control mice. Bars represent means ± SEM normalized to GAPDH (n=3). *$p<0.05$ relative to control. (B) Co-immunoprecipitation assay of HEK293 cells transfected with plasmids expressing myc-tagged human IPMK and Ctip2. IPMK binds Ctip2.

3.3.3 Regulation of IPMK at the protein level

Since the depletion of IPMK protein in Q111 cells is substantially greater than the loss of IPMK mRNA, we investigated whether HD is associated with alterations in IPMK protein stability. We monitored the turnover of IPMK by examining its rate of depletion following inhibition of protein synthesis with cycloheximide (Figure 3.9). In Q7 cells, cycloheximide treatment requires about 8 h to secure 45% depletion. By contrast, 4 h after cycloheximide administration, IPMK protein levels in Q111 cells are reduced about 80%. The calculated half-life for IPMK turnover in Q7 cells is 8.9 h, which is reduced to 2 h in Q111 cells.

There are two main protein degradation pathways: the ubiquitin-proteasome system and the lysosomal degradation pathway (124). We sought to determine whether these pathways contribute to altered IPMK protein stability and/or reduced IPMK expression in HD. Impairing the proteasomal degradation pathway using MG132 does not alter IPMK protein levels in Q7 and Q111 cells (Figure 3.10A). By contrast, inhibition of the lysosomal degradation pathway using bafilomycin rescues IPMK protein levels in Q111 cells (Figure 3.10B). Thus, IPMK depletion in Q111 cells is associated with decreased protein stability involving lysosomal degradation as well as diminished IPMK transcription.

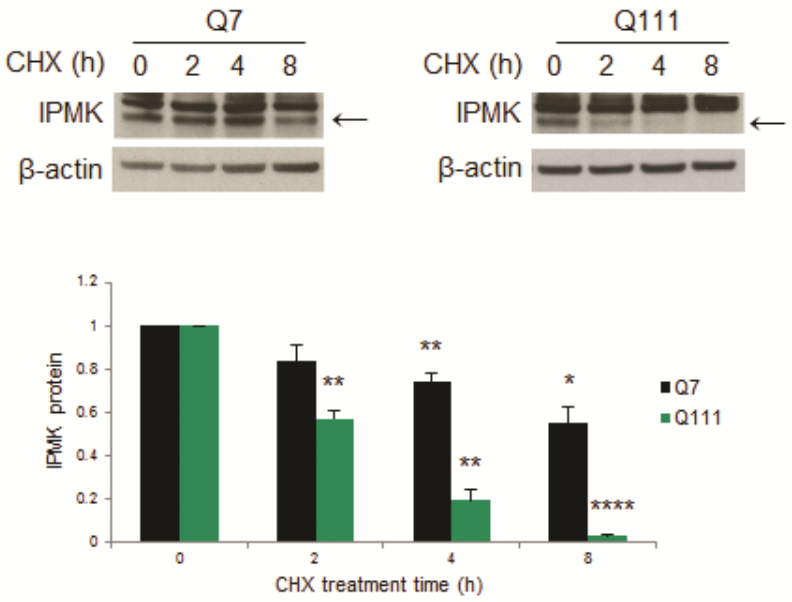

Figure 3.9. IPMK protein stability is altered in a cellular model of HD

IPMK protein levels in Q7 and Q111 cells following treatment with translational inhibitor cycloheximide (CHX). Bars represent means ± SEM normalized to β-actin or GAPDH (n=4). For Q7 cells, **p<0.01 and *p<0.05 relative to the Q7 0-h CHX treatment control. For Q111 cells, **p<0.01 and ****p<0.0001 relative to the Q111 0-h CHX control.

Figure 3.10. Lysosomal protein degradation contributes to altered IPMK protein levels in HD

(Figure on following page)

(A) Treatment of Q7 and Q111 cells with proteasomal inhibitor MG132 did not alter IPMK protein expression. Bars represent means ± SEM normalized to β-actin (n=3). *$p<0.05$ and **$p<0.01$ relative to Q7 control. (B) Bafilomycin (Baf), an inhibitor of lysosomal degradation, restores IPMK protein levels in the Q111 cells without altering IPMK protein levels in the Q7 cells. Bars represent means ± SEM normalized to β-actin (n=3). *$p<0.05$ relative to Q111 empty vector control.

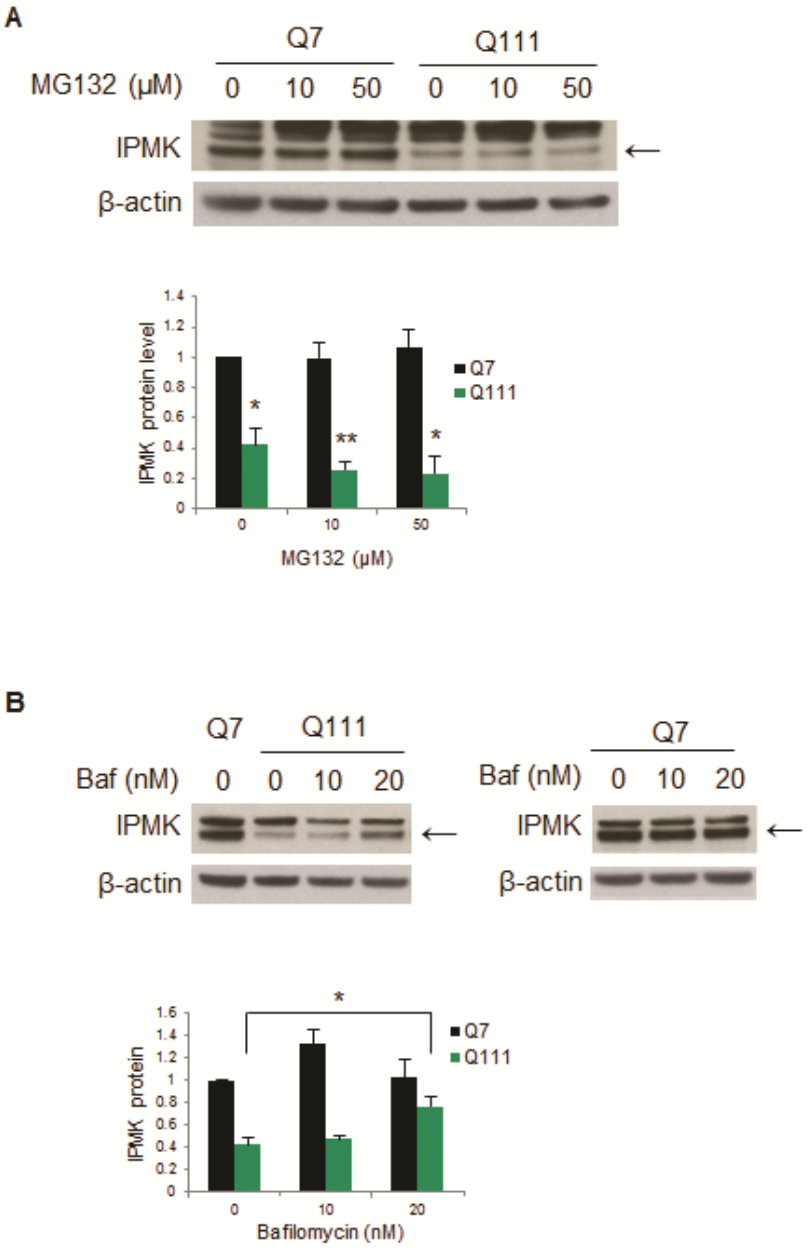

Figure 3.10. Lysosomal protein degradation contributes to altered IPMK protein levels in HD

(Figure legend on previous page)

One potential mechanism for depleting IPMK might involve mHtt binding IPMK and increasing turnover. We examined this possibility by monitoring binding between the two proteins in a HEK293 overexpression model (Figure 3.11A). IPMK binds robustly to the N-terminal fragment of mHtt (N171-82Q) but not to wild type Htt (N171-18Q). Mapping experiments indicate that binding to mHtt is determined predominantly by the N-terminal portion of IPMK, as IPMK fragments 1-124 and 1-209 bind robustly to mHtt, while fragments 125-416 and 210-416 bind very little (Figure 3.11B). These results are summarized along with the other binding partners of IPMK in Figure 3.11C.

Figure 3.11. IPMK binds selectively to mHtt

(Figure on following page)

(A) Co-immunoprecipitation assay of HEK293 cells transfected with plasmids expressing myc-tagged human IPMK and the N-terminal fragment of either wild type Htt (Htt-flag) or mHtt (mHtt-flag). IPMK binds selectively to the N-terminal fragment of mHtt and not wild type Htt. (B) N-terminal fragments (1-124 and 1-209) and C-terminal fragments (125-416 and 210-416) of human IPMK were overexpressed with the N-terminal fragment of mHtt (mHtt-flag) in HEK293 cells. Co-immunoprecipitation assays indicate that the N-terminal fragments of IPMK bind mHtt. (C) Diagram of IPMK demonstrating the positions of the fragments and their interactions with binding partners of IPMK. The key domains for inositol binding (IP), ATP binding (ATP), and catalytic activity (Ser-Ser-Leu-Leu or SSLL), as well as nuclear localization signal (NLS) are shown.

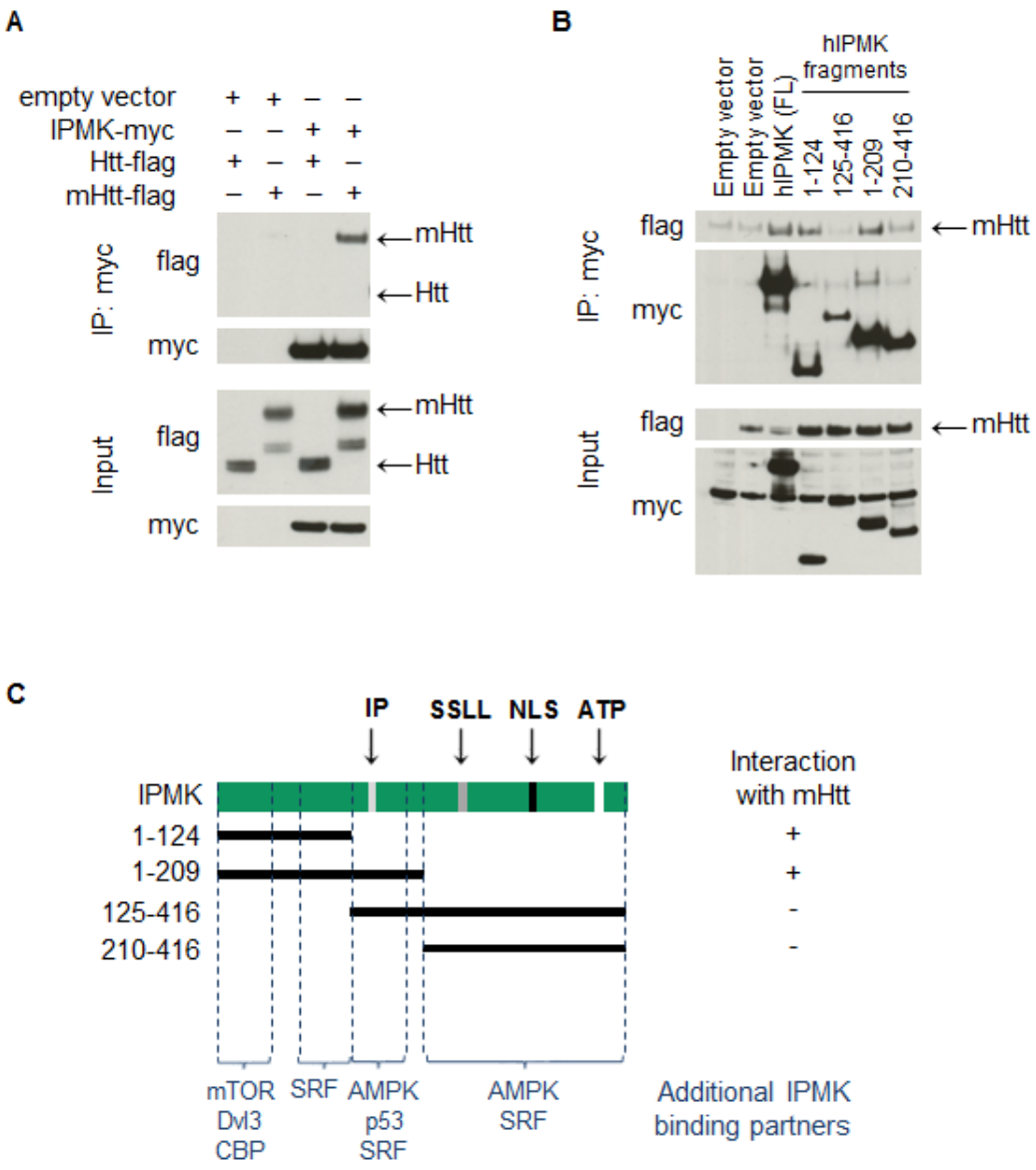

Figure 3.11. IPMK binds selectively to mHtt

(Figure legend on previous page)

3.3.4 Role of IPMK in neuronal dysfunction

IPMK has both pro-survival and pro-apoptotic effects due to the myriad of downstream signaling targets, which differ based on the cellular context. We wondered whether the depletion of IPMK in HD contributes to the pathophysiology and behavioral phenotypes in HD. If this were the case, then restoring the depleted IPMK should be beneficial. We assessed mitochondrial metabolic activity of cells by the MTT assay (Figure 3.12A). Metabolic activity of Q111 cells is only half that of Q7 cells (183). Overexpressing IPMK alleviates this abnormality (Figure 3.12A).

IPMK possesses inositol phosphate kinase and PI3-kinase activities, and also displays various non-catalytic actions (7, 10, 11, 51, 184). To ascertain which of these activities mediates the beneficial effects of IPMK, we overexpressed IPMK K129A-S235A (IPMK-KASA), which is devoid of both inositol phosphate kinase and PI3-kinase activities. We also overexpressed the *Arabidobsis thaliana* ortholog, atIPK2β, which possesses inositol phosphate kinase but not PI3-kinase activity and has been shown to restore inositol phosphate production in IPMK null MEFs (7). Neither IPMK-KASA nor atIPK2β rescue the depressed metabolic activity of Q111 cells (Figure 3.12B). The lack of activity of IPMK-KASA indicates that catalytic activity of IPMK is required for rescue. The inactivity of atIPK2β suggests that PI3-kinase activity of IPMK is responsible for restoring the metabolic activity of Q111 cells.

Figure 3.12. The lipid kinase activity of IPMK rescues the mitochondrial metabolic activity deficit in a cellular model of HD

(Figure on following page)

(A) Q7 and Q111 cells were transfected with 1 or 2 μg mouse IPMK plasmid. IPMK rescues the mitochondrial metabolic activity deficit in Q111 cells as measured by the MTT assay. Bars represent means ± SEM (n=6 for Q7 and Q111 empty vector controls and n=4 for IPMK overexpression groups). *$p<0.05$ and ****$p<0.0001$ relative to the Q7 empty vector control. **$p<0.01$ relative to the Q111 empty vector control. (B) The IPMK activity required to rescue the metabolic activity deficit in Q111 cells was identified. Q7 and Q111 cells were transfected with either wild type IPMK, which displays non-catalytic and catalytic activities, the kinase-dead mutant of IPMK (IPMK-KASA), which lacks both PI3-kinase and soluble inositol phosphate kinase activities, or atIPK2β, which displays only soluble kinase activity. Neither IPMK-KASA nor atIPK2β rescued the metabolic activity deficit as measured by the MTT assay. Bars represent means ± SEM (n=4). *$p<0.05$ and **$p<0.01$ relative to the Q7 empty vector control (unless otherwise indicated).

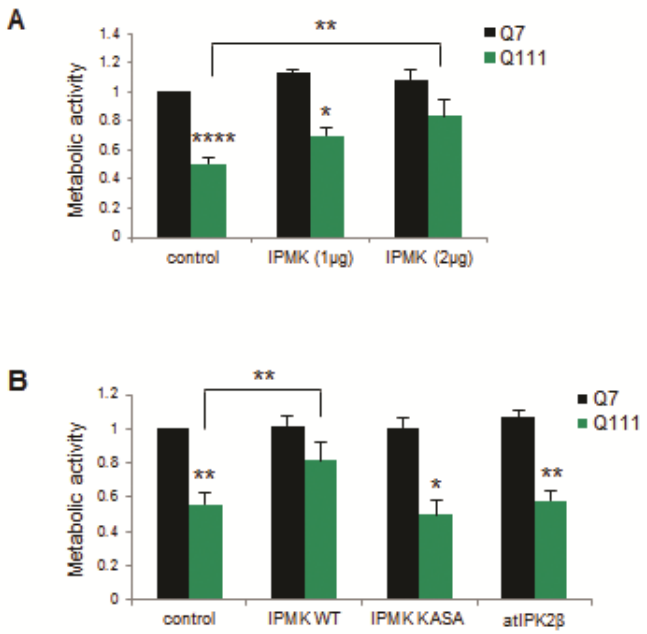

Figure 3.12. The lipid kinase activity of IPMK rescues the mitochondrial metabolic activity deficit in a cellular model of HD

(Figure legend on previous page)

The PI3-kinase activity of IPMK generates PIP_3, which is indirectly visualized using a GFP-tagged Akt pleckstrin homology domain construct (Akt-PH-GFP). In general, GFP fluorescence localizes to the membrane in the presence of PIP_3 and remains diffuse in the cytoplasm in the absence of PIP_3. In Q7 cells, Akt-PH-GFP is localized to the cell membrane, indicating the presence of PIP_3 (Figure 3.13A). In Q111 cells, Akt-PH-GFP expression is diffuse throughout the cytoplasm, but localizes to the cell membrane upon over-expression of IPMK, consistent with increased PIP_3 production (Figure 3.13B).

PIP_3 physiologically activates Akt protein kinase. Akt signaling deficits have previously been described in HD striatum and lymphoblasts (185). We observe a 70% - 80% depletion of phospho-Akt levels in Q111 cells at the T308 and S473 sites (Figure 3.14A and Figure 3.14B). The loss of phospho-Akt at both sites is reversed by overexpressing IPMK in Q111 cells (Figure 3.15A and Figure 3.15B).

The loss of IPMK is pathogenic as assessed by mitochondrial metabolic activity in a cellular model of HD. Restoring IPMK rescues the metabolic activity deficit in a lipid kinase activity-dependent manner. This is consistent with the significant improvement in Akt signaling downstream of increased PIP_3 production.

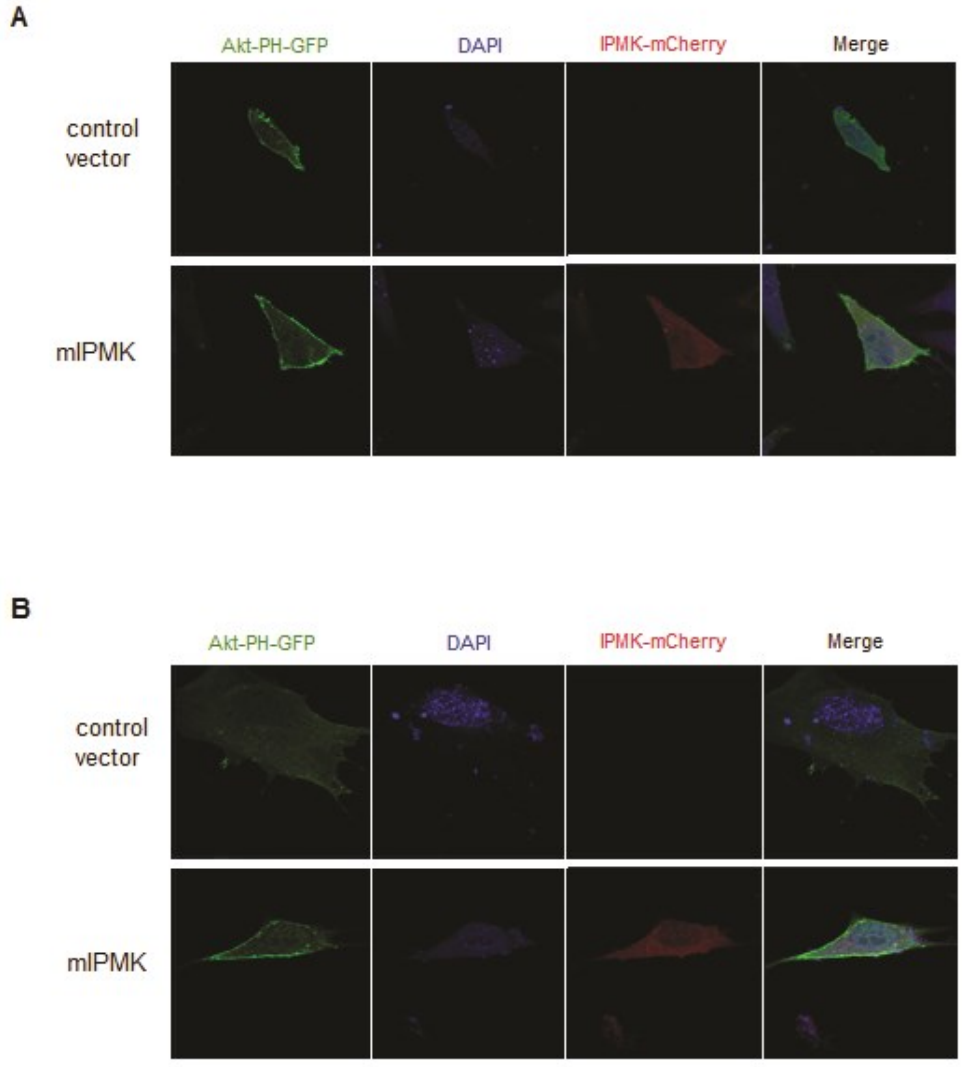

Figure 3.13. IPMK rescues Akt-PH-GFP localization in a cellular model of HD

(A) Q7 cells were transfected with Akt-PH-GFP and either a control vector or IPMK-mCherry. Akt-PH-GFP is localized to the cell membrane with or without IPMK-mCherry. Localization to the cell membrane appears to increase in the presence of IPMK-mCherry. (B) Q111 cells were transfected with Akt-PH-GFP and either a control vector or IPMK-mCherry. In the presence of IPMK-mCherry, Akt-PH-GFP localizes to the cell membrane.

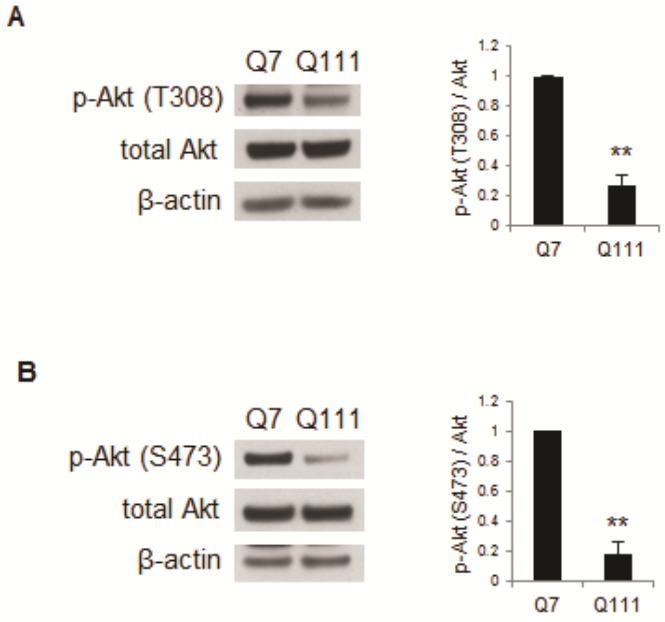

Figure 3.14. Akt signaling is altered in a cellular model of HD

(A) Akt phosphorylation at the T308 site [p-Akt (T308)] is decreased in Q111 cells. Bars represent means ± SEM normalized to total Akt (n=3). **p<0.01 relative to the Q7 control. (B) Akt phosphorylation at the S473 site [p-Akt (S473)] is also decreased in Q111 cells. Bars represent means ± SEM normalized to total Akt (n=3). **p<0.01 relative to the Q7 control.

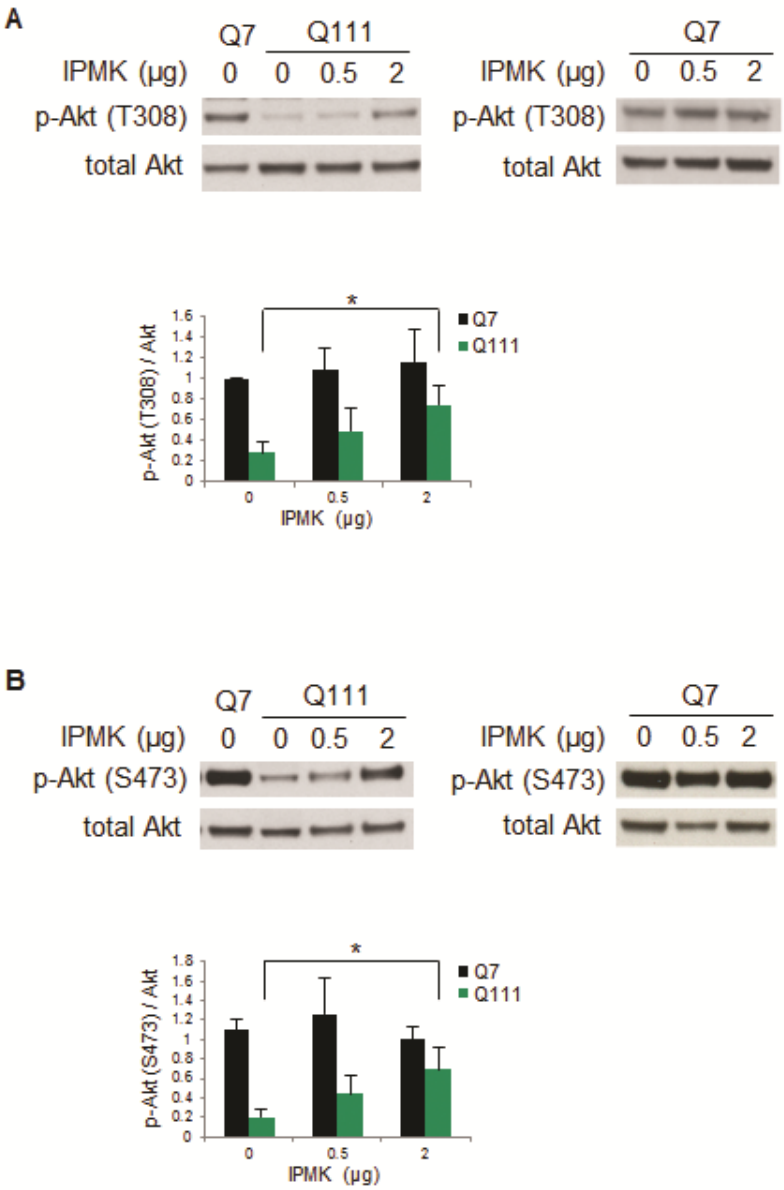

Figure 3.15. Akt signaling deficit in a cellular model of HD is rescued by IPMK

(A) IPMK overexpression rescues the loss of p-Akt (T308). Bars represent means ± SEM normalized to total Akt (n=4). *$p<0.05$ relative to the Q111 empty vector control sample. (B) IPMK overexpression rescues the loss of p-Akt (S473). Bars represent means ± SEM normalized to total Akt (n=4). *$p<0.05$ relative to the Q111 empty vector control sample.

3.3.5 Effect of IPMK down-regulation on HD phenotype *in vivo*

IPMK is protective in the cellular model of HD. Thus, we hypothesized that either down-regulating or over-expressing IPMK in an animal model of HD would worsen or reverse the behavioral phenotype, respectively. Since IPMK gene knockout is embryonic lethal in mice (42), the R6/2 mice (also referred to as HD mice) were crossed with IPMK Het mice to study the effect of IPMK down-regulation on HD behavioral phenotype. Despite the smaller litter size, all four possible genotypes from the R6/2 and IPMK Het breeding pairs (wild type, HD, IPMK Het, and HD;IPMK Het) were observed in equal Mendelian ratios (Table 3.4). Male and female F1 mice were born in equal numbers. The R6/2 transgenic mouse model of HD is one of the most severe models of the disease. These animals display early and rapid deficits in locomotor activity, motor coordination, and general habitus, which become more pronounced as the disease progresses. Onset of motor symptoms occurs at approximately five to eight weeks of age depending on the behavioral test selected.

HD and HD;IPMK Het animals demonstrate a similar decline in body weight and survival (Figure 3.16A and Figure 3.16B). Furthermore, the loss of one allele of IPMK does not further impair rotarod performance (Figure 3.17) or open field activity (data not shown). Since IPMK Het mice do not exhibit an overt phenotype but IPMK knockout animals are embryonic lethal, IPMK is likely happlosufficient. Furthermore, the severity of the R6/2 phenotype may obscure the effect of the loss of only one allele of IPMK.

Table 3.4. Genotype ratio of R6/2 and IPMK heterozygous crossing

	WT	***HD***	***IPMK Het***	***HD;IPMK Het***	***total***
Male	8	6	7	5	26
Female	10	7	4	7	28
total	18	13	11	12	54

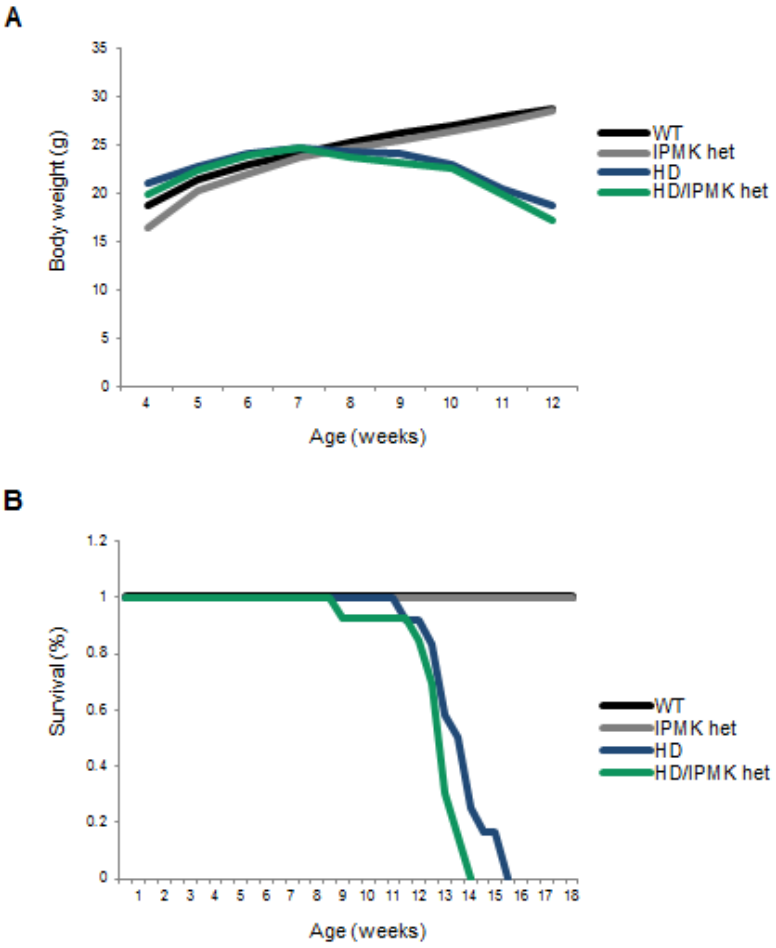

Figure 3.16. Weight and survival of F1 generation from R6/2 and IPMK Het pair

(A) R6/2 and R6/2;IPMK Het animals show a similar and gradual decrease in body weight over time. IPMK Het mice display a normal weight gain comparable to WT animals (n=8 for wild type, n=7 for IPMK Het, n=6 for R6/2, n=5 for R6/2;IPMK Het). (B) The Kaplan-Meier curve indicates that the loss of one allele of IPMK in R6/2 animals does not significantly alter survival compared to R6/2 mice. Both male and female animals were included in similar ratios for the survival curve (n=18 for wild type, n=11 for IPMK Het, n=13 for R6/2, n=12 for R6/2;IPMK Het).

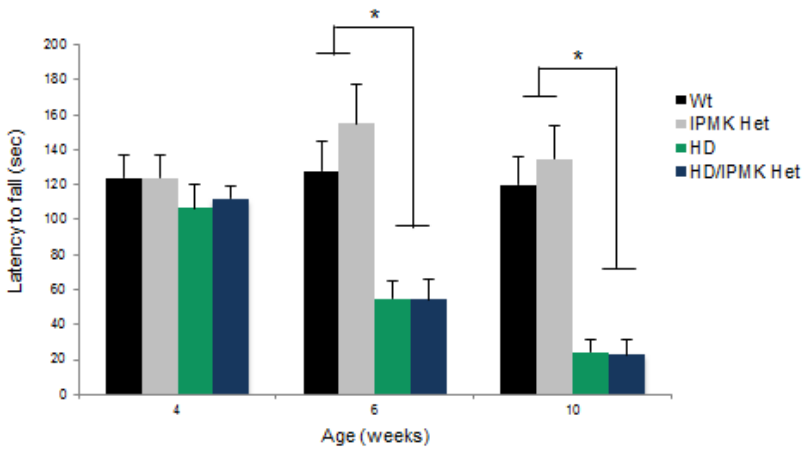

Figure 3.17. Loss of allele of IPMK does not alter R6/2 rotarod performance

R6/2 and R6/2;IPMK Het animals display similar deficits on rotarod testing. IPMK Het rotarod performance is comparable to wild type animal (n=7 for wild type, n=7 for IPMK Het, n=5 for R6/2, n=5 for R6/2;IPMK Het). *$p<0.05$ relative to wild type mice or IPMK Het mice.

3.3.6 Effect of IPMK delivery on HD phenotype *in vivo*

We next investigated the effects of IPMK overexpression on striatal pathology and behavioral phenotype of R6/2 mice. Direct administration of IPMK-expressing AAV2 in the striatum of R6/2 mice covers almost half of the striatal area (Figure 3.18A) at two weeks post-injection. We confirmed robust expression of IPMK in the striatum 10 weeks post-injection (Figure 3.18B). Interestingly, the expression of the unknown 49-kDa band is also elevated in tissues obtained from animals receiving the IPMK virus. The intrastriatal injections were performed at 3 weeks of age. Behavioral phenotypes were assessed at 6, 8, and 10 weeks of age. Striatal pathology was studied at 10 weeks (Figure 3.18C).

Although no effects were observed on weight and survival (Figure 3.19A and Figure 3.19B), viral overexpression of IPMK in the striatum of R6/2 mice reduced the number of EM48-positive mHtt aggregates by approximately 75% at 10 weeks of age (Figure 3.20A and Figure 3.20B). Furthermore, the size of these aggregates also decreased by about 30% (Figures 3.20C). No changes in aggregate number or size were observed in the cortex, which did not receive IPMK (Figure 3.20D).

HD striatal pathology also includes a decline in the size of MSN (186). Thus, Nissl staining was used to assess neuronal size. IPMK overexpression in wild type animals did not affect MSN size (Figure 3.21A) whereas IPMK delivery in R6/2 mice appears to increase the cross-sectional area of MSNs relative to control R6/2 MSNs (Figure 3.21B).

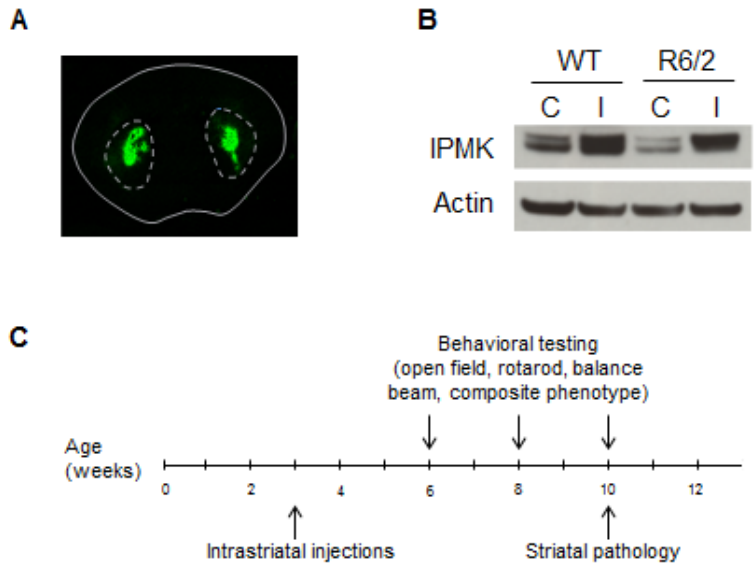

Figure 3.18. AAV2-mediated delivery of IPMK in striatum of R6/2 animals

(A) Coronal section of mouse brain demonstrating intrastriatal virus expression two weeks post-injection. (B) Striatal tissue obtained from R6/2 mice 10 weeks post-injection with either GFP control AAV2 (denoted C) or IPMK-expressing AAV2 (denoted I) confirm increased IPMK expression in wild type and R6/2 animals receiving IPMK-expressing AAV2. (C) Intrastriatal injections were performed at 3 weeks followed by behavior testing at 6, 8, and 10 weeks of age. Pathology was assessed at 10 weeks.

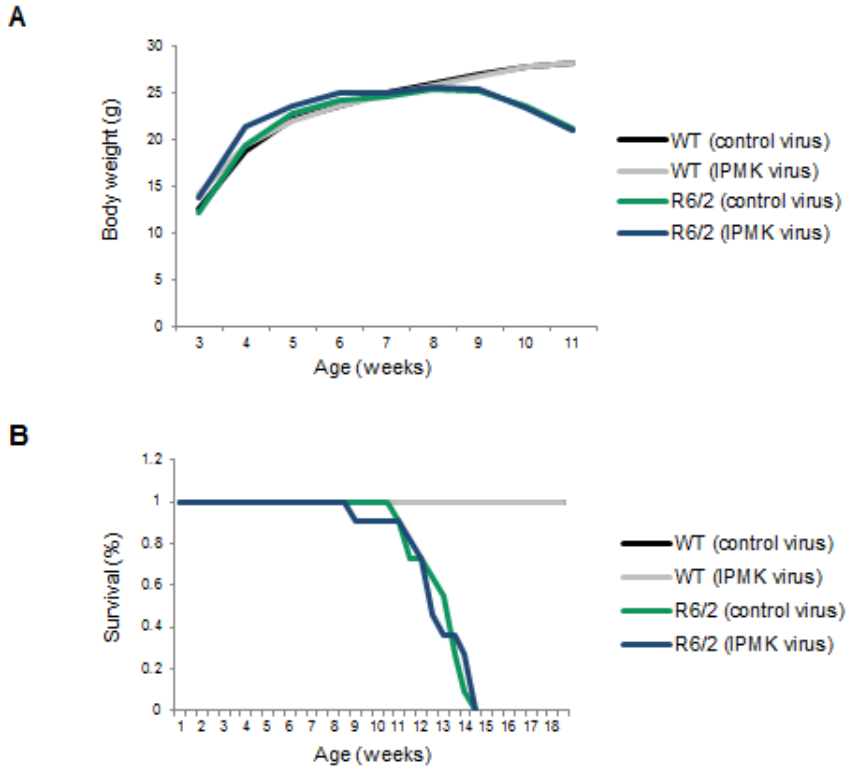

Figure 3.19. IPMK overexpression does not affect body weight and survival of R6/2 animals

(A) R6/2 mice injected with either control or IPMK virus show a similar and gradual decrease in weight over time. IPMK overexpression did not affect wild type (WT) mice. (n=10 for wild type with control virus, n=9 for wild type with IPMK virus, n=17 for R6/2 with control virus, and n=13 for R6/2 with IPMK virus). (B) The Kaplan-Meier curve indicates that striatal overexpression of IPMK did not alter survival in wild type or R6/2 mice (n=10 for wild type with control virus, n=11 for wild type with IPMK virus, n=11 for R6/2 with control virus, n=11 for R6/2 with IPMK virus).

Figure 3.20. Effect of IPMK on EM48-positive aggregates

(Figure on following page)

(A) EM48-positive mHtt aggregates are present in R6/2 striatum and absent in wild type striatum. Virus-mediated over-expression of IPMK reduces the number and the size of mHtt aggregates. Scale bar represents 50 μm. (B) Quantitation of number of mHtt aggregates per 40x field of view measuring 0.1 mm^2. Bars represent mean number of aggregates ± SEM (n=3 animals). **$p<0.01$ relative to the number of R6/2 control aggregates. (C) Quantitation of size of mHtt aggregates based on cross-sectional area of aggregates. Bars represent mean size of aggregates ± SEM (n=3 animals). *$p<0.05$ relative to the size of aggregates in R6/2 control sections. (D) EM48-positive mHtt aggregates are also evident in R6/2 cortex and used as a negative control. No changes in aggregate number or size were detected due to the striatal localization of the injections.

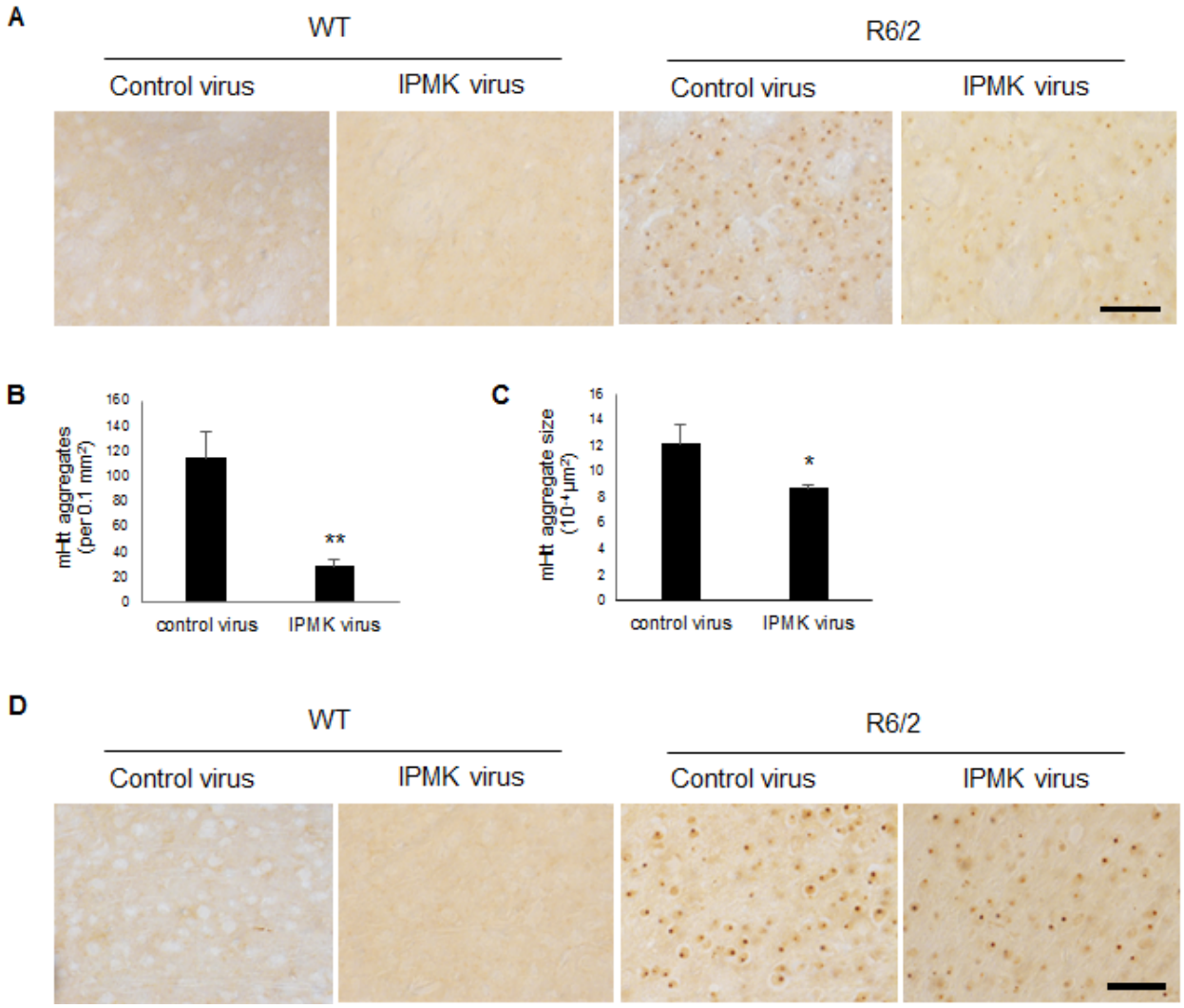

Figure 3.20. Effect of IPMK on EM48-positive aggregates

(Figure legend on previous page)

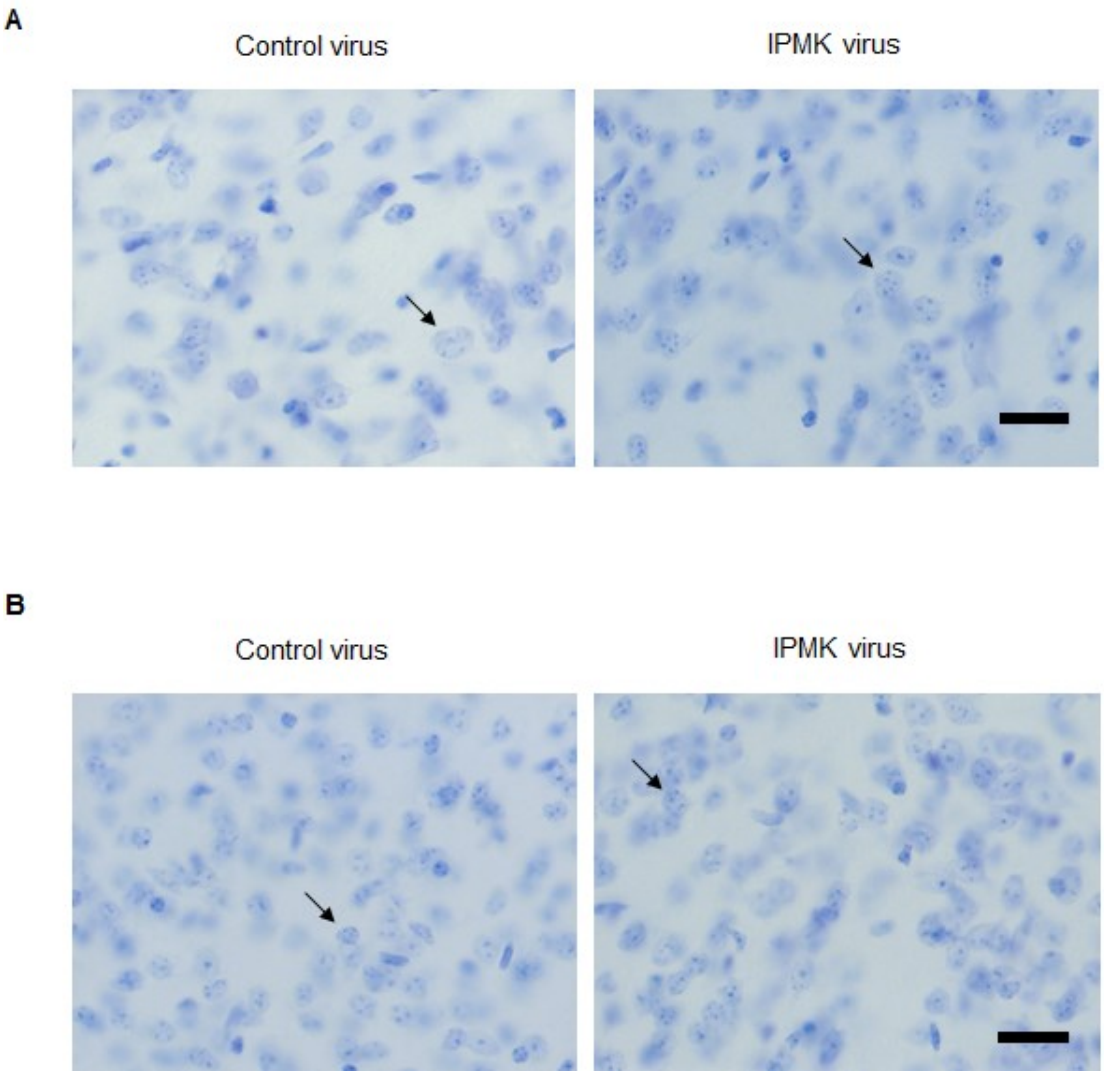

Figure 3.21. IPMK delivery improves medium spiny neuron size

(A) Overexpression of IPMK in wild type animals does not alter the size of MSNs as visualized by Nissl staining. Scale bar represents 20 µm. (n=3 animals per group). (B) MSNs in R6/2 animals appear smaller in size compared to wild type MSNs as detected by Nissl staining. IPMK overexpression in R6/2 animals appears to rescue MSN size. Scale bar represents 50 µm (n=3 animals per group).

Changes in reactive astrocytes measured by GFAP immunoreactivity was also investigated. Little reactive astrocytosis is present in wild type striatum (Figure 3.22) and most was associated with the injection tract. There is evidence of mild astrogliosis in R6/2 striatum as previously reported (187). However, IPMK delivery did not affect astrogliosis (Figure 3.22). Due to AAV2-mediated delivery, only neurons expressed IPMK. Thus, IPMK might not influence astrocyte function in these *in vivo* studies.

The pathological changes described correspond with the delay in motor deficits observed in R6/2 animals. Repletion of IPMK restores central locomotor activity of the R6/2 mice to levels that are not significantly lower than those of wild type mice at 6 weeks (Figure 3.23). However, IPMK overexpression does not significantly improve rotarod performance (Figure 3.24A) likely due to the earlier onset of this particular deficit. In a balance beam model, the time to cross is increased 8-fold in R6/2 mice compared to wild type animals (Figure 3.24B). This time is reduced by half in IPMK-replenished mice. We also evaluated a composite phenotype (180) of HD abnormalities, which consist of hindlimb clasping, gait abnormalities, kyphosis and ledge walking (Figure 3.25A). The composite phenotype score is reduced almost by half with IPMK repletion. This is consistent with improvement in gait, specifically stride length, in R6/2 mice receiving the IPMK-expressing virus (Figure 3.25B and Figure 3.25C). Furthermore, there is reduced forepaw-hindpaw print overlap in the R6/2 animals, which appears to improve with IPMK delivery (Figure 3.25C). We did not observe significant differences in balance beam and composite score in R6/2 animals relative to wild type mice prior to 10 weeks of age.

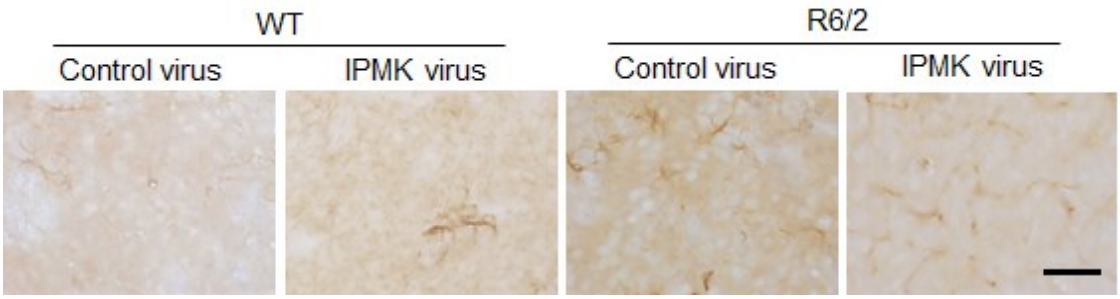

Figure 3.22. IPMK does not alter reactive astrocytosis

GFAP staining confirms the absence of reactive astrocytes in wild type tissue with or without IPMK over-expression. Mild astrocytosis is observed in R6/2 animals and is not affected by neuron-specifc AAV2-mediated IPMK delivery. Scale bar represents 50 μm (n=3 animals per group).

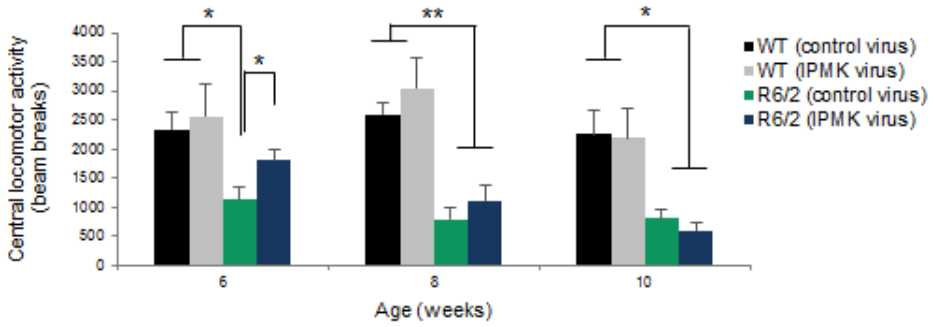

Figure 3.23. Virus-mediated expression of IPMK delays open field deficits

IPMK overexpression delays impairment of central locomotor activity. Bars represent means ± SEM beam breaks (n=9-12 animals per group). *p<0.05 and **p<0.01 relative to either wild type or R6/2 mice injected with control virus.

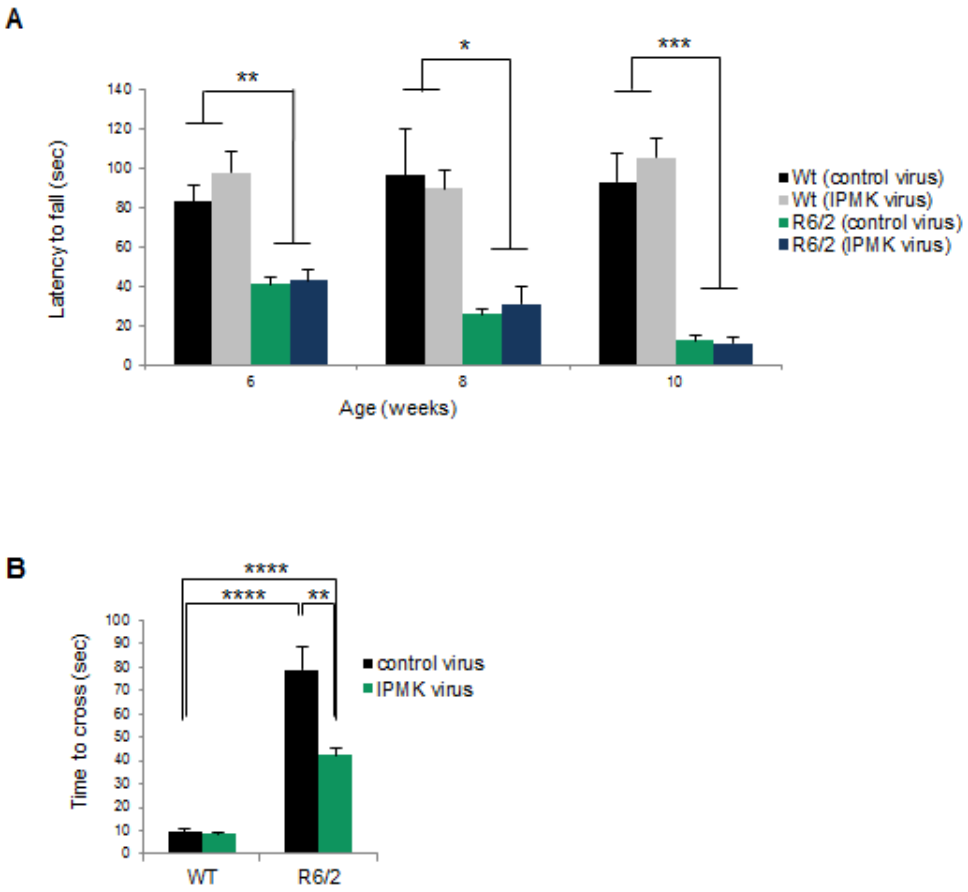

Figure 3.24. Virus-mediated delivery of IPMK improves motor coordination impaired in late disease stage

(A) IPMK overexpression does not affect rotarod performance at 6, 8, and 10 weeks of age. Bars represent means ± SEM time to fall in seconds (n=7-11 animals per group). *p<0.05, **p<0.01 and ***p<0.001 relative to wild type mice injected with either control or IPMK virus. (B) IPMK restores motor coordination and balance assessed by balance beam performance. Bars represent means ± SEM total time to cross beam (n=7-10 animals per group). **p<0.01 and ****p<0.0001 relative to either wild type or R6/2 mice injected with control virus.

Figure 3.25. Virus-mediated delivery of IPMK improves gait and general phenotype

(Figure on following page)

(A) General phenotype based on clasping, kyphosis, gait, and ledge walking are presented as a composite score, which is improved by IPMK overexpression. Bars represent means ± SEM (n=9-10 animals per group). *$p<0.05$ relative to R6/2 mice receiving control virus. (B) IPMK overexpression improves R6/2 animal gait, specifically stride length at 10 weeks of age. Bars represent means ± SEM stride length in centimeters (cm) (n=6-10 animals per group). *$p<0.05$, **$p<0.01$ and ****$p<0.0001$ relative to wild type mice or R6/2 mice injected with control virus as indicated. (C) Representative footprint test results with forepaws and hindpaws indicated in red and blue, respectively.

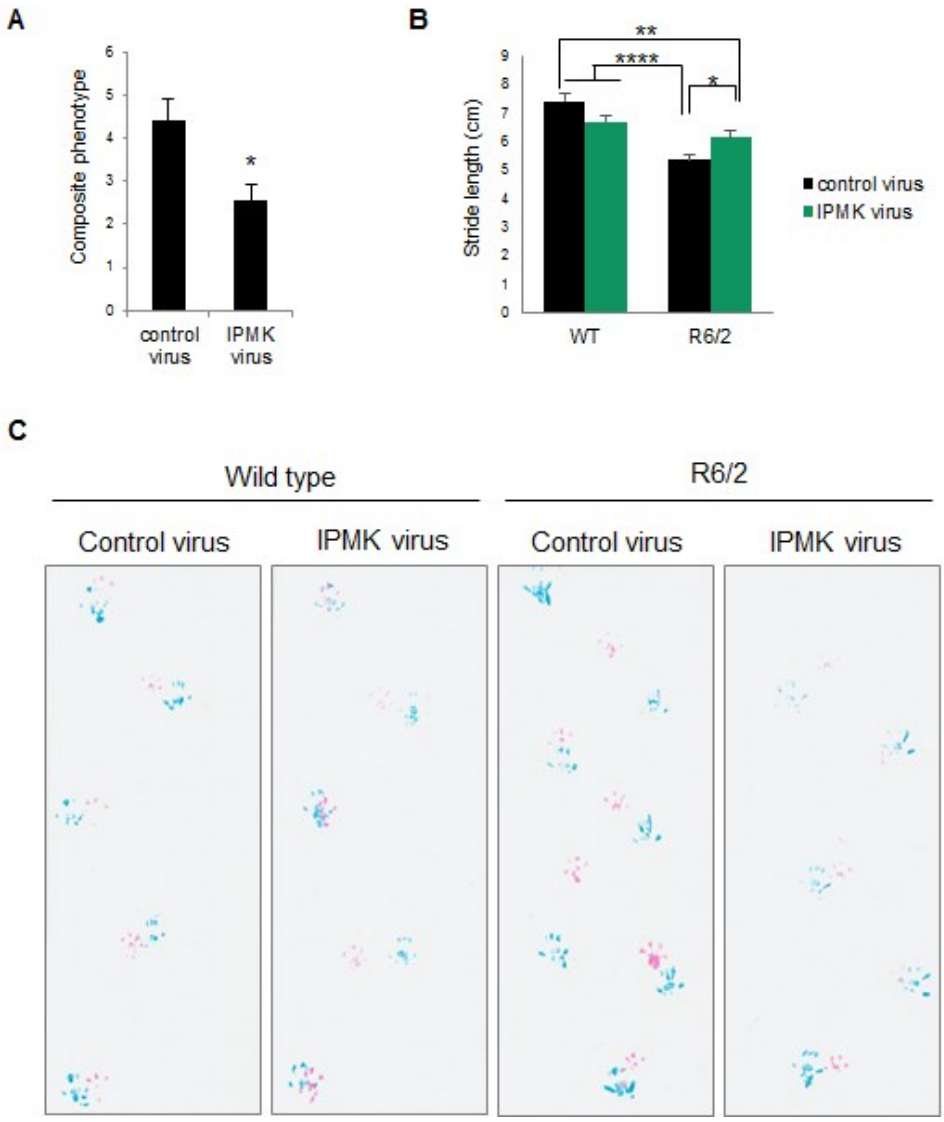

Figure 3.25. Virus-mediated delivery of IPMK improves gait and general phenotype

(Figure legend on previous page)

3.4 Discussion

In the present study we report a dramatic depletion of IPMK in post-mortem HD striatal tissues, as well as in Q111 HD cells and the R6/2 and zQ175 murine models of HD. The depletion of IPMK occurs at both transcriptional and protein stability levels and corresponds with decreased Akt signaling. IPMK depletion appears to mediate, at least in part, the pathology and motor deficits in HD. Viral expression of IPMK in the striatum of R6/2 mice, the brain region primarily affected in clinical HD, delays locomotor deficits of the animals and reduces the number and size of aggregates.

The striatal-enriched transcription factor Ctip2 appears to determine IPMK transcription. Its overexpression reverses the IPMK depletion in Q111 cells. Ctip2 protein itself is also selectively expressed in striatal medium spiny neurons (151), the cell type uniquely lost in HD (182). The depletion of Ctip2 in the striatum, cortex and hippocampus of R6/2 mice is consistent with the altered expression pattern of IPMK in these mice. Interestingly, Ctip2 overexpression in Q7 cells does not change IPMK protein levels suggesting a potential negative feedback effect of IPMK or other targets on Ctip2 expression and/or transcriptional activity. This is further supported by the increased expression of Ctip2 in conditional IPMK knockout animals.

Altered IPMK protein stability and lysosomal degradation also contribute to the loss of IPMK protein in the cellular model of HD. Although macroautophagy and the ubiquitin proteasome system are both impaired in HD, chaperone-mediated autophagy is

constitutively up-regulated in early stages of the disease, thereby increasing the turnover of both wild type Htt and mHtt fragments (128). The selective interaction of IPMK with the N-terminal fragment of mHtt might explain the loss of IPMK through lysosomal degradation in Q111 cells but not Q7 cells.

We provide several lines of evidence that the depletion of IPMK is pathogenic in HD. Overexpressing IPMK restores to normal the depressed mitochondrial metabolic activity of Q111 cells, an action that appears to be determined by the PI3-kinase activity of IPMK. IPMK and the p110 PI3-kinase act coordinately in generating PIP_3 (7), a classic stimulant of Akt (188). Phospho-Akt depletion in Q111 cells is rescued by overexpressing IPMK. Overexpression of constitutively active Akt is sufficient to rescue pathologic phenotypes, such as the formation of nuclear inclusions, in primary rat brain cultures expressing mHtt (101). Akt also regulates inclusions indirectly by phosphorylating other proteins such as the ADP-ribosylation factor-interacting protein arfaptin2, which rescues mHtt-induced proteasomal impairment and decreases neuronal intranuclear inclusions (189). Compensatory mechanisms have been shown to target Akt and increase its activation during early stages of HD. Decreased levels of PH domain leucine-rich repeat protein phosphatase 1 (PHLPP1), a phosphatase that targets the S473 site of Akt, contribute to enhancement of Akt phosphorylation at early stages of HD (190).

Akt also rescues additional cellular deficits caused by mHtt. mHtt is phosphorylated by Akt at the S421 site, which restores fast axonal transport by altering the mHtt interaction

with dynactin (191). Conversely, excitotoxic stimulation of NMDA receptors reduces mHtt S421 phosphorylation (192). mHtt increases the mitochondrial susceptibility to Ca^{2+}-induced mitochondrial depolarization (193). In healthy cells, these depolarized mitochondria are targeted for autophagy by parkin, in a process that requires hexokinase 2 (HK2) (194). Akt, which is known to promote cell survival, phosphorylates HK2 at the T473 residue thereby increasing HK2 association with mitochondria (195). Impaired Akt signaling in HD could thus be affecting mitophagy thereby contributing to mitochondrial dysfunction.

As the R6/2 animals used in this study express the N-terminal fragment of mHtt, rather than full-length mHtt, the observed effects of IPMK likely do not require direct phosphorylation of mHtt by Akt. Thus, through the multiple downstream effects of Akt, including arfaptin2, IPMK deficits may account for the notably pleiotropic manifestations of HD. The lipid kinase activity of IPMK may have additional functions in the context of HD. IPMK is required for mRNA export of specific transcripts such as the recombinase Rad51, which is associated with double-stranded DNA break repair (56). DNA repair responses to genotoxic stress are impaired in HD (196, 197).

Several signaling pathways implicated in HD converge on Akt. The BDNF pathway is altered in HD due to decreased transcription and release of BDNF at the corticostriatal synapses (141, 198), as well as impaired TrkB receptor signaling (143). Augmenting this pathway may be beneficial, as TrkB agonists extend survival in murine models of HD (199). Similarly, synaptic, but not extrasynaptic, NMDA receptors enhance Akt

phosphorylation and neuroprotection (200). More recently, the CB_1 cannabinoid receptor, which is highly expressed in MSNs, was found to exert neuroprotective effects through the activation of the PI3K/Akt pathway. Viral-mediated over-expression of CB_1 rescued pathological deficits in R6/2 mice (201).

Intrastriatal delivery of IPMK in R6/2 mice similarly improved neuropathological and motor deficits in the R6/2 model of HD. IPMK overexpression had the greatest effects on balance beam performance and gait. The motor deficits assessed using these tests appear during later symptomatic stages (after 8.5 weeks of age) in R6/2 animals (169). IPMK overexpression resulted in moderate to no effects on open field and rotarod testing, respectively, likely because the corresponding motor deficits occur at five weeks of age. Thus, earlier delivery of IPMK may have greater effects on the behavioral phenotype of these R6/2 animals. In addition to motor deficits, early clinical manifestations of HD include cognitive symptoms (72). IPMK regulates the induction of immediate early genes, required for learning, memory and behavior, as mice deleted for IPMK display aberrant spatial memory (11).

Altered histone modifications contribute to transcriptional dysregulation in HD. H3K4 trimethylation (H3K4me3) patterns in HD are rescued when expression of Jarid1c, an H3K4me3 demethylase, is reduced (202). Furthermore, HDAC4 knock-down restores deficient BDNF transcription in R6/2 mice (203), and the HDAC inhibitor, suberoylanilide hydroxamic acid, rescues motor deficits in R6/2 mice (174). HDAC complex formation requires IP_4 (37). Thus, the soluble inositol phosphate product of

IPMK enhances histone deacetylase activity. However, it is unclear how the lipid kinase and inositol phosphate kinase activities of IPMK are differentially regulated. *In vitro* competition assays indicate that the IPMK substrate PIP_2 competes successfully with IP_3 and IP_4 (51), which might be expected to favor the PI3-kinase activity of IPMK.

The inositol phosphate kinase activity of IPMK also generates IP_5, which inhibits the PH domain of Akt and subsequently impairs Akt signaling (24-27). Therefore, the inositol phosphate kinase activity of IPMK directly opposes the effects of its lipid kinase activity. Although the catalytic sites of IPMK may have higher affinity for PIP_2 compared to the inositol phosphates (51), it is necessary to study the molecular mechanisms that regulate the switch in the catalytic activities of IPMK.

Additional clinical features of HD include peripheral organ dysfunction such as weight loss, skeletal muscle wasting, as well as metabolic and endocrine alterations (75). IPMK influences metabolism by inhibiting AMPK activation (9). AMPK promotes catabolic pathways while inhibiting various anabolic pathways such as cholesterol and triglyceride synthesis (60). Interestingly, a pathologic increase in AMPK phosphorylation has been demonstrated in HD patients and in the R6/2 model (204). IPMK delivery in R6/2 animals did not improve body weight and survival, probably because IPMK was expressed only in the striatum. Conceivably, widespread expression of IPMK in HD models may improve peripheral organ dysfunction.

The circadian rhythm is also altered in HD (76). Microarray analysis of SRF-treated wild type and IPMK null MEFs indicate that period circadian clock 1 (Per1) is down-regulated in the absence of IPMK (62). Per1 acts in concert with several other core clock proteins to regulate circadian rhythm. Interestingly, AMPK is thought to transmit energy-dependent signals to the molecular clock by destabilizing Per proteins and cryptochrome (Cry) proteins (205). Furthermore, impaired function of other clock genes including brain and muscle Arnt-like protein 1 (Bmal1), circadian locomotor output cycles kaput (Clock), and neuronal PAS domain protein 2 (Npas2), have been implicated in neurodegeneration (206). The expression of the clock genes Per1, Per2, Cry2 and Bmal1 were not altered in the suprachiasmatic nucleus of conditional IPMK knockout animals (data not shown). Since SRF is an immediate early transcription factor responding to peripheral stimuli (207), further studies include investigating the effects of IPMK on clock gene expression in peripheral organs such as the liver. IPMK may be influencing aspects of circadian rhythm dysfunction in HD through SRF.

Several proteins, specifically mTOR, Dvl3, CBP, AMPK, and p53 have been shown to bind to specific exons of IPMK. The interaction of mHtt with the N-terminal fragment of IPMK might interfere with non-catalytic functions of IPMK that require this binding site, specifically mTOR, Dvl3, CBP, and SRF. The effect of mHtt on these pathways remains to be investigated.

The small G-protein Rhes sumoylates mHtt resulting in cytotoxicity (159), which is further enhanced through the interaction of Rhes and mHtt with acyl-CoA binding

domain containing 3 (ACBD3) (208). An *in vivo* screen for SUMO1 substrates demonstrated that Ctip2 is sumoylated (156). Perhaps Rhes also modulates the Ctip2-IPMK-Akt signaling pathway through the regulation of Ctip2 or IPMK.

Our findings suggest that the IPMK depletion in HD is pathogenic by dint of diminished PI3-kinase activity with less PIP_3 available to activate Akt. Approaches targeting the Ctip2-IPMK pathway may thus ameliorate neuronal dysfunction in HD.

3.5 Conclusion

Huntington's disease (HD) is a progressive neurodegenerative disorder mainly affecting the striatum. The striatal-enriched protein Ctip2 is depleted in HD and has been identified as a putative transcription factor for IPMK, a multi-functional enzyme with a soluble inositol phosphate kinase activity, a lipid kinase activity, and several non-catalytic activities including its role as a transcriptional co-activator.

The present study implicates the impairment of the Ctip2-IPMK-Akt signaling pathway in the pathophysiology of HD (Figure 3.26). IPMK is depleted in post-mortem HD striatal tissues and various cellular and animal models of the disease. The reduced levels of IPMK protein and mRNA result from mHtt-induced loss of expression and function of Ctip2, as well as decreased IPMK protein stability. Over-expression of IPMK rescues the mitochondrial metabolic activity deficit in a cell model of HD. This rescue requires the lipid kinase activity of IPMK, thereby involving the Akt signaling pathway. Consistent with the cellular data, over-expression of IPMK in the striatum improves the striatal pathology and psychomotor performance of a transgenic mouse model of HD.

Although our studies mainly focused on the role of IPMK in modulating Akt signaling in the striatum, this pleiotropic enzyme may also be involved in other aspects of HD pathogenesis, including mitochondrial deficits, impaired axonal transport, and peripheral organ dysfunction. Additional studies focusing on the other systemic effects of IPMK, as well as the mechanisms regulating IPMK activity, are required to better understand the

role of this multi-functional protein in the complex network of impaired pathways and cellular processes resulting in HD. The Ctip2-IPMK-Akt signaling pathway provides a novel therapeutic target and approach to enhancing Akt signaling in HD and potentially other neurodegenerative diseases.

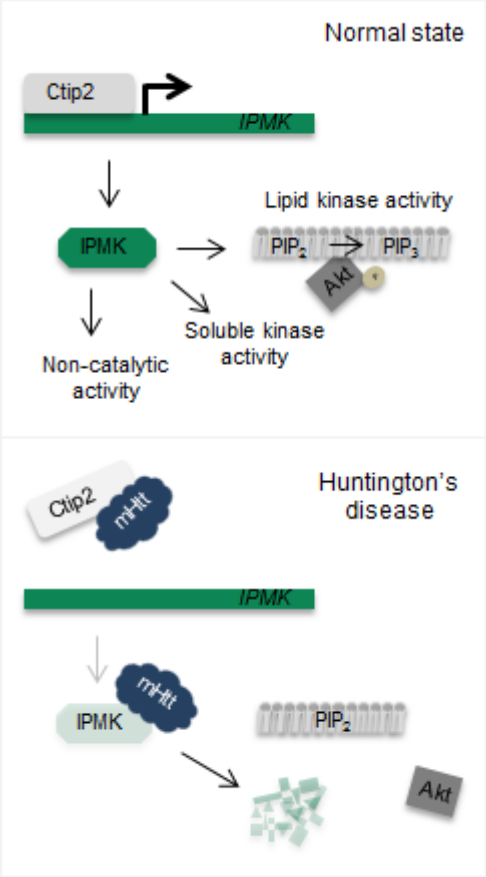

Figure 3.26. Summary of Ctip2-IPMK-Akt signaling pathway in HD

In normal striatal cells, Ctip2 induces IPMK. IPMK displays several functions including the lipid kinase activity, which enhances Akt signaling. In HD, Ctip2 transcriptional activity and expression is inhibited by mHtt resulting in decreased IPMK transcription. Decreased IPMK protein stability, likely caused by the selective interaction with mHtt, further reduces IPMK protein levels. This results in the loss of Akt phosphorylation.

3.6 References

1. Irvine RF & Schell MJ (2001) Back in the water: the return of the inositol phosphates. *Nat Rev Mol Cell Biol* 2(5):327-338.
2. Nalaskowski MM, Deschermeier C, Fanick W, & Mayr GW (2002) The human homologue of yeast ArgRIII protein is an inositol phosphate multikinase with predominantly nuclear localization. *Biochem J* 366(Pt 2):549-556.
3. Ongusaha PP, Hughes PJ, Hirata M, Davey J, & Michell RH (1997) The inositol 1,4,5-trisphosphate 6-kinase of Schizosaccharomyces pombe. *Biochem Soc Trans* 25(1):105S.
4. Saiardi A*, et al.* (2001) Mammalian inositol polyphosphate multikinase synthesizes inositol 1,4,5-trisphosphate and an inositol pyrophosphate. *Proc Natl Acad Sci U S A* 98(5):2306-2311.
5. York JD, Odom AR, Murphy R, Ives EB, & Wente SR (1999) A phospholipase C-dependent inositol polyphosphate kinase pathway required for efficient messenger RNA export. *Science* 285(5424):96-100.
6. Hatch AJ & York JD (2010) SnapShot: Inositol phosphates. *Cell* 143(6):1030-1030 e1031.
7. Maag D*, et al.* (2011) Inositol polyphosphate multikinase is a physiologic PI3-kinase that activates Akt/PKB. *Proc Natl Acad Sci U S A* 108(4):1391-1396.
8. Morgan-Lappe S*, et al.* (2006) RNAi-based screening of the human kinome identifies Akt-cooperating kinases: a new approach to designing efficacious multitargeted kinase inhibitors. *Oncogene* 25(9):1340-1348.

9. Bang S, *et al.* (2012) AMP-activated protein kinase is physiologically regulated by inositol polyphosphate multikinase. *Proc Natl Acad Sci U S A* 109(2):616-620.

10. Kim S, *et al.* (2011) Amino acid signaling to mTOR mediated by inositol polyphosphate multikinase. *Cell Metab* 13(2):215-221.

11. Xu R, *et al.* (2013) Inositol polyphosphate multikinase is a transcriptional coactivator required for immediate early gene induction. *Proc Natl Acad Sci U S A* 110(40):16181-16186.

12. Xu R, *et al.* (2013) Inositol polyphosphate multikinase is a coactivator of p53-mediated transcription and cell death. *Sci Signal* 6(269):ra22.

13. Berridge MJ (1993) Inositol trisphosphate and calcium signalling. *Nature* 361(6410):315-325.

14. Chang SC & Majerus PW (2006) Inositol polyphosphate multikinase regulates inositol 1,4,5,6-tetrakisphosphate. *Biochem Biophys Res Commun* 339(1):209-216.

15. Leyman A, *et al.* (2007) The absence of expression of the three isoenzymes of the inositol 1,4,5-trisphosphate 3-kinase does not prevent the formation of inositol pentakisphosphate and hexakisphosphate in mouse embryonic fibroblasts. *Cell Signal* 19(7):1497-1504.

16. Odom AR, Stahlberg A, Wente SR, & York JD (2000) A role for nuclear inositol 1,4,5-trisphosphate kinase in transcriptional control. *Science* 287(5460):2026-2029.

17. Shen X, Xiao H, Ranallo R, Wu WH, & Wu C (2003) Modulation of ATP-dependent chromatin-remodeling complexes by inositol polyphosphates. *Science* 299(5603):112-114.

18. Steger DJ, Haswell ES, Miller AL, Wente SR, & O'Shea EK (2003) Regulation of chromatin remodeling by inositol polyphosphates. *Science* 299(5603):114-116.

19. El Alami M, Messenguy F, Scherens B, & Dubois E (2003) Arg82p is a bifunctional protein whose inositol polyphosphate kinase activity is essential for nitrogen and PHO gene expression but not for Mcm1p chaperoning in yeast. *Mol Microbiol* 49(2):457-468.

20. Dubois E, Dewaste V, Erneux C, & Messenguy F (2000) Inositol polyphosphate kinase activity of Arg82/ArgRIII is not required for the regulation of the arginine metabolism in yeast. *FEBS Lett* 486(3):300-304.

21. Taylor R, Jr., Chen PH, Chou CC, Patel J, & Jin SV (2012) KCS1 deletion in Saccharomyces cerevisiae leads to a defect in translocation of autophagic proteins and reduces autophagosome formation. *Autophagy* 8(9):1300-1311.

22. Saiardi A, Caffrey JJ, Snyder SH, & Shears SB (2000) Inositol polyphosphate multikinase (ArgRIII) determines nuclear mRNA export in Saccharomyces cerevisiae. *FEBS Lett* 468(1):28-32.

23. Hirata M, Kanematsu T, Takeuchi H, & Yagisawa H (1998) Pleckstrin homology domain as an inositol compound binding module. *Jpn J Pharmacol* 76(3):255-263.

24. Komander D*, et al.* (2004) Structural insights into the regulation of PDK1 by phosphoinositides and inositol phosphates. *Embo J* 23(20):3918-3928.

25. Jackson SG, Al-Saigh S, Schultz C, & Junop MS (2011) Inositol pentakisphosphate isomers bind PH domains with varying specificity and inhibit phosphoinositide interactions. *BMC Struct Biol* 11:11.

26. Maffucci T*, et al.* (2005) Inhibition of the phosphatidylinositol 3-kinase/Akt pathway by inositol pentakisphosphate results in antiangiogenic and antitumor effects. *Cancer Res* 65(18):8339-8349.

27. Piccolo E*, et al.* (2004) Inositol pentakisphosphate promotes apoptosis through the PI 3-K/Akt pathway. *Oncogene* 23(9):1754-1765.

28. Fukuda M, Kojima T, Kabayama H, & Mikoshiba K (1996) Mutation of the pleckstrin homology domain of Bruton's tyrosine kinase in immunodeficiency impaired inositol 1,3,4,5-tetrakisphosphate binding capacity. *J Biol Chem* 271(48):30303-30306.

29. Huang YH*, et al.* (2007) Positive regulation of Itk PH domain function by soluble IP4. *Science* 316(5826):886-889.

30. Fukuda M & Mikoshiba K (1996) Structure-function relationships of the mouse Gap1m. Determination of the inositol 1,3,4,5-tetrakisphosphate-binding domain. *J Biol Chem* 271(31):18838-18842.

31. Cullen PJ*, et al.* (1995) Identification of a specific Ins(1,3,4,5)P4-binding protein as a member of the GAP1 family. *Nature* 376(6540):527-530.

32. MacDonald BT, Tamai K, & He X (2009) Wnt/beta-catenin signaling: components, mechanisms, and diseases. *Dev Cell* 17(1):9-26.

33. Wang Y & Wang HY (2012) Dvl3 translocates IPMK to the cell membrane in response to Wnt. *Cell Signal* 24(12):2389-2395.

34. Gao Y & Wang HY (2007) Inositol pentakisphosphate mediates Wnt/beta-catenin signaling. *J Biol Chem* 282(36):26490-26502.

35. Solyakov L*, et al.* (2004) Regulation of casein kinase-2 (CK2) activity by inositol phosphates. *J Biol Chem* 279(42):43403-43410.

36. St-Denis NA & Litchfield DW (2009) Protein kinase CK2 in health and disease: From birth to death: the role of protein kinase CK2 in the regulation of cell proliferation and survival. *Cell Mol Life Sci* 66(11-12):1817-1829.

37. Watson PJ, Fairall L, Santos GM, & Schwabe JW (2012) Structure of HDAC3 bound to co-repressor and inositol tetraphosphate. *Nature* 481(7381):335-340.

38. Quignard JF, Rakotoarisoa L, Mironneau J, & Mironneau C (2003) Stimulation of L-type Ca2+ channels by inositol pentakis- and hexakisphosphates in rat vascular smooth muscle cells. *J Physiol* 549(Pt 3):729-737.

39. Hermosura MC*, et al.* (2000) InsP4 facilitates store-operated calcium influx by inhibition of InsP3 5-phosphatase. *Nature* 408(6813):735-740.

40. Coates M (1975) Studies on the interaction of organic phosphates with haemoglobin in an amphibian (Bufo marinus), a reptile (Trachydosaurus rugosus) and man. *Aust J Biol Sci* 28(4):367-378.

41. Fujii M & York JD (2005) A role for rat inositol polyphosphate kinases rIPK2 and rIPK1 in inositol pentakisphosphate and inositol hexakisphosphate production in rat-1 cells. *J Biol Chem* 280(2):1156-1164.

42. Frederick JP*, et al.* (2005) An essential role for an inositol polyphosphate multikinase, Ipk2, in mouse embryogenesis and second messenger production. *Proc Natl Acad Sci U S A* 102(24):8454-8459.

43. Saiardi A, Resnick AC, Snowman AM, Wendland B, & Snyder SH (2005) Inositol pyrophosphates regulate cell death and telomere length through phosphoinositide 3-kinase-related protein kinases. *Proc Natl Acad Sci U S A* 102(6):1911-1914.

44. York SJ, Armbruster BN, Greenwell P, Petes TD, & York JD (2005) Inositol diphosphate signaling regulates telomere length. *J Biol Chem* 280(6):4264-4269.

45. Illies C*, et al.* (2007) Requirement of inositol pyrophosphates for full exocytotic capacity in pancreatic beta cells. *Science* 318(5854):1299-1302.

46. Saiardi A, Sciambi C, McCaffery JM, Wendland B, & Snyder SH (2002) Inositol pyrophosphates regulate endocytic trafficking. *Proc Natl Acad Sci U S A* 99(22):14206-14211.

47. Jadav RS, Chanduri MV, Sengupta S, & Bhandari R (2013) Inositol pyrophosphate synthesis by inositol hexakisphosphate kinase 1 is required for homologous recombination repair. *J Biol Chem* 288(5):3312-3321.

48. Bhandari R*, et al.* (2007) Protein pyrophosphorylation by inositol pyrophosphates is a posttranslational event. *Proc Natl Acad Sci U S A* 104(39):15305-15310.

49. Saiardi A, Bhandari R, Resnick AC, Snowman AM, & Snyder SH (2004) Phosphorylation of proteins by inositol pyrophosphates. *Science* 306(5704):2101-2105.

50. Vanhaesebroeck B, Stephens L, & Hawkins P (2012) PI3K signalling: the path to discovery and understanding. *Nat Rev Mol Cell Biol* 13(3):195-203.

51. Resnick AC*, et al.* (2005) Inositol polyphosphate multikinase is a nuclear PI3-kinase with transcriptional regulatory activity. *Proc Natl Acad Sci U S A* 102(36):12783-12788.

52. Backer JM (2008) The regulation and function of Class III PI3Ks: novel roles for Vps34. *Biochem J* 410(1):1-17.

53. Wang X, Hills LB, & Huang YH (2015) Lipid and Protein Co-Regulation of PI3K Effectors Akt and Itk in Lymphocytes. *Front Immunol* 6:117.

54. Fruman DA & Rommel C (2014) PI3K and cancer: lessons, challenges and opportunities. *Nat Rev Drug Discov* 13(2):140-156.

55. Blind RD, Suzawa M, & Ingraham HA (2012) Direct modification and activation of a nuclear receptor-PIP(2) complex by the inositol lipid kinase IPMK. *Sci Signal* 5(229):ra44.

56. Wickramasinghe VO*, et al.* (2013) Human inositol polyphosphate multikinase regulates transcript-selective nuclear mRNA export to preserve genome integrity. *Mol Cell* 51(6):737-750.

57. Okada M, Jang SW, & Ye K (2008) Akt phosphorylation and nuclear phosphoinositide association mediate mRNA export and cell proliferation activities by ALY. *Proc Natl Acad Sci U S A* 105(25):8649-8654.

58. El Bakkoury M, Dubois E, & Messenguy F (2000) Recruitment of the yeast MADS-box proteins, ArgRI and Mcm1 by the pleiotropic factor ArgRIII is required for their stability. *Mol Microbiol* 35(1):15-31.

59. Bosch D & Saiardi A (2012) Arginine transcriptional response does not require inositol phosphate synthesis. *J Biol Chem* 287(45):38347-38355.

60. Hardie DG, Hawley SA, & Scott JW (2006) AMP-activated protein kinase--development of the energy sensor concept. *J Physiol* 574(Pt 1):7-15.

61. Sheng M & Greenberg ME (1990) The regulation and function of c-fos and other immediate early genes in the nervous system. *Neuron* 4(4):477-485.

62. Kim E*, et al.* (2013) Inositol polyphosphate multikinase is a coactivator for serum response factor-dependent induction of immediate early genes. *Proc Natl Acad Sci U S A* 110(49):19938-19943.

63. Loss O, Wu CT, Riccio A, & Saiardi A (2013) Modulation of inositol polyphosphate levels regulates neuronal differentiation. *Mol Biol Cell* 24(18):2981-2989.

64. Kublun I, Ehm P, Brehm MA, & Nalaskowski MM (2014) Efficacious inhibition of Importin alpha/beta-mediated nuclear import of human inositol phosphate multikinase. *Biochimie* 102:117-123.

65. Meyer R*, et al.* (2012) Nucleocytoplasmic shuttling of human inositol phosphate multikinase is influenced by CK2 phosphorylation. *Biol Chem* 393(3):149-160.

66. Tang B*, et al.* (2011) Genome-wide identification of Bcl11b gene targets reveals role in brain-derived neurotrophic factor signaling. *PLoS One* 6(9):e23691.

67. Wakabayashi Y*, et al.* (2003) Bcl11b is required for differentiation and survival of alphabeta T lymphocytes. *Nat Immunol* 4(6):533-539.

68. Le Douce V, Cherrier T, Riclet R, Rohr O, & Schwartz C (2014) The many lives of CTIP2: from AIDS to cancer and cardiac hypertrophy. *J Cell Physiol* 229(5):533-537.

69. Bates GP (2005) History of genetic disease: the molecular genetics of Huntington disease - a history. *Nat Rev Genet* 6(10):766-773.

70. Ross CA*, et al.* (2014) Huntington disease: natural history, biomarkers and prospects for therapeutics. *Nat Rev Neurol* 10(4):204-216.

71. Beighton P & Hayden MR (1981) Huntington's chorea. *S Afr Med J* 59(8):250.

72. Ross CA & Tabrizi SJ (2011) Huntington's disease: from molecular pathogenesis to clinical treatment. *Lancet Neurol* 10(1):83-98.

73. Paulsen JS (2011) Cognitive impairment in Huntington disease: diagnosis and treatment. *Curr Neurol Neurosci Rep* 11(5):474-483.

74. Hayden MR, Berkowicz AL, Beighton PH, & Yiptong C (1981) Huntington's chorea on the island of Mauritius. *S Afr Med J* 60(26):1001-1002.

75. van der Burg JM, Bjorkqvist M, & Brundin P (2009) Beyond the brain: widespread pathology in Huntington's disease. *Lancet Neurol* 8(8):765-774.

76. Morton AJ (2013) Circadian and sleep disorder in Huntington's disease. *Exp Neurol* 243:34-44.

77. Gerfen CR (1992) The neostriatal mosaic: multiple levels of compartmental organization in the basal ganglia. *Annu Rev Neurosci* 15:285-320.

78. Kita H & Kitai ST (1988) Glutamate decarboxylase immunoreactive neurons in rat neostriatum: their morphological types and populations. *Brain Res* 447(2):346-352.

79. Vonsattel JP & DiFiglia M (1998) Huntington disease. *J Neuropathol Exp Neurol* 57(5):369-384.

80. de la Monte SM, Vonsattel JP, & Richardson EP, Jr. (1988) Morphometric demonstration of atrophic changes in the cerebral cortex, white matter, and neostriatum in Huntington's disease. *J Neuropathol Exp Neurol* 47(5):516-525.

81. Cudkowicz M & Kowall NW (1990) Degeneration of pyramidal projection neurons in Huntington's disease cortex. *Ann Neurol* 27(2):200-204.

82. Hedreen JC, Peyser CE, Folstein SE, & Ross CA (1991) Neuronal loss in layers V and VI of cerebral cortex in Huntington's disease. *Neurosci Lett* 133(2):257-261.

83. Davies SW & Scherzinger E (1997) Nuclear inclusions in Huntington's disease. *Trends Cell Biol* 7(11):422.

84. Vonsattel JP*, et al.* (1985) Neuropathological classification of Huntington's disease. *J Neuropathol Exp Neurol* 44(6):559-577.

85. Wichmann T & DeLong MR (1996) Functional and pathophysiological models of the basal ganglia. *Curr Opin Neurobiol* 6(6):751-758.

86. Galvan L, Andre VM, Wang EA, Cepeda C, & Levine MS (2012) Functional Differences Between Direct and Indirect Striatal Output Pathways in Huntington's Disease. *J Huntingtons Dis* 1(1):17-25.

87. Albin RL, Reiner A, Anderson KD, Penney JB, & Young AB (1990) Striatal and nigral neuron subpopulations in rigid Huntington's disease: implications for the functional anatomy of chorea and rigidity-akinesia. *Ann Neurol* 27(4):357-365.

88. Gertler TS, Chan CS, & Surmeier DJ (2008) Dichotomous anatomical properties of adult striatal medium spiny neurons. *J Neurosci* 28(43):10814-10824.

89. Cepeda C, *et al.* (2008) Differential electrophysiological properties of dopamine D1 and D2 receptor-containing striatal medium-sized spiny neurons. *Eur J Neurosci* 27(3):671-682.

90. The Huntington's Disease Collaborative Research Group (1993) A novel gene containing a trinucleotide repeat that is expanded and unstable on Huntington's disease chromosomes. *Cell* 72(6):971-983.

91. Bertram L & Tanzi RE (2005) The genetic epidemiology of neurodegenerative disease. *J Clin Invest* 115(6):1449-1457.

92. Trottier Y, Biancalana V, & Mandel JL (1994) Instability of CAG repeats in Huntington's disease: relation to parental transmission and age of onset. *J Med Genet* 31(5):377-382.

93. Dehay B & Bertolotti A (2006) Critical role of the proline-rich region in Huntingtin for aggregation and cytotoxicity in yeast. *J Biol Chem* 281(47):35608-35615.

94. Gao YG, *et al.* (2006) Structural insights into the specific binding of huntingtin proline-rich region with the SH3 and WW domains. *Structure* 14(12):1755-1765.

95. Cattaneo E, Zuccato C, & Tartari M (2005) Normal huntingtin function: an alternative approach to Huntington's disease. *Nat Rev Neurosci* 6(12):919-930.

96. Aiken CT, *et al.* (2009) Phosphorylation of threonine 3: implications for Huntingtin aggregation and neurotoxicity. *J Biol Chem* 284(43):29427-29436.

97. Gu X, *et al.* (2009) Serines 13 and 16 are critical determinants of full-length human mutant huntingtin induced disease pathogenesis in HD mice. *Neuron* 64(6):828-840.

98. Steffan JS, *et al.* (2004) SUMO modification of Huntingtin and Huntington's disease pathology. *Science* 304(5667):100-104.

99. Bhat KP, Yan S, Wang CE, Li S, & Li XJ (2014) Differential ubiquitination and degradation of huntingtin fragments modulated by ubiquitin-protein ligase E3A. *Proc Natl Acad Sci U S A* 111(15):5706-5711.

100. Yanai A, *et al.* (2006) Palmitoylation of huntingtin by HIP14 is essential for its trafficking and function. *Nat Neurosci* 9(6):824-831.

101. Humbert S, *et al.* (2002) The IGF-1/Akt pathway is neuroprotective in Huntington's disease and involves Huntingtin phosphorylation by Akt. *Dev Cell* 2(6):831-837.

102. Rangone H, *et al.* (2004) The serum- and glucocorticoid-induced kinase SGK inhibits mutant huntingtin-induced toxicity by phosphorylating serine 421 of huntingtin. *Eur J Neurosci* 19(2):273-279.

103. Jeong H, *et al.* (2009) Acetylation targets mutant huntingtin to autophagosomes for degradation. *Cell* 137(1):60-72.

104. DiFiglia M, *et al.* (1995) Huntingtin is a cytoplasmic protein associated with vesicles in human and rat brain neurons. *Neuron* 14(5):1075-1081.

105. Tong Y, *et al.* (2011) Spatial and temporal requirements for huntingtin (Htt) in neuronal migration and survival during brain development. *J Neurosci* 31(41):14794-14799.

106. Duyao MP, *et al.* (1995) Inactivation of the mouse Huntington's disease gene homolog Hdh. *Science* 269(5222):407-410.

107. Nasir J*, et al.* (1995) Targeted disruption of the Huntington's disease gene results in embryonic lethality and behavioral and morphological changes in heterozygotes. *Cell* 81(5):811-823.

108. Molero AE*, et al.* (2009) Impairment of developmental stem cell-mediated striatal neurogenesis and pluripotency genes in a knock-in model of Huntington's disease. *Proc Natl Acad Sci U S A* 106(51):21900-21905.

109. Caron NS, Hung CL, Atwal RS, & Truant R (2014) Live cell imaging and biophotonic methods reveal two types of mutant huntingtin inclusions. *Hum Mol Genet* 23(9):2324-2338.

110. Ross CA & Poirier MA (2004) Protein aggregation and neurodegenerative disease. *Nat Med* 10 Suppl:S10-17.

111. Sugars KL & Rubinsztein DC (2003) Transcriptional abnormalities in Huntington disease. *Trends Genet* 19(5):233-238.

112. Benn CL*, et al.* (2008) Huntingtin modulates transcription, occupies gene promoters in vivo, and binds directly to DNA in a polyglutamine-dependent manner. *J Neurosci* 28(42):10720-10733.

113. Desplats PA, Lambert JR, & Thomas EA (2008) Functional roles for the striatal-enriched transcription factor, Bcl11b, in the control of striatal gene expression and transcriptional dysregulation in Huntington's disease. *Neurobiol Dis* 31(3):298-308.

114. Dunah AW*, et al.* (2002) Sp1 and TAFII130 transcriptional activity disrupted in early Huntington's disease. *Science* 296(5576):2238-2243.

115. Shimohata T, Onodera O, & Tsuji S (2000) Interaction of expanded polyglutamine stretches with nuclear transcription factors leads to aberrant transcriptional regulation in polyglutamine diseases. *Neuropathology* 20(4):326-333.

116. Boutell JM, *et al.* (1999) Aberrant interactions of transcriptional repressor proteins with the Huntington's disease gene product, huntingtin. *Hum Mol Genet* 8(9):1647-1655.

117. McCampbell A, *et al.* (2000) CREB-binding protein sequestration by expanded polyglutamine. *Hum Mol Genet* 9(14):2197-2202.

118. Steffan JS, *et al.* (2000) The Huntington's disease protein interacts with p53 and CREB-binding protein and represses transcription. *Proc Natl Acad Sci U S A* 97(12):6763-6768.

119. McCampbell A, *et al.* (2001) Histone deacetylase inhibitors reduce polyglutamine toxicity. *Proc Natl Acad Sci U S A* 98(26):15179-15184.

120. Steffan JS, *et al.* (2001) Histone deacetylase inhibitors arrest polyglutamine-dependent neurodegeneration in Drosophila. *Nature* 413(6857):739-743.

121. Liu KY, *et al.* (2015) Disruption of the nuclear membrane by perinuclear inclusions of mutant huntingtin causes cell-cycle re-entry and striatal cell death in mouse and cell models of Huntington's disease. *Hum Mol Genet* 24(6):1602-1616.

122. Bennett EJ, *et al.* (2007) Global changes to the ubiquitin system in Huntington's disease. *Nature* 448(7154):704-708.

123. Rubinsztein DC (2006) The roles of intracellular protein-degradation pathways in neurodegeneration. *Nature* 443(7113):780-786.

124. Levine B & Kroemer G (2008) Autophagy in the pathogenesis of disease. *Cell* 132(1):27-42.

125. Tan JM, *et al.* (2008) Lysine 63-linked ubiquitination promotes the formation and autophagic clearance of protein inclusions associated with neurodegenerative diseases. *Hum Mol Genet* 17(3):431-439.

126. Komatsu M, *et al.* (2006) Loss of autophagy in the central nervous system causes neurodegeneration in mice. *Nature* 441(7095):880-884.

127. Ravikumar B, *et al.* (2004) Inhibition of mTOR induces autophagy and reduces toxicity of polyglutamine expansions in fly and mouse models of Huntington disease. *Nat Genet* 36(6):585-595.

128. Koga H, *et al.* (2011) Constitutive upregulation of chaperone-mediated autophagy in Huntington's disease. *J Neurosci* 31(50):18492-18505.

129. Kim J, *et al.* (2010) Mitochondrial loss, dysfunction and altered dynamics in Huntington's disease. *Hum Mol Genet* 19(20):3919-3935.

130. Cui L, *et al.* (2006) Transcriptional repression of PGC-1alpha by mutant huntingtin leads to mitochondrial dysfunction and neurodegeneration. *Cell* 127(1):59-69.

131. Wang JQ, *et al.* (2013) Dysregulation of mitochondrial calcium signaling and superoxide flashes cause mitochondrial genomic DNA damage in Huntington disease. *J Biol Chem* 288(5):3070-3084.

132. Heiskanen KM, Bhat MB, Wang HW, Ma J, & Nieminen AL (1999) Mitochondrial depolarization accompanies cytochrome c release during apoptosis in PC6 cells. *J Biol Chem* 274(9):5654-5658.

133. Coyle JT & Schwarcz R (1976) Lesion of striatal neurones with kainic acid provides a model for Huntington's chorea. *Nature* 263(5574):244-246.

134. Okamoto S, *et al.* (2009) Balance between synaptic versus extrasynaptic NMDA receptor activity influences inclusions and neurotoxicity of mutant huntingtin. *Nat Med* 15(12):1407-1413.

135. Kaufman AM, *et al.* (2012) Opposing roles of synaptic and extrasynaptic NMDA receptor signaling in cocultured striatal and cortical neurons. *J Neurosci* 32(12):3992-4003.

136. Rubinsztein DC, *et al.* (1997) Genotypes at the GluR6 kainate receptor locus are associated with variation in the age of onset of Huntington disease. *Proc Natl Acad Sci U S A* 94(8):3872-3876.

137. Tang TS, *et al.* (2005) Disturbed Ca2+ signaling and apoptosis of medium spiny neurons in Huntington's disease. *Proc Natl Acad Sci U S A* 102(7):2602-2607.

138. Altar CA, *et al.* (1997) Anterograde transport of brain-derived neurotrophic factor and its role in the brain. *Nature* 389(6653):856-860.

139. Huang EJ & Reichardt LF (2003) Trk receptors: roles in neuronal signal transduction. *Annu Rev Biochem* 72:609-642.

140. Fenner BM (2012) Truncated TrkB: beyond a dominant negative receptor. *Cytokine Growth Factor Rev* 23(1-2):15-24.

141. Zuccato C, *et al.* (2001) Loss of huntingtin-mediated BDNF gene transcription in Huntington's disease. *Science* 293(5529):493-498.

142. Gauthier LR, *et al.* (2004) Huntingtin controls neurotrophic support and survival of neurons by enhancing BDNF vesicular transport along microtubules. *Cell* 118(1):127-138.

143. Plotkin JL, *et al.* (2014) Impaired TrkB receptor signaling underlies corticostriatal dysfunction in Huntington's disease. *Neuron* 83(1):178-188.

144. Tai YF, *et al.* (2007) Microglial activation in presymptomatic Huntington's disease gene carriers. *Brain* 130(Pt 7):1759-1766.

145. Pavese N, *et al.* (2006) Microglial activation correlates with severity in Huntington disease: a clinical and PET study. *Neurology* 66(11):1638-1643.

146. Shin JY, *et al.* (2005) Expression of mutant huntingtin in glial cells contributes to neuronal excitotoxicity. *J Cell Biol* 171(6):1001-1012.

147. Bjorkqvist M, *et al.* (2008) A novel pathogenic pathway of immune activation detectable before clinical onset in Huntington's disease. *J Exp Med* 205(8):1869-1877.

148. Bradford J, *et al.* (2009) Expression of mutant huntingtin in mouse brain astrocytes causes age-dependent neurological symptoms. *Proc Natl Acad Sci U S A* 106(52):22480-22485.

149. Desplats PA, *et al.* (2006) Selective deficits in the expression of striatal-enriched mRNAs in Huntington's disease. *J Neurochem* 96(3):743-757.

150. Arlotta P, *et al.* (2005) Neuronal subtype-specific genes that control corticospinal motor neuron development in vivo. *Neuron* 45(2):207-221.

151. Arlotta P, Molyneaux BJ, Jabaudon D, Yoshida Y, & Macklis JD (2008) Ctip2 controls the differentiation of medium spiny neurons and the establishment of the cellular architecture of the striatum. *J Neurosci* 28(3):622-632.

152. Ip BK, Bayatti N, Howard NJ, Lindsay S, & Clowry GJ (2011) The corticofugal neuron-associated genes ROBO1, SRGAP1, and CTIP2 exhibit an anterior to posterior gradient of expression in early fetal human neocortex development. *Cereb Cortex* 21(6):1395-1407.

153. Molyneaux BJ, Arlotta P, Hirata T, Hibi M, & Macklis JD (2005) Fezl is required for the birth and specification of corticospinal motor neurons. *Neuron* 47(6):817-831.

154. Thomas EA (2006) Striatal specificity of gene expression dysregulation in Huntington's disease. *J Neurosci Res* 84(6):1151-1164.

155. Senawong T*, et al.* (2003) Involvement of the histone deacetylase SIRT1 in chicken ovalbumin upstream promoter transcription factor (COUP-TF)-interacting protein 2-mediated transcriptional repression. *J Biol Chem* 278(44):43041-43050.

156. Tirard M*, et al.* (2012) In vivo localization and identification of SUMOylated proteins in the brain of His6-HA-SUMO1 knock-in mice. *Proc Natl Acad Sci U S A* 109(51):21122-21127.

157. Falk JD*, et al.* (1999) Rhes: A striatal-specific Ras homolog related to Dexras1. *J Neurosci Res* 57(6):782-788.

158. Henley JM, Craig TJ, & Wilkinson KA (2014) Neuronal SUMOylation: mechanisms, physiology, and roles in neuronal dysfunction. *Physiol Rev* 94(4):1249-1285.

159. Subramaniam S, Sixt KM, Barrow R, & Snyder SH (2009) Rhes, a striatal specific protein, mediates mutant-huntingtin cytotoxicity. *Science* 324(5932):1327-1330.

160. Mealer RG, Subramaniam S, & Snyder SH (2013) Rhes deletion is neuroprotective in the 3-nitropropionic acid model of Huntington's disease. *J Neurosci* 33(9):4206-4210.

161. Baiamonte BA, Lee FA, Brewer ST, Spano D, & LaHoste GJ (2013) Attenuation of Rhes activity significantly delays the appearance of behavioral symptoms in a mouse model of Huntington's disease. *PLoS One* 8(1):e53606.

162. McGeer PL & McGeer EG (1976) Enzymes associated with the metabolism of catecholamines, acetylcholine and gaba in human controls and patients with Parkinson's disease and Huntington's chorea. *J Neurochem* 26(1):65-76.

163. Schwarz M, Turski L, & Sontag KH (1984) CGS 8216, Ro 15-1788 and methyl-beta-carboline-3-carboxylate, but not EMD 41717 antagonize the muscle relaxant effect of diazepam in genetically spastic rats. *Life Sci* 35(14):1445-1451.

164. Beal MF*, et al.* (1986) Replication of the neurochemical characteristics of Huntington's disease by quinolinic acid. *Nature* 321(6066):168-171.

165. Brouillet E*, et al.* (1993) Age-dependent vulnerability of the striatum to the mitochondrial toxin 3-nitropropionic acid. *J Neurochem* 60(1):356-359.

166. Huang LS, *et al.* (2006) 3-nitropropionic acid is a suicide inhibitor of mitochondrial respiration that, upon oxidation by complex II, forms a covalent adduct with a catalytic base arginine in the active site of the enzyme. *J Biol Chem* 281(9):5965-5972.

167. Pouladi MA, Morton AJ, & Hayden MR (2013) Choosing an animal model for the study of Huntington's disease. *Nat Rev Neurosci* 14(10):708-721.

168. Mangiarini L, *et al.* (1996) Exon 1 of the HD gene with an expanded CAG repeat is sufficient to cause a progressive neurological phenotype in transgenic mice. *Cell* 87(3):493-506.

169. Carter RJ, *et al.* (1999) Characterization of progressive motor deficits in mice transgenic for the human Huntington's disease mutation. *J Neurosci* 19(8):3248-3257.

170. Menalled LB, *et al.* (2012) Comprehensive behavioral and molecular characterization of a new knock-in mouse model of Huntington's disease: zQ175. *PLoS One* 7(12):e49838.

171. Yamamoto A, Lucas JJ, & Hen R (2000) Reversal of neuropathology and motor dysfunction in a conditional model of Huntington's disease. *Cell* 101(1):57-66.

172. Beal MF & Ferrante RJ (2004) Experimental therapeutics in transgenic mouse models of Huntington's disease. *Nat Rev Neurosci* 5(5):373-384.

173. Paul BD, *et al.* (2014) Cystathionine gamma-lyase deficiency mediates neurodegeneration in Huntington's disease. *Nature* 509(7498):96-100.

174. Hockly E, *et al.* (2003) Suberoylanilide hydroxamic acid, a histone deacetylase inhibitor, ameliorates motor deficits in a mouse model of Huntington's disease. *Proc Natl Acad Sci U S A* 100(4):2041-2046.

175. Thomas EA, *et al.* (2008) The HDAC inhibitor 4b ameliorates the disease phenotype and transcriptional abnormalities in Huntington's disease transgenic mice. *Proc Natl Acad Sci U S A* 105(40):15564-15569.

176. Carroll JB, *et al.* (2011) Potent and selective antisense oligonucleotides targeting single-nucleotide polymorphisms in the Huntington disease gene / allele-specific silencing of mutant huntingtin. *Mol Ther* 19(12):2178-2185.

177. Benraiss A, *et al.* (2013) Sustained mobilization of endogenous neural progenitors delays disease progression in a transgenic model of Huntington's disease. *Cell Stem Cell* 12(6):787-799.

178. Kwon Y, Hofmann T, & Montell C (2007) Integration of phosphoinositide- and calmodulin-mediated regulation of TRPC6. *Mol Cell* 25(4):491-503.

179. Savitt JM, Jang SS, Mu W, Dawson VL, & Dawson TM (2005) Bcl-x is required for proper development of the mouse substantia nigra. *J Neurosci* 25(29):6721-6728.

180. Guyenet SJ, *et al.* (2010) A simple composite phenotype scoring system for evaluating mouse models of cerebellar ataxia. *J Vis Exp* (39).

181. Trettel F, *et al.* (2000) Dominant phenotypes produced by the HD mutation in STHdh(Q111) striatal cells. *Hum Mol Genet* 9(19):2799-2809.

182. Reiner A, *et al.* (1988) Differential loss of striatal projection neurons in Huntington disease. *Proc Natl Acad Sci U S A* 85(15):5733-5737.

183. Gines S*, et al.* (2003) Specific progressive cAMP reduction implicates energy deficit in presymptomatic Huntington's disease knock-in mice. *Hum Mol Genet* 12(5):497-508.

184. Saiardi A, Erdjument-Bromage H, Snowman AM, Tempst P, & Snyder SH (1999) Synthesis of diphosphoinositol pentakisphosphate by a newly identified family of higher inositol polyphosphate kinases. *Curr Biol* 9(22):1323-1326.

185. Colin E*, et al.* (2005) Akt is altered in an animal model of Huntington's disease and in patients. *Eur J Neurosci* 21(6):1478-1488.

186. Klapstein GJ*, et al.* (2001) Electrophysiological and morphological changes in striatal spiny neurons in R6/2 Huntington's disease transgenic mice. *J Neurophysiol* 86(6):2667-2677.

187. Tong X*, et al.* (2014) Astrocyte Kir4.1 ion channel deficits contribute to neuronal dysfunction in Huntington's disease model mice. *Nat Neurosci* 17(5):694-703.

188. Pearce LR, Komander D, & Alessi DR (2010) The nuts and bolts of AGC protein kinases. *Nat Rev Mol Cell Biol* 11(1):9-22.

189. Rangone H*, et al.* (2005) Phosphorylation of arfaptin 2 at Ser260 by Akt Inhibits PolyQ-huntingtin-induced toxicity by rescuing proteasome impairment. *J Biol Chem* 280(23):22021-22028.

190. Saavedra A*, et al.* (2010) PH domain leucine-rich repeat protein phosphatase 1 contributes to maintain the activation of the PI3K/Akt pro-survival pathway in Huntington's disease striatum. *Cell Death Differ* 17(2):324-335.

191. Zala D*, et al.* (2008) Phosphorylation of mutant huntingtin at S421 restores anterograde and retrograde transport in neurons. *Hum Mol Genet* 17(24):3837-3846.

192. Metzler M*, et al.* (2010) Phosphorylation of huntingtin at Ser421 in YAC128 neurons is associated with protection of YAC128 neurons from NMDA-mediated excitotoxicity and is modulated by PP1 and PP2A. *J Neurosci* 30(43):14318-14329.

193. Choo YS, Johnson GV, MacDonald M, Detloff PJ, & Lesort M (2004) Mutant huntingtin directly increases susceptibility of mitochondria to the calcium-induced permeability transition and cytochrome c release. *Hum Mol Genet* 13(14):1407-1420.

194. McCoy MK, Kaganovich A, Rudenko IN, Ding J, & Cookson MR (2014) Hexokinase activity is required for recruitment of parkin to depolarized mitochondria. *Hum Mol Genet* 23(1):145-156.

195. Roberts DJ, Tan-Sah VP, Smith JM, & Miyamoto S (2013) Akt phosphorylates HK-II at Thr-473 and increases mitochondrial HK-II association to protect cardiomyocytes. *J Biol Chem* 288(33):23798-23806.

196. Qi ML*, et al.* (2007) Proteome analysis of soluble nuclear proteins reveals that HMGB1/2 suppress genotoxic stress in polyglutamine diseases. *Nat Cell Biol* 9(4):402-414.

197. Enokido Y*, et al.* (2010) Mutant huntingtin impairs Ku70-mediated DNA repair. *J Cell Biol* 189(3):425-443.

198. Zuccato C, *et al.* (2003) Huntingtin interacts with REST/NRSF to modulate the transcription of NRSE-controlled neuronal genes. *Nat Genet* 35(1):76-83.

199. Jiang M, *et al.* (2013) Small-molecule TrkB receptor agonists improve motor function and extend survival in a mouse model of Huntington's disease. *Hum Mol Genet* 22(12):2462-2470.

200. Wang YB, *et al.* (2012) Adaptor protein APPL1 couples synaptic NMDA receptor with neuronal prosurvival phosphatidylinositol 3-kinase/Akt pathway. *J Neurosci* 32(35):11919-11929.

201. Blazquez C, *et al.* (2015) The CB cannabinoid receptor signals striatal neuroprotection via a PI3K/Akt/mTORC1/BDNF pathway. *Cell Death Differ* .

202. Vashishtha M, *et al.* (2013) Targeting H3K4 trimethylation in Huntington disease. *Proc Natl Acad Sci U S A* 110(32):E3027-3036.

203. Mielcarek M, *et al.* (2013) HDAC4 reduction: a novel therapeutic strategy to target cytoplasmic huntingtin and ameliorate neurodegeneration. *PLoS Biol* 11(11):e1001717.

204. Ju TC, *et al.* (2011) Nuclear translocation of AMPK-alpha1 potentiates striatal neurodegeneration in Huntington's disease. *J Cell Biol* 194(2):209-227.

205. Jordan SD & Lamia KA (2013) AMPK at the crossroads of circadian clocks and metabolism. *Mol Cell Endocrinol* 366(2):163-169.

206. Musiek ES, *et al.* (2013) Circadian clock proteins regulate neuronal redox homeostasis and neurodegeneration. *J Clin Invest* 123(12):5389-5400.

207. Gerber A, *et al.* (2013) Blood-borne circadian signal stimulates daily oscillations in actin dynamics and SRF activity. *Cell* 152(3):492-503.

208. Sbodio JI, Paul BD, Machamer CE, & Snyder SH (2013) Golgi protein ACBD3 mediates neurotoxicity associated with Huntington's disease. *Cell Rep* 4(5):890-897.

CURRICULUM VITAE

Ishrat Ahmed updated 5/23/2015

August 2, 1987
Trois-Rivières, Québec, Canada

Educational History

Ph.D. expected	2017	Program in Neuroscience Advisor: Solomon H. Snyder, MD	Johns Hopkins School of Medicine
M.D. expected	2017	Medical Scientist Training Program	Johns Hopkins School of Medicine
M.S.	2009	Cellular and Molecular Biology	Johns Hopkins University
B.S.	2009	Cellular and Molecular Biology French literature (minor)	Johns Hopkins University

Professional experience

Course participant	2015	Neural stem cells: Development and brain repair Neuroscience School of Advanced Studies (selected participant)
Course participant	2014	Emerging Women's Leadership Program
Course participant	2014	NINDS/AUPN/ANA/CNS Combining Clinical and Research Careers in Neuroscience course (selected participant)
Clinical research	2010	Lab of Alfredo Quinones-Hinojosa, MD Johns Hopkins School of Medicine
Research assistant	2006-2009	Labs of Ted Dawson, MD-PhD and Dr. Joseph Savitt, MD-PhD Institute for Cell Engineering, Johns Hopkins School of Medicine
Research apprentice	2004-2006	Lab of Manish Patankar, PhD University of Wisconsin School of Medicine

Scholarships, fellowships, and awards

Glenn/AFAR Scholarship for Research in the Biology of Aging	2015	$5000	Stipend support
UniStem Scholarship	2015	$1500	Course support
Neurostereology Fellowship Award	2013	$500	Course support
Medical Scientist Training Program	2009-2017	$20-30,000/yr	Stipend support
Keystone Symposia Scholarship	2009	$1200	Meeting support
Parkinson's Disease Foundation Summer Student Fellowship	2008	$3000	Stipend support
Technology Fellowship Grant	2008	$2000	Stipend support
Second Decade Society Internship Grant	2007	$2000	Stipend support
Second Decade Society Internship Grant	2006	$2000	Stipend support
Health Occupations Students of America Scholarship	2006	$1000	Tuition support
Barry M. Goldwater Scholarship	2007-2009	$8000/yr	Tuition support
Bloomberg Scholarship	2005-2009	$30-36,000/yr	Tuition support
Robert C. Byrd Scholarship	2005-2009	$1500/yr	Tuition support
John Cameron Scholarship	2005	$1000	Tuition support
National Honor Society Scholarship	2005	$1000	Tuition support
Health Occupations Students of America Scholarship	2005	$1000	Tuition support
Presidential Freedom Scholarship	2005	$500	Tuition support

Additional academic awards

2009	William D. McElroy Award for Meritorious Research	Johns Hopkins University
2008	Phi Beta Kappa	Phi Beta Kappa Society
2005	Young Epidemiology Scholars Competition Regional Finalist	Robert Wood Johnson
2004	Young Epidemiology Scholars Competition Regional Finalist	Foundation

Publications

Ahmed I, Sbodio JI, Harraz MM, Tyagi R, Grima JC, Albacarys LK, Hubbi ME, Xu R, Kim S, Paul BD, Snyder SH. Huntington's disease: Neural dysfunctions linked to inositol polyphosphate multikinase. *Manuscript under review*

Hubbi ME, Gilkes DM, Hu H, Kshitiz, **Ahmed I**, Semenza GL (2014) Cyclin-dependent kinases regulate lysosomal degradation of hypoxia-inducible factor 1α to promote cell-cycle progression. Proc Natl Acad Sci USA 11(32):3325-3334.

Xu R, Paul BD, Smith DR, Tyagi R, Rao F, Khan AB, Blech DJ, Vandiver MS, Harraz MM, Guha P, **Ahmed I**, Sen N, Gallagher M, Snyder SH (2013) Inositol polyphosphate multikinase is a transcriptional coactivator required for immediate early gene induction. Proc Natl Acad Sci USA 110(40):16181-6.

Hubbi ME, Hu H, Kshitiz, **Ahmed I**, Levchenko A, Semenza GL (2013) Chaperone-mediated autophagy targets hypoxia-inducible factor 1α (HIF-1α) for lysosomal degradation. J Biol Chem 288(15): 10703-14.

Ahmed I*, Liang Y*, Schools S, Dawson VL, Dawson TM, Savitt JM. (2012) Development and characterization of a new Parkinson's disease model resulting from impaired autophagy. J Neurosci 32(46):16503-9.

Pendleton C*, **Ahmed I***, Quinones-Hinojosa A. (2011) Neurotransplantation: *Lux et Veritas*, Fiction or Reality? J Neurosurg Sci 55(4):297-304.

Abstracts

Ahmed I, Sbodio JI, Harraz MM, Tyagi R, Albacarys LK, Hubbi ME, Grima JC, Xu R, Kim S, Paul BD, Snyder SH. Depletion of inositol polyphosphate multikinase mediates neuronal dysfunction in Huntington's disease. Cure Huntington's Disease Initiative (CHDI) Annual HD Therapeutics Conference, Palm Springs, CA, February 2015.

Ahmed I, Paul BD, Sbodio JI, Harraz MM, Tyagi R, Albacarys LK, Hubbi ME, Grima JC, Kim S, Snyder SH. Neuronal dysfunction in Huntington's disease linked to inositol polyphosphate multikinase. Cold Spring Harbor Laboratory meeting. Neurodegenerative Diseases: Biology and Therapeutics, Cold Spring Harbor, NY, December 2014.

Ahmed I, Sbodio JI, Harraz MM, Tyagi R, Albacarys LK, Xu R, Grima JC, Kim S, Paul BD, Snyder SH. Loss of inositol polyphosphate multikinase contributes to neurodegeneration in Huntington's disease. Society for Neuroscience, Washington D.C., November 2014. ***Selected for podium presentation***

Ahmed I, Koldobskiy MA, Ho GP, Snyder SH. S-nitrosylation of p53 regulates response to cellular stress. Cure Huntington's Disease Initiative (CHDI) Annual HD Therapeutics Conference, Palm Springs, CA, February 2014.

Koldobskiy MA, **Ahmed I**, Ho GP, Snowman A, Raabe E, Eberhart C, Snyder SH. S-nitrosylation of the p53 tumor suppressor protein in medulloblastoma. Society for Neuro-Oncology, San Francisco, CA, November 2013.

Ahmed I, Koldobskiy MA, Ho GP, Snyder SH. Regulation of p53 by nitric oxide. Society for Neuroscience, San Diego, CA, November 2013.

Ahmed I, Ho GP, Koldobskiy MA, Snyder SH. S-nitrosylation regulates p53. Society for Neuroscience, New Orleans, LA, October 2012.

Ahmed I, Raza S, Quinones-Hinojosa A. Assessment of surgical outcomes of mediobasal temporal lobe tumor resection via transcortical approaches. Scholarly Concentrations Project Symposium, Baltimore, MD, January 2011.

Ahmed I, Schools SE, Savitt JM. Dopamine neurons are sensitive to impaired autophagy in vivo. Keystone Symposium on Molecular and Cellular Biology-Neurodegenerative Diseases: New Molecular Mechanisms, Keystone, CO, February 2009. ***Selected for podium presentation***

Mejias-Estevez RM, Schools SE, **Ahmed I**, Ginty DD, Zhang C, Shokat KM, Dawson VL, Dawson TM, Savitt JM. RET knock-in mice: a new chemical/genetic tool for studying the role of RET kinase in development and aging. Society for Neuroscience, San Diego, CA, November 2007.

Savitt JM, Mejias R, Schools SE, **Ahmed I**, Ginty DD, Zhang C, Shokat KM, Dawson TM. Cell-type specific and inducible knockout of GDNF receptor function in mice. American Neurological Association, Washington D.C., October 2007.

Service and Leadership

2013-2015	MCAT instructor, Post-Baccalaureate Premedical Program and Odyssey Program, Johns Hopkins University
2013-2015	NeXXt Scholars Mentoring Fellow, New York Academy of Sciences
2012-2014	MSTP student committee, Johns Hopkins School of Medicine
2012-2013	MCAT instructor, Examkrackers Inc, Baltimore MD
2011-2014	Student Editorial Assistant, Medicine journal, Johns Hopkins Medicine
2010	Project HEALTH volunteer, Johns Hopkins Bayview Medical Center
2009-2012	Co-founder, Co-Director of Grants and Research, Charm City Clinic, Baltimore, MD
2009-2011	Advisor, Health Occupations Students of America, Johns Hopkins University

Mentoring

Adarsha Malla	Undergraduate student, Department of Biomedical Engineering (2013-2015)
Jonathan Grima	Rotation student, Department of Neuroscience (2013)